Astroparticle Physics 2023/24

Wednesday 8:30 - 10:15 HG 03.054
Thursday 15:30 - 17:15 HG 03.082

- lectures
- student presentations
- oral exam, ca. 45 min

Jörg R. Hörandel
HG 02.728
j.horandel@astro.ru.nl
http://particle.astro.ru.nl/goto.html?astropart2324

birth of cosmic rays
CRs: supernova remnants
neutrinos: e.g. Sun *(lecture 9)*

propagation of CRs in the Galaxy
interactions with ISM *(lecture 9)*

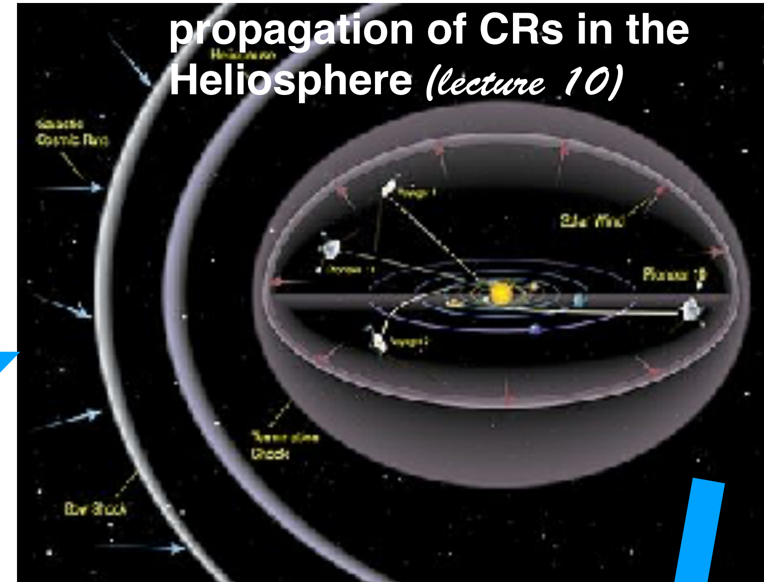

propagation of CRs in the Heliosphere *(lecture 10)*

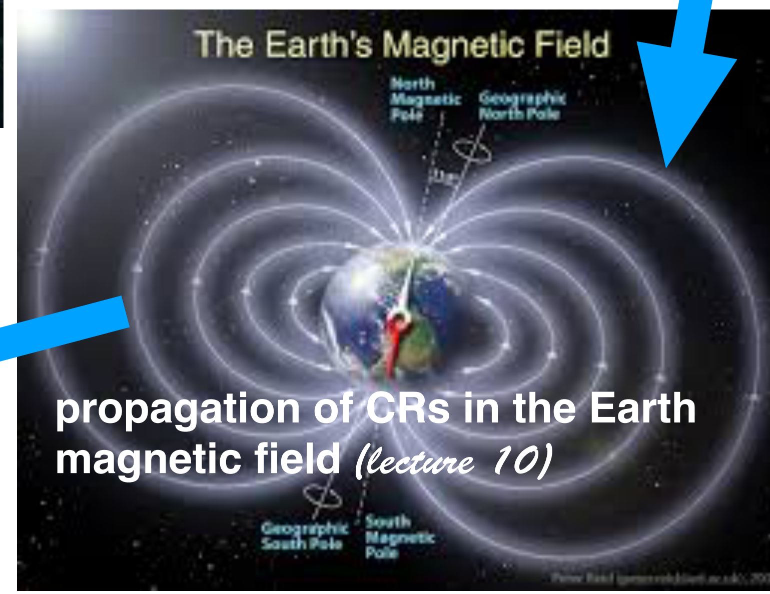

propagation of CRs in the Earth magnetic field *(lecture 10)*

CRs at the top of the atmosphere *(lecture 11)*

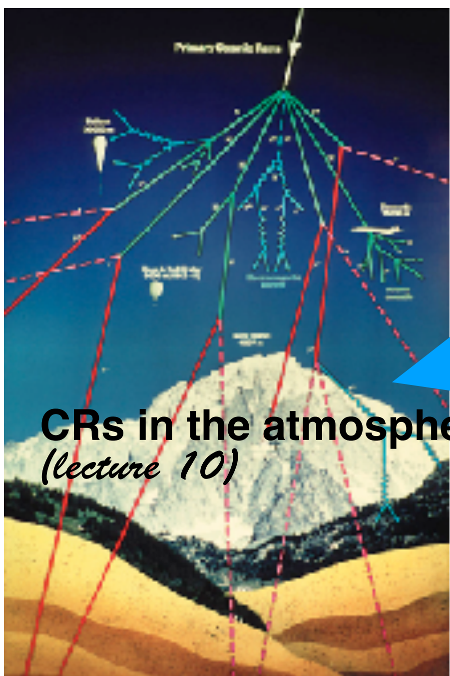

CRs in the atmosphere *(lecture 10)*

CRs underground *(lecture 12)*
neutrino oscillations *(lecture 12+13)*

Particles and the Cosmos

J. Blümer et al. / Progress in Particle and Nuclear Physics 63 (2009) 293–338

~1000/m² s

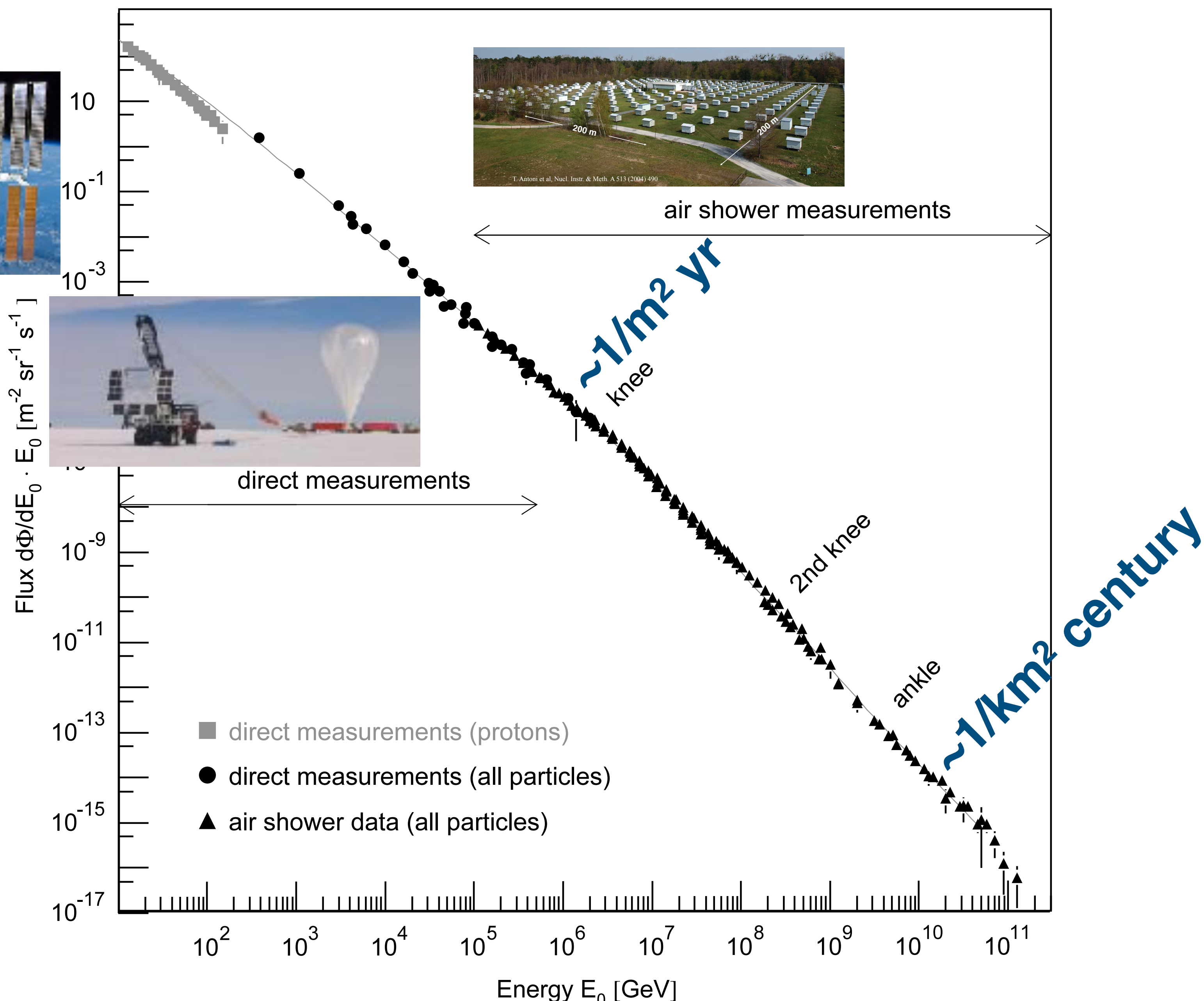

energy spectrum of cosmic rays extends to extremely high energies:

10^{20} eV ~16 J

Origin of cosmic rays
multi messenger technique

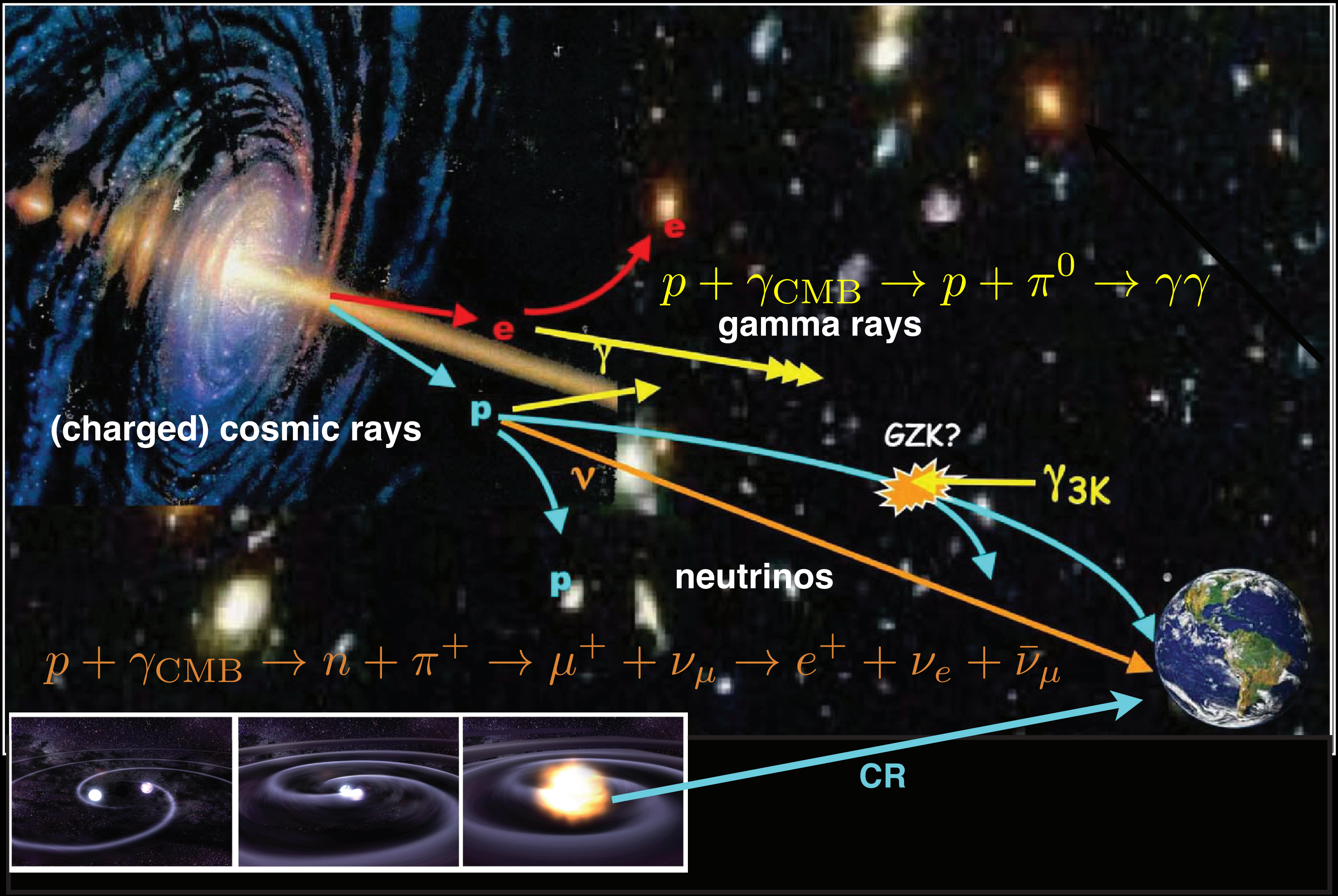

RESEARCH ARTICLE SUMMARY

NEUTRINO ASTROPHYSICS

Multimessenger observations of a flaring blazar coincident with high-energy neutrino IceCube-170922A

The IceCube Collaboration, *Fermi*-LAT, MAGIC, *AGILE*, ASAS-SN, HAWC, H.E.S.S., *INTEGRAL*, Kanata, Kiso, Kapteyn, Liverpool Telescope, Subaru, *Swift/NuSTAR*, VERITAS, and VLA/17B-403 teams*†

INTRODUCTION: Neutrinos are tracers of cosmic-ray acceleration: electrically neutral and traveling at nearly the speed of light, they can escape the densest environments and may be traced back to their source of origin. High-energy neutrinos are expected to be produced in blazars: intense extragalactic radio, optical, x-ray, and, in some cases, γ-ray sources characterized by relativistic jets of plasma pointing close to our line of sight. Blazars are among the most powerful objects in the Universe and are widely speculated to be sources of high-energy cosmic rays. These cosmic rays generate high-energy neutrinos and γ-rays, which are produced when the cosmic rays accelerated in the jet interact with nearby gas or photons. On 22 September 2017, the cubic-kilometer IceCube Neutrino Observatory detected a ~290-TeV neutrino from a direction consistent with the flaring γ-ray blazar TXS 0506+056. We report the details of this observation and the results of a multiwavelength follow-up campaign.

RATIONALE: Multimessenger astronomy aims for globally coordinated observations of cosmic rays, neutrinos, gravitational waves, and electromagnetic radiation across a broad range of wavelengths. The combination is expected to yield crucial

mic rays. The discovery of an extraterrestrial diffuse flux of high-energy neutrinos, announced by IceCube in 2013, has characteristic properties that hint at contributions from extragalactic sources, although the individual sources remain as yet unidentified. Continuously monitoring the entire sky for astrophysical neutrinos, IceCube provides real-time triggers for observatories around the world measuring γ-rays, x-rays, optical, radio, and gravitational waves, allowing for the potential identification of even rapidly fading sources.

RESULTS: A high-energy neutrino-induced muon track was detected on 22 September 2017, automatically generating an alert that was distributed worldwide within 1 min of detection and prompted follow-up searches by telescopes over a broad range of wavelengths. On 28 September 2017, the *Fermi* Large Area Telescope Collaboration reported that the direction of the neutrino was coincident with a cataloged γ-ray source, 0.1° from the neutrino direction. The source, a blazar known as TXS 0506+056 at a measured redshift of 0.34, was in a flaring state at the time with enhanced γ-ray activity in the GeV range. Follow-up observations by imaging atmospheric Cherenkov telescopes, notably the Major Atmospheric Gamma Imaging Cherenkov (MAGIC) telescopes, revealed periods where the detected γ-ray flux from the blazar reached energies up to 400 GeV. Measurements of the source have also been completed at x-ray, optical, and radio wavelengths. We have investigated models associating neutrino and γ-ray production and find that correlation of the neutrino with the flare of TXS 0506+056 is statistically significant at the level of 3 standard deviations (sigma). On the basis of the redshift of TXS 0506+056, we derive constraints for the muon-neutrino luminosity for this source and find them to be similar to the luminosity observed in γ-rays.

CONCLUSION: The energies of the γ-rays and the neutrino indicate that blazar jets may accelerate cosmic rays to at least several PeV. The observed association of a high-energy neutrino with a blazar during a period of enhanced γ-ray emission suggests that blazars may indeed be one of the long-

ON OUR WEBSITE

Read the full article at http://dx.doi.org/10.1126/science.aat1378

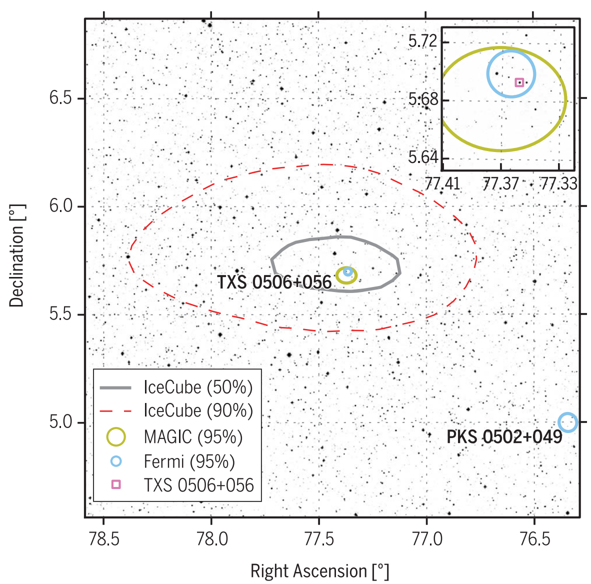

Multimessenger observations of blazar TXS 0506+056. The

NATA FOR THE R-BAND IN MAGNIFIED VIEW

Follow-up of GW170817 with PAO (neutrinos)

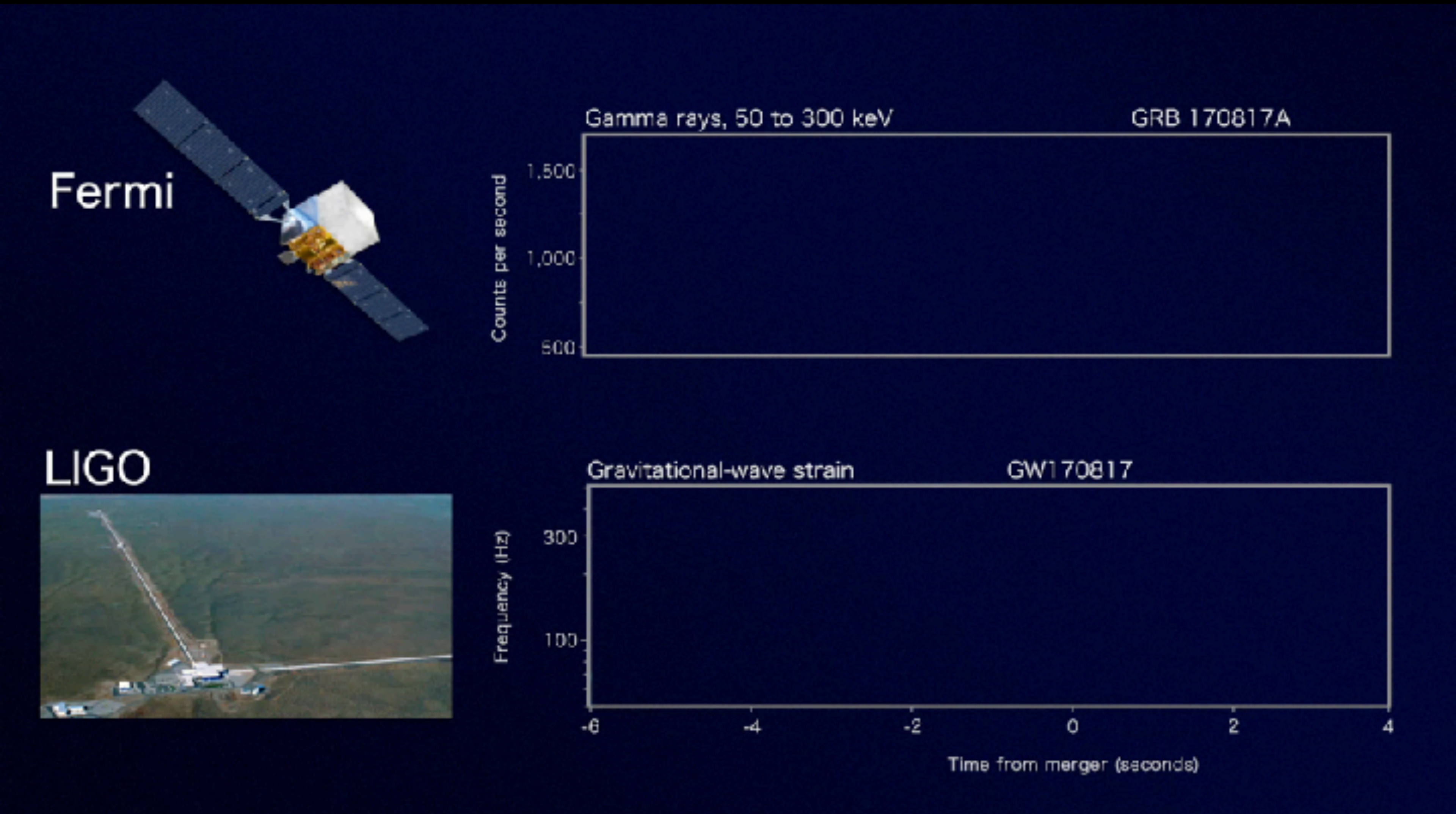

Follow-up of GW170817 with PAO (neutrinos)

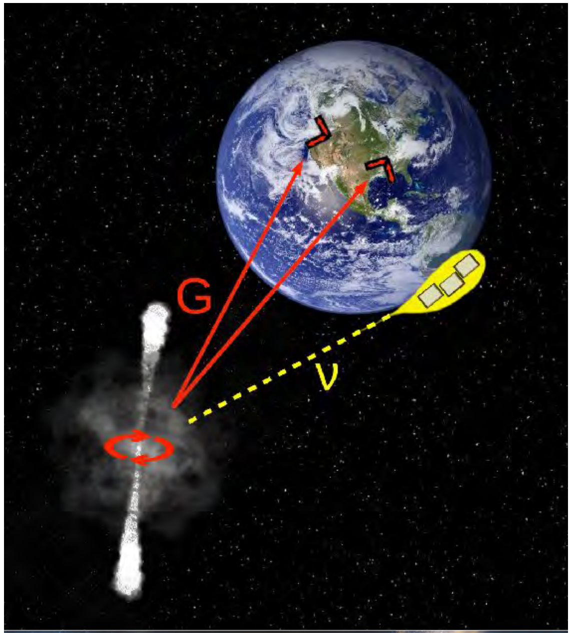

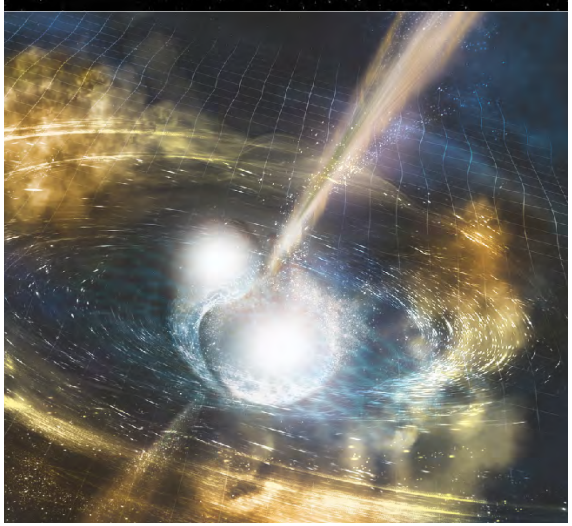

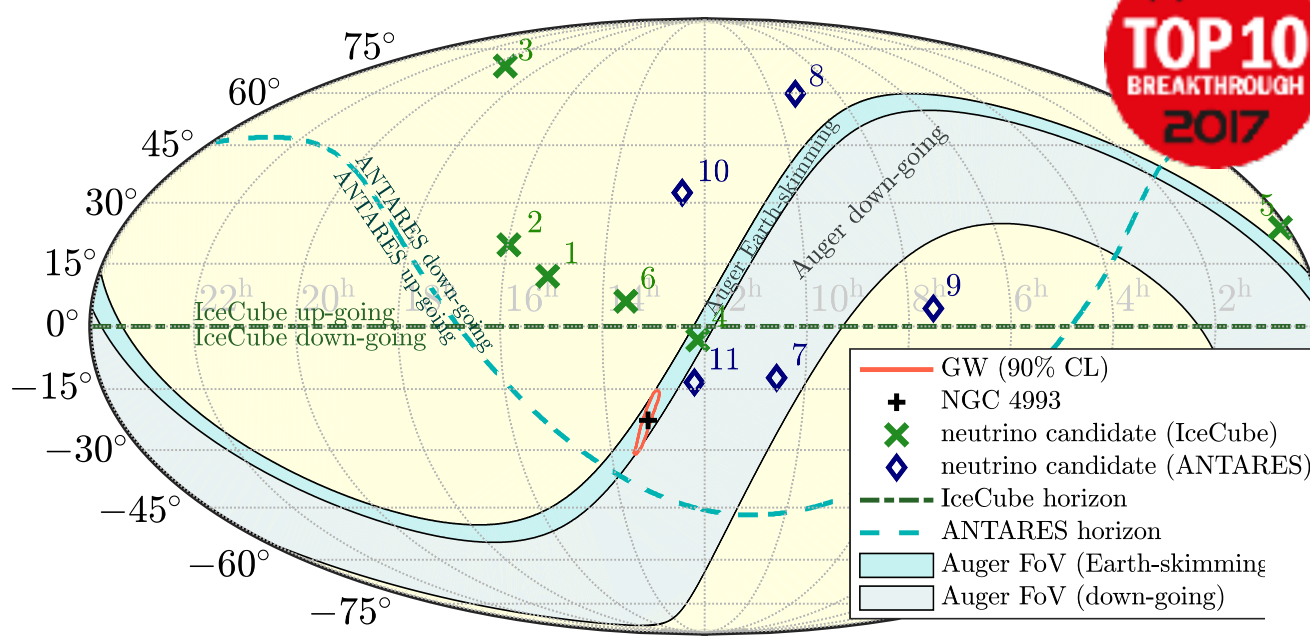

The Astrophysical Journal Letters, 848:L12 (59pp), 2017 October 20
https://doi.org/10.3847/2041-8213/aa91c9

Multi-messenger Observations of a Binary Neutron Star Merger

LIGO Scientific Collaboration and Virgo Collaboration, Fermi GBM, INTEGRAL, IceCube Collaboration, AstroSat Cadmium Zinc Telluride Imager Team, IPN Collaboration, The Insight-Hxmt Collaboration, ANTARES Collaboration, The Swift Collaboration, AGILE Team, The 1M2H Team, The Dark Energy Camera GW-EM Collaboration and the DES Collaboration, The DLT40 Collaboration, GRAWITA: GRAvitational Wave Inaf TeAm, The Fermi Large Area Telescope Collaboration, ATCA: Australia Telescope Compact Array, ASKAP: Australian SKA Pathfinder, Las Cumbres Observatory Group, OzGrav, DWF (Deeper, Wider, Faster Program), AST3, and CAASTRO Collaborations, The VINROUGE Collaboration, MASTER Collaboration, J-GEM, GROWTH, JAGWAR, Caltech-NRAO, TTU-NRAO, and NuSTAR Collaborations, Pan-STARRS, The MAXI Team, TZAC Consortium, KU Collaboration, Nordic Optical Telescope, ePESSTO, GROND, Texas Tech University, SALT Group, TOROS: Transient Robotic Observatory of the South Collaboration, The BOOTES Collaboration, MWA: Murchison Widefield Array, The CALET Collaboration, IKI-GW Follow-up Collaboration, H.E.S.S. Collaboration, LOFAR Collaboration, LWA: Long Wavelength Array, HAWC Collaboration, The Pierre Auger Collaboration, ALMA Collaboration, Euro VLBI Team, Pi of the Sky Collaboration, The Chandra Team at McGill University, DFN: Desert Fireball Network, ATLAS, High Time Resolution Universe Survey, RIMAS and RATIR, and SKA South Africa/MeerKAT
(See the end matter for the full list of authors.)

Received 2017 October 3; revised 2017 October 6; accepted 2017 October 6; published 2017 October 16

Follow-up of GW170817 with PAO (neutrinos)

The Astrophysical Journal Letters, 850:L35 (18pp), 2017 December 1
https://doi.org/10.3847/2041-8213/aa9aed

Search for High-energy Neutrinos from Binary Neutron Star Merger GW170817 with ANTARES, IceCube, and the Pierre Auger Observatory

ANTARES Collaboration, IceCube Collaboration, The Pierre Auger Collaboration, and LIGO Scientific Collaboration and Virgo Collaboration

PAO in pre-defined +/- 500 s window as sensitive as IceCube

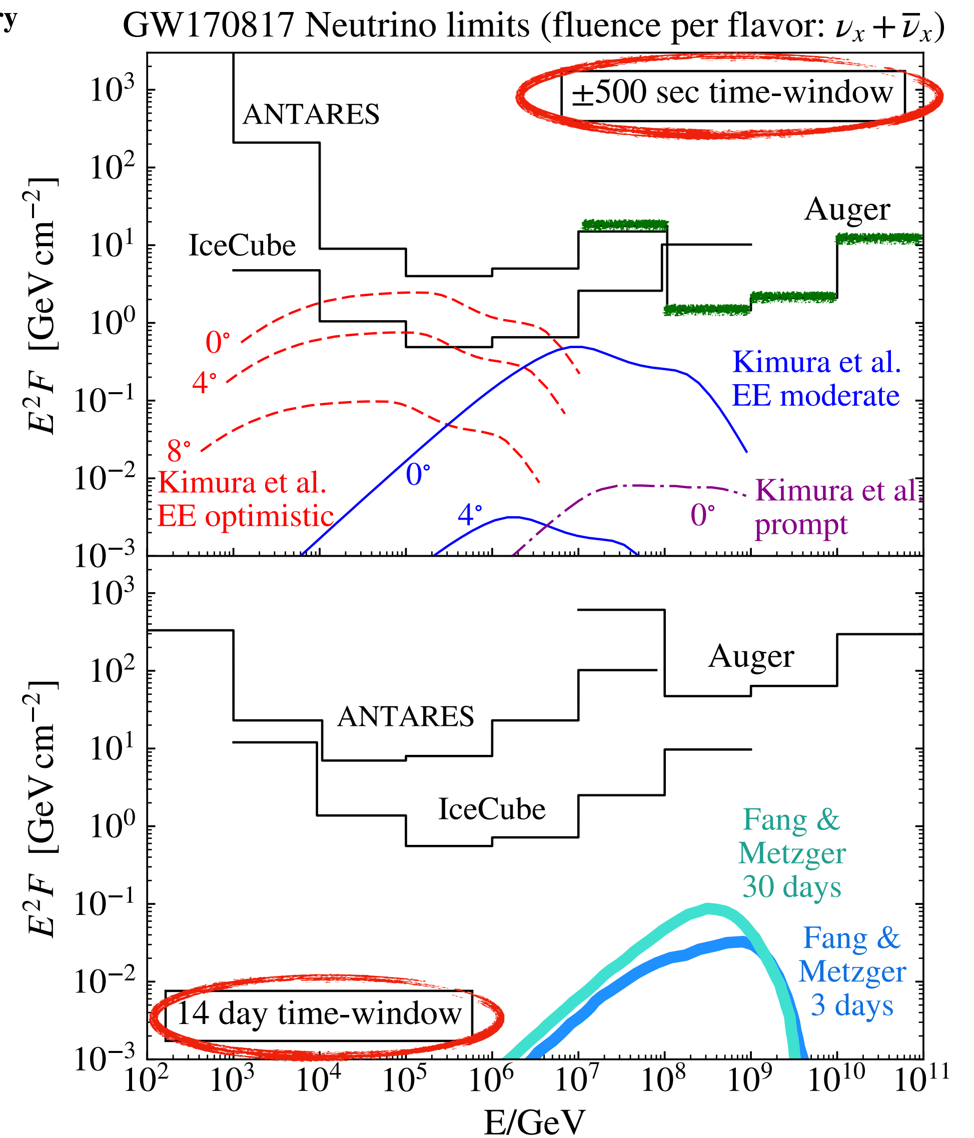

A&A 619, A71 (2018)
https://doi.org/10.1051/0004-6361/201832640

Astronomy & Astrophysics

The γ-ray spectrum of the core of Centaurus A as observed with H.E.S.S. and *Fermi*-LAT

ABSTRACT

Centaurus A (Cen A) is the nearest radio galaxy discovered as a very-high-energy (VHE; 100 GeV–100 TeV) γ-ray source by the High Energy Stereoscopic System (H.E.S.S.). It is a faint VHE γ-ray emitter, though its VHE flux exceeds both the extrapolation from early *Fermi*-LAT observations as well as expectations from a (misaligned) single-zone synchrotron-self Compton (SSC) description. The latter satisfactorily reproduces the emission from Cen A at lower energies up to a few GeV. New observations with H.E.S.S., comparable in exposure time to those previously reported, were performed and eight years of *Fermi*-LAT data were accumulated to clarify the spectral characteristics of the γ-ray emission from the core of Cen A. The results allow us for the first time to achieve the goal of constructing a representative, contemporaneous γ-ray core spectrum of Cen A over almost five orders of magnitude in energy. Advanced analysis methods, including the template fitting method, allow detection in the VHE range of the core with a statistical significance of 12σ on the basis of 213 hours of total exposure time. The spectrum in the energy range of 250 GeV–6 TeV is compatible with a power-law function with a photon index $\Gamma = 2.52 \pm 0.13_{\rm stat} \pm 0.20_{\rm sys}$. An updated *Fermi*-LAT analysis provides evidence for spectral hardening by $\Delta\Gamma \simeq 0.4 \pm 0.1$ at γ-ray energies above $2.8^{+1.0}_{-0.6}$ GeV at a level of 4.0σ. The fact that the spectrum hardens at GeV energies and extends into the VHE regime disfavour a single-zone SSC interpretation for the overall spectral energy distribution (SED) of the core and is suggestive of a new γ-ray emitting component connecting the high-energy emission above the break energy to the one observed at VHE energies. The absence of significant variability at both GeV and TeV energies does not yet allow disentanglement of the physical nature of this component, though a jet-related origin is possible and a simple two-zone SED model fit is provided to this end.

Key words. gamma rays: galaxies – radiation mechanisms: non-thermal

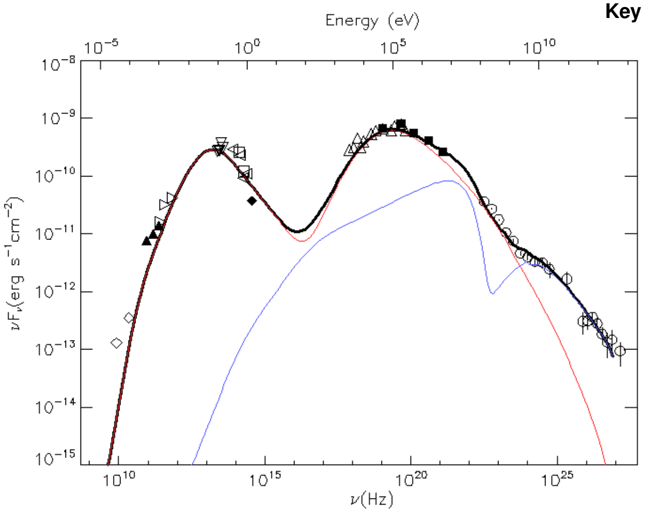

Fig. 3. SED of Cen A core with model fits as described in text. The red curve corresponds to an SSC component designed to fit the radio to sub-GeV data. The blue curve corresponds to a second SSC component added to account for the highest energy data. The black curve corresponds to the sum of the two components. SED points as derived from H.E.S.S. and *Fermi*-LAT data in this paper are shown with open circles. Observations from the radio band to the MeV γ-ray band are from TANAMI (◇), SEST (▲), JCMT (▹), MIDI (▽), NAOS/CONICA (◃), NICMOS (□), WFPC2 (♦), *Suzaku* (△), OSSE/COMPTEL (■). The acronyms are described in Appendix B.

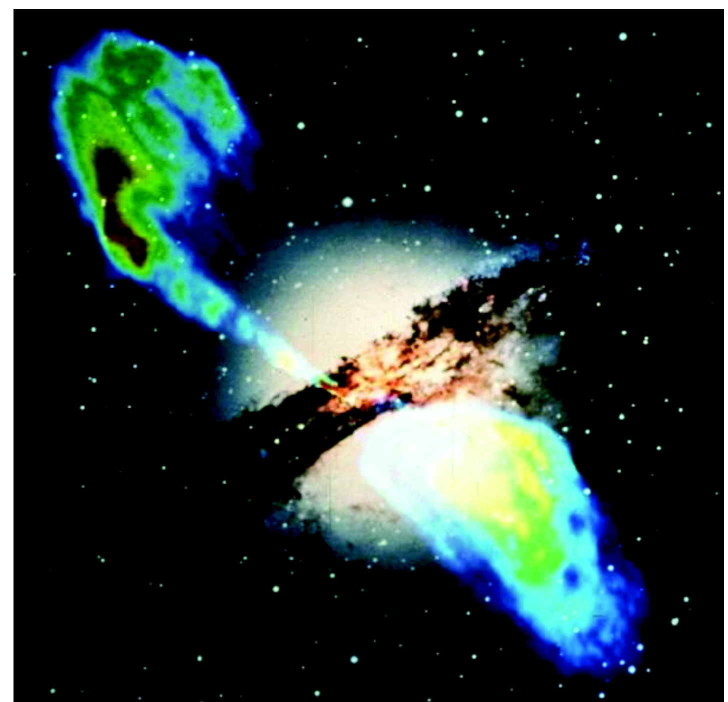

Anisotropy detected at >5.2 sigma
dipole amplitude 6.5%

COSMIC RAYS

Observation of a large-scale anisotropy in the arrival directions of cosmic rays above 8×10^{18} eV

The Pierre Auger Collaboration*†

physicsworld TOP 10 BREAKTHROUGH 2017

$E>8*10^{18}$ eV $3*10^{4}$ CRs

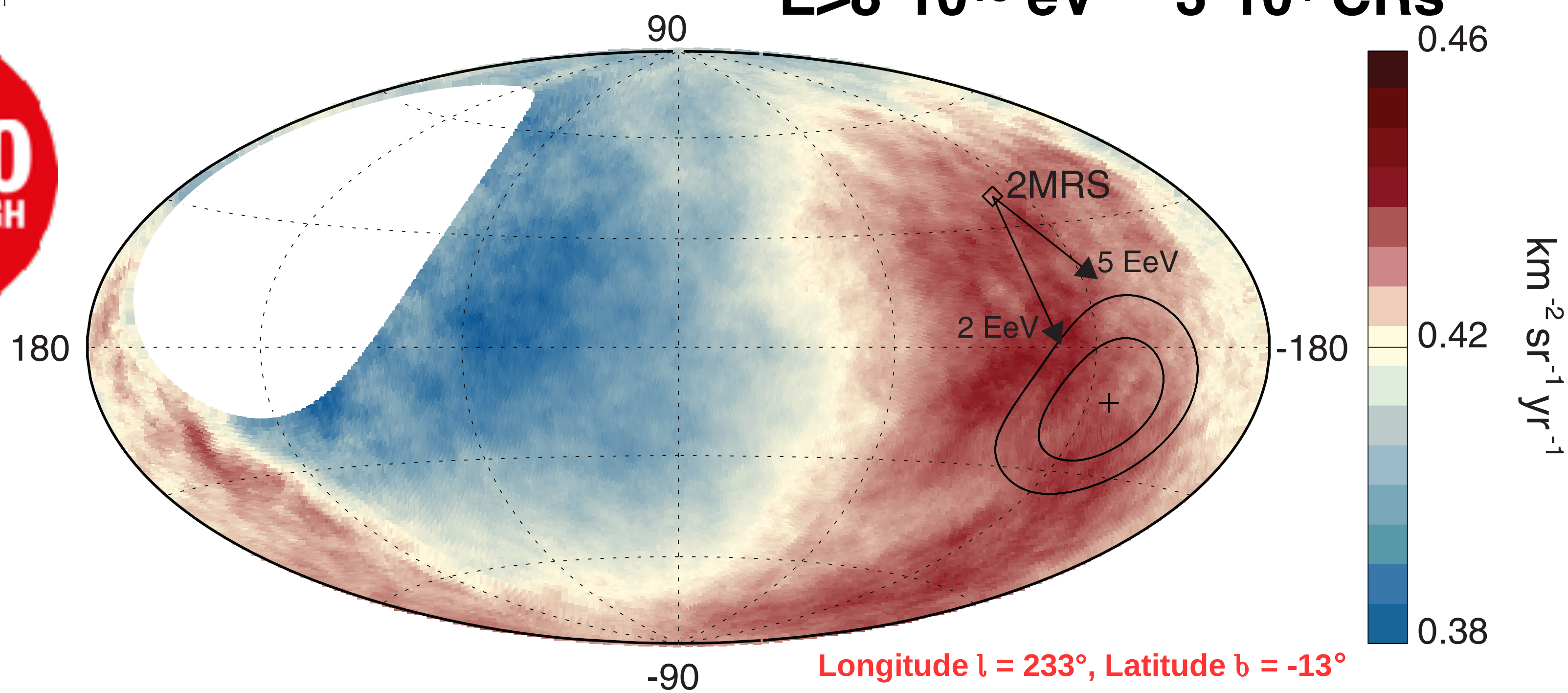

Longitude l = 233°, Latitude b = -13°

Fig. 3. Map showing the fluxes of particles in galactic coordinates. Sky map in galactic coordinates showing the cosmic-ray flux for $E \geq 8$ EeV smoothed with a 45° top-hat function. The galactic center is at the origin. The cross indicates the measured dipole direction; the contours denote the 68% and 95% confidence level regions. The dipole in the 2MRS galaxy distribution is indicated. Arrows show the deflections expected for a particular model of the galactic magnetic field (*8*) on particles with E/Z = 5 or 2 EeV.

A. Aab et al., Science 357 (2017) 1266

Astroparticle Physics

messengers from the Universe

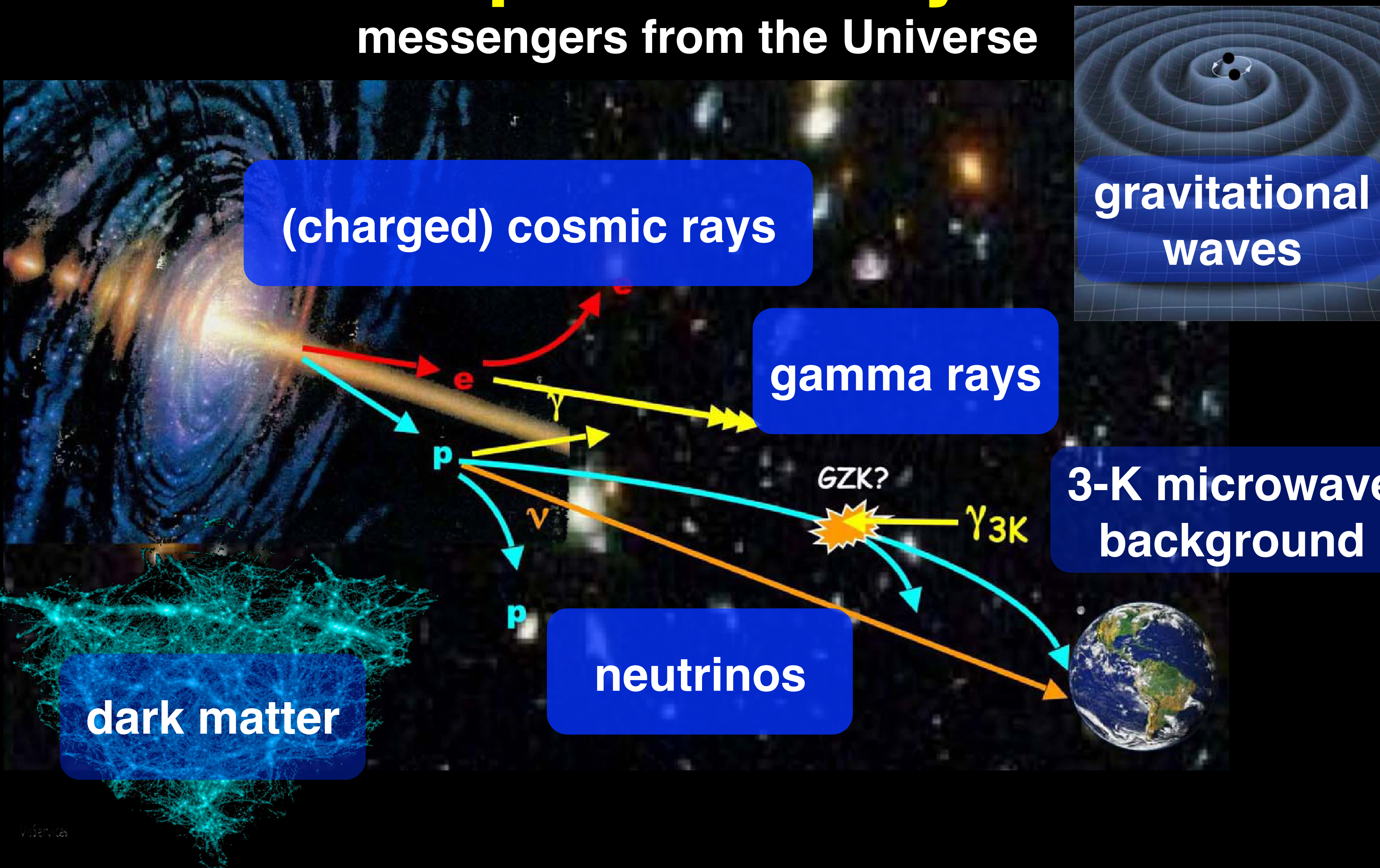

Literature

Particles & Cosmos: Stanev

Astroparticle Physics:
Tom Gaisser, Cosmic rays and particle physics
Cambridge University Press (2016)

+ primary literature (journal articles)

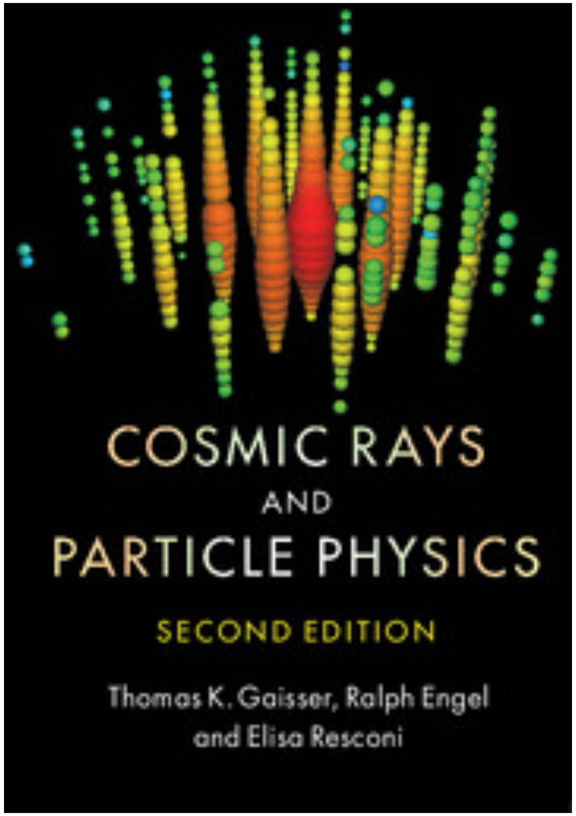

Astroparticle Physics 2023/24

1. Historical introduction - basic properties of cosmic rays
2. Hadronic interactions and accelerator data
3. Cascade equations
4. Electromagnetic cascades
5. Extensive air showers
6. Detectors for extensive air showers
7. High-energy cosmic rays and the knee in the energy spectrum of cosmic rays
8. Radio detection of extensive air showers
9. Acceleration, Astrophysical accelerators and beam dumps
10. Extragalactic propagation of cosmic rays
11. Ultra-high-energy energy cosmic rays
12. Astrophysical gamma rays and neutrinos
13. Neutrino astronomy
14. Gamma-ray astronomy

Student talks

- Students will present selected topics, based on journal publications.
- Learn how to derive information from primary literature.
- Presentation followed by discussion and questions.
- 60 min presentation, 15 min discussion
- You are expected to participate in discussions and ask questions.
- Your presentation + interaction will be part of your grade.

Student talks

- Air showers - Matthews Heitler model ____________
- Radio detection of air showers ____________
- CR anisotropy at TeV energies, IceCube/Top, HAWC ____________
- the knee in the energy spectrum of cosmic rays ____________
- Detectors for UHE CRs, Auger, TA ____________
- GZK effect and the end of the CR spectrum, Auger, TA ____________
- CR mass composition at highest energies, Auger, TA ____________
- CR anisotropy at highest energies, Auger, TA ____________
- IceCube project + results (neutrino) ____________
- KM3NeT project + results (neutrino) ____________
- H.E.S.S. project and results (gamma ray) ____________
- Fermi satellite project and results (gamma ray) ____________
- Cherenkov Telescope Array - CTA ____________
- Origin of the heavy elements from GW events ____________
- Cosmic magnetic fields ____________

lecture 1

Historical introduction

Basic properties of Cosmic Rays

Discovery of Radioactivity

Henri Becquerel

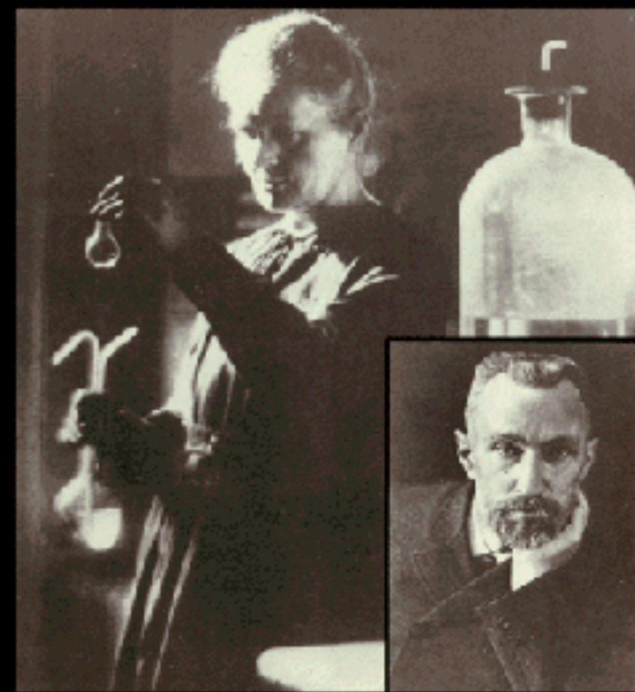

Marie & Pierre Curie

Nobel Prize 1903

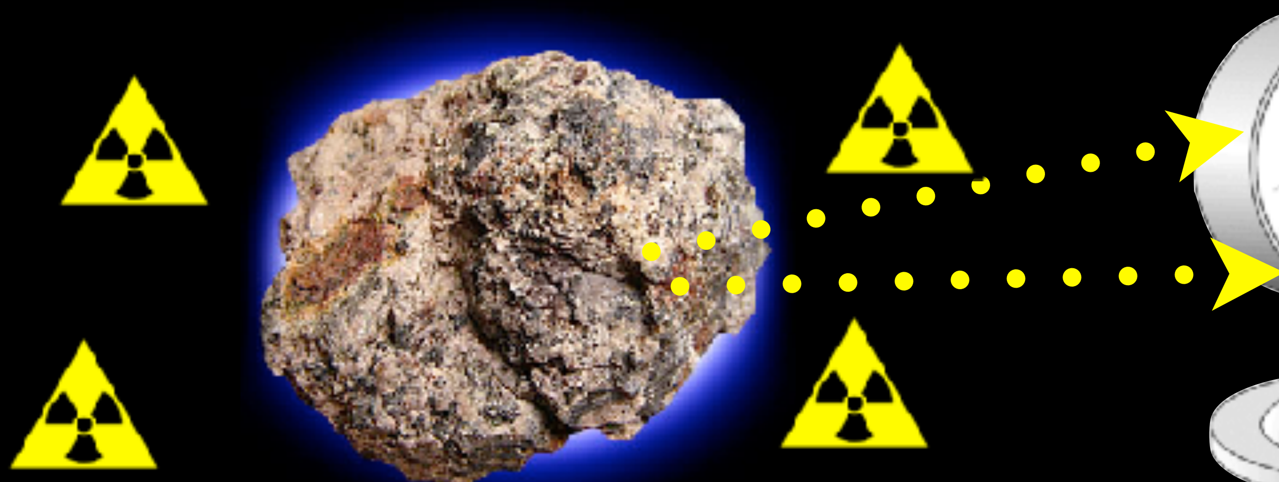

Physikalische Zeitschrift. 10. Jahrgang. No. 8. (1909) 251

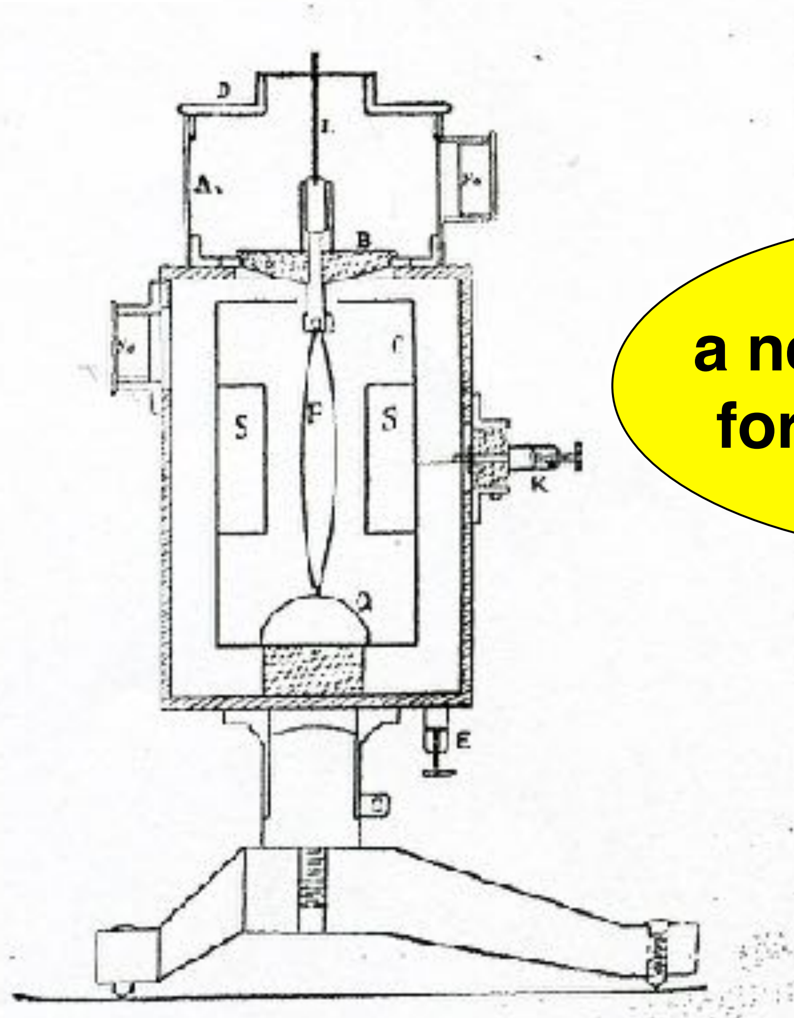

Ein neues Elektrometer für statische Ladungen.

Dritte Mitteilung[1]).

Von Th. Wulf.

a new electrometer
for static charges

Mitteilung enthält einige
her beschriebenen Appa-
öhung seiner Transport-

Sir J.J.Thomson
Nobel Prize 1906

Conduction of electricity through gases (1928):

It would be one of the romances of science if these obscure and prosaic minute leakages of electricity from well-insulated bodies should be the means by which the most fundamental problems in the evolution of the cosmos came to be investigated.

Detector used by Wilson to investigate ionization of air

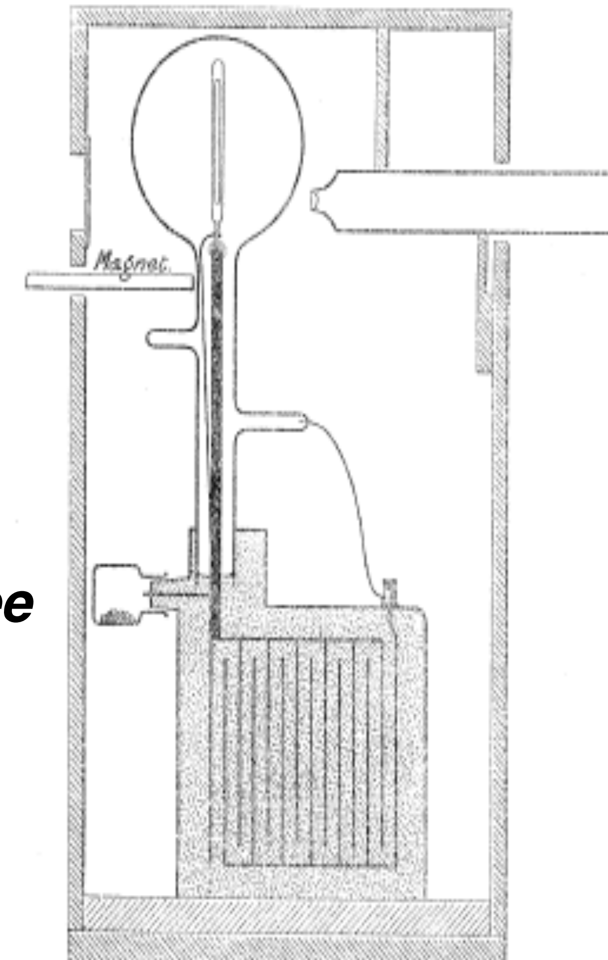

"the continuous production of ions in dust-free air could be explained as being due to radiation from sources outside our atmosphere, possibly radiation like Röntgen rays or cathode rays, but of enormously greater penetrating power"

C T R Wilson, Proc Roy Soc A 68 (1901) 151

Über den Ursprung der in der Atmosphäre vorhandenen γ-Strahlung.

Von Th. Wulf.

on the origin of gamma radiation in the atmosphere

Tabelle I.

Strahlung der Wände von Gebäuden.

Ort	Material	Alter	Strahlung Ionen pro ccm u. Sekunde
Abtei Maria Laach bei Andernach a. Rh. . .	Vulkanisch Tuff	50 Jahre	13,7
Valkenburg, Colleg, Holland-L.	Ziegelsteine	15 "	5,7
Löwen, Colleg, Belgien	Ziegelsteine	—	8,0
Namur, Colleg N. D. de la paix, Belgien . . .	Ziegelsteine	ca. 100	5,7
Wynandsrade Kasteel, Holland	Ziegelsteine	200 Jahre	0,0

Nur in dem alten holländischen Kasteel Wynandsrade, vor fast 200 Jahren aus Ziegelsteinen erbaut, zeigte sich kein Unterschied in der Strahlung im Zimmer und im Freien. — Am stärksten war die Strahlung in Maria Laach in einem

Man kann den Inhalt dieser Arbeit kurz so zusammenfassen. Es wird über Versuche berichtet, welche beweisen, daß an dem Beobachtungsort die durchdringende Strahlung von primär radioaktiven Substanzen verursacht wird, welche in den obersten Erdschichten liegen, bis etwa 1 m unter der Oberfläche.

Wenn ein Teil der Strahlung aus der Atmosphäre stammt, so ist er doch so klein, daß er sich mit den gebrauchten Mitteln nicht nachweisen ließ.

Die zeitlichen S … ankungen in der γ-Strahlun … eben … de … ie …

the radiation originates from the soil
maybe a small contribution from the atmosphere

~1910

Theodor Wulf

1909: Soddy & Russel: attenuation of gamma rays follows an exponential law

$$I = I_0 e^{-\mu L}$$

Discovery of Cosmic Rays

Viktor Franz Hess 7. August 1912

Early cosmic-ray work published in German

Jörg R. Hörandel

Citation: AIP Conf. Proc. **1516**, 52 (2013); doi: 10.1063/1.4792540

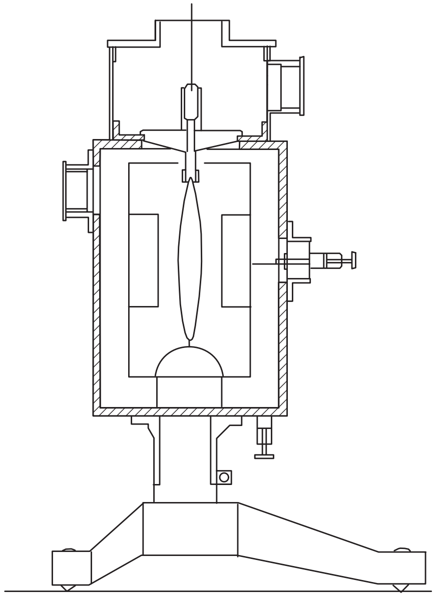

FIGURE 1. *Left*: Electrometer after Th. Wulf [5]. *Right*: Two grandsons of V.F. Hess revealing a plaque to commemorate the discovery of cosmic rays on August 7th, 2012, close to the presumed landing site of V.F. Hess in Pieskow close to Berlin. It reads: "To commemorate the discovery of cosmic rays. On 7 August 1912 landed the Austrian physicist Victor F. Hess with a hydrogen balloon close to Pieskow. On the journey from Lower-Bohemia he reached an altitude of 5300 m and he proved the existence of a penetrating, ionizing radiation from outer space. For the discovery of cosmic rays V.F. Hess has been awarded the Nobel Prize in Physics in 1936. The participants of the symposium '100 years cosmic rays', Bad Saarow-Pieskow, 7 August 2012".

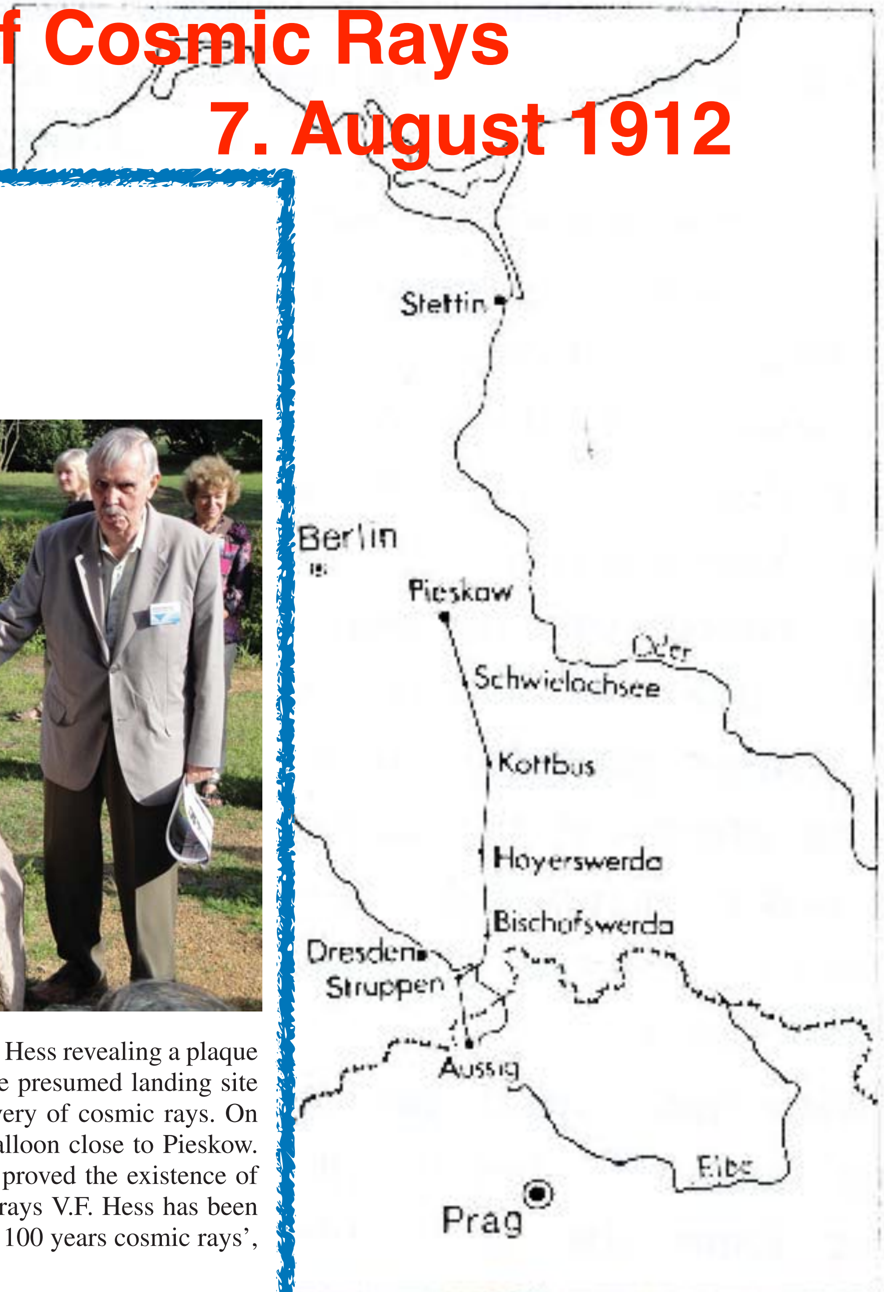

Aeronautisches Gelände im Wiener Prater, vo
seine ersten Freiballon-Forschungsfahrten u
schichtliche Mu

Hess on

Route des Entdeckungsfluges der kosmischen Strahlung.

Aus der Abteilung für Geophysik, Meteorologie und Erdmagnetismus:

Viktor F. Hess (Wien), Über Beobachtungen der durchdringenden Strahlung bei sieben Freiballonfahrten.

on the observation of the penetrating radiation during 7 balloon campaigns

Im Vorjahre habe ich bereits Gelegenheit gehabt, zwei Ballonfahrten zur Erforschung der durchdringenden Strahlung zu unterneh-

7. Fahrt (7. August 1912).

Ballon: „Böhmen" (1680 cbm Wasserstoff). Führer: Hauptmann W. Hoffory.
Meteorolog. Beobachter: E. Wolf. Luftelektr. Beobachter: V. F. Hess.

hydrogen!

altitude

intensity

		Mittlere Höhe		Beobachtete Strahlung				Temp.	Relat. Feucht. Proz.
		absolut	relativ m	Apparat 1 q_1	Apparat 2 q_2	Apparat 3 q_3	reduz. q_3		
1	$15^h\,15$—$16^h\,15$	156	0	17,3	12,9	—	—	—	—
2	$16^h\,15$—$17^h\,15$	156	0	15,9	11,0	18,4	18,4	$1\frac{1}{2}$ Tag vor dem Aufstiege (in Wien)	
3	$17^h\,15$—$18^h\,15$	156	0	15,8	11,2	[illegible]	17,5		
4	[illegible]	1700	1400	15,8	14,4	[illegible]	[illegible]	$+6,4^0$	60
[illegible]	[illegible]	2750	2500	17,3	[illegible]	[illegible]	[illegible]	$+1,4^0$	41
[illegible]	[illegible]	3850	3600	19,8	[illegible]	[illegible]	[illegible]	$-6,8^0$	64
7	[illegible]	4800	4700	40,7	[illegible]	[illegible]	[illegible]	$-9,8^0$	40
		(4400–[illegible])					—		
8	$10^h\,45$—$11^h\,15$	4400	4200	28,1	22,7	—	—	—	—
9	$11^h\,15$—$11^h\,45$	1300	1200	(9,7)	11,5	—	—	—	—
10	$11^h\,45$—$12^h\,10$	250	150	11,9	10,7	—	—	$+16,0^0$	68
11	$12^h\,25$—$13^h\,12$	140	0	15,0	11,6	—	—	(nach der Landung in Pieskow, Brandenburg)	

wurde.

Elektrometers gesetzter Zinkstift von

Aus der Abteilung für Geophysik, Meteorologie und Erdmagnetismus:

Viktor F. Hess (Wien), Über Beobachtungen der durchdringenden Strahlung bei sieben

V.F. Hess in 1936–37, on the occasion of Nobel prize.

Nobel Prize 1936

erweitertes Beobachtungsmaterial wurde.

der Atmosphäre zurückzuführen.

Die Ergebnisse der vorliegenden Beobachtungen scheinen am ehesten durch die Annahme erklärt werden zu können, daß eine Strahlung von sehr hoher Durchdringungskraft von oben her in unsere Atmosphäre eindringt, und auch noch in deren untersten Schichten einen Teil der in geschlossenen Gefäßen beobachteten Ionisation hervorruft. Die Intensität dieser Strahlung scheint zeitlichen Schwankungen unterworfen zu sein, welche bei einstündigen Ablesungsintervallen noch erkennbar sind. Da ich im Ballon weder bei Nacht noch bei einer Sonnenfinsternis eine Verringerung der Strahlung fand, so kann man wohl kaum die Sonne als Ursache dieser hypothetischen Strahlung ansehen, wenigstens solange man nur an eine direkte γ-Strahlung mit geradliniger Fortpflanzung denkt.

Daß die Zunahme der Strahlung erst jenseits 3000 m so stark merklich wird, ist nicht

Absorption in the atmosphere

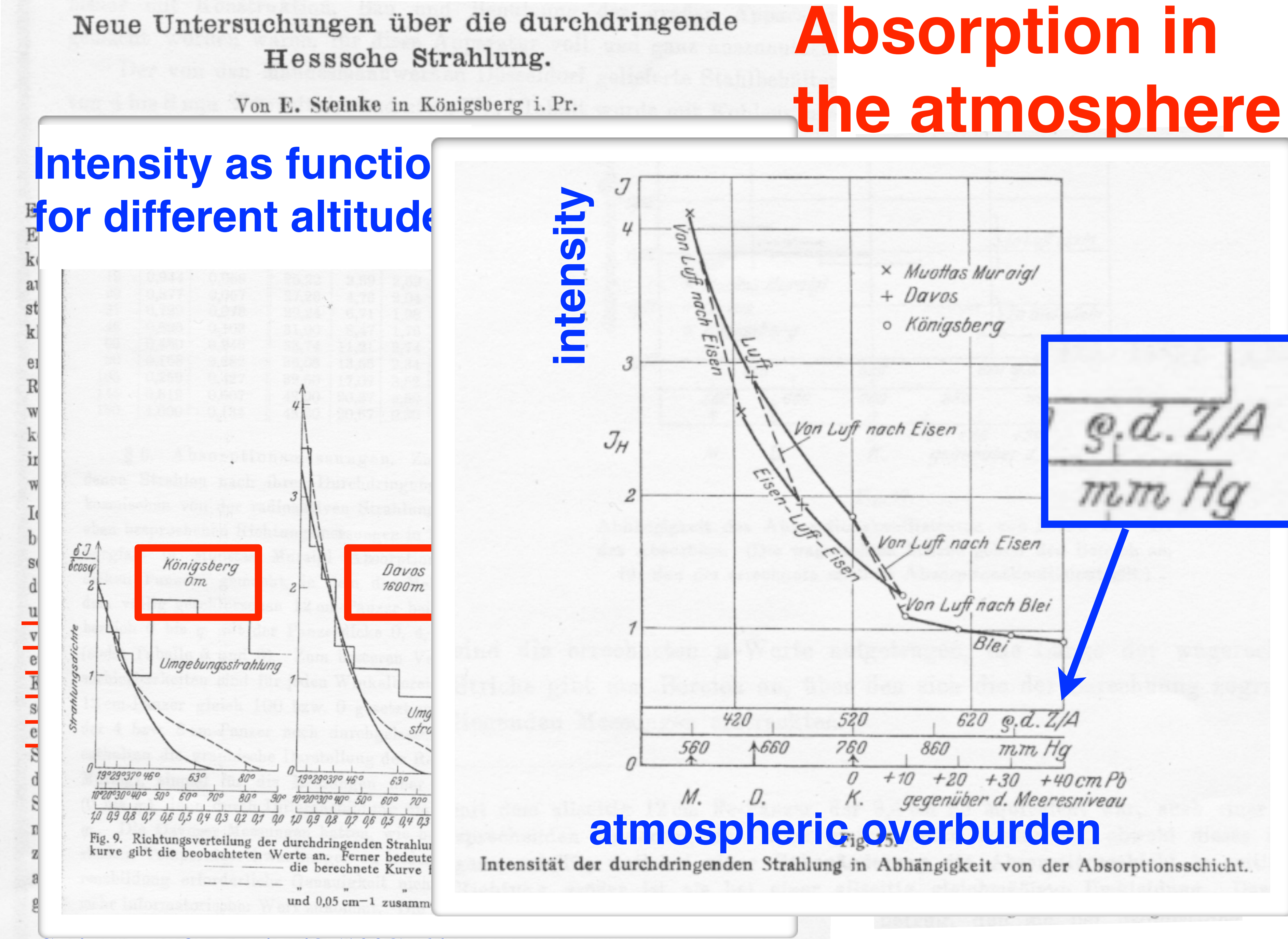

E. Steinke, Z. f. Physik 48 (1928) 647

Barometric effect

Über Schwankungen und Barometereffekt der kosmischen Ultrastrahlung im Meeresniveau.

Von **E. Steinke** in Königsberg i. Pr.

Während d
stunden au
Dicke, teil
material e
teils perio
Schwanku
dische Sch
mäßige In
endlich pe
während d
kungen, i
für das Au
zeitlichen

with
ect

on of

si

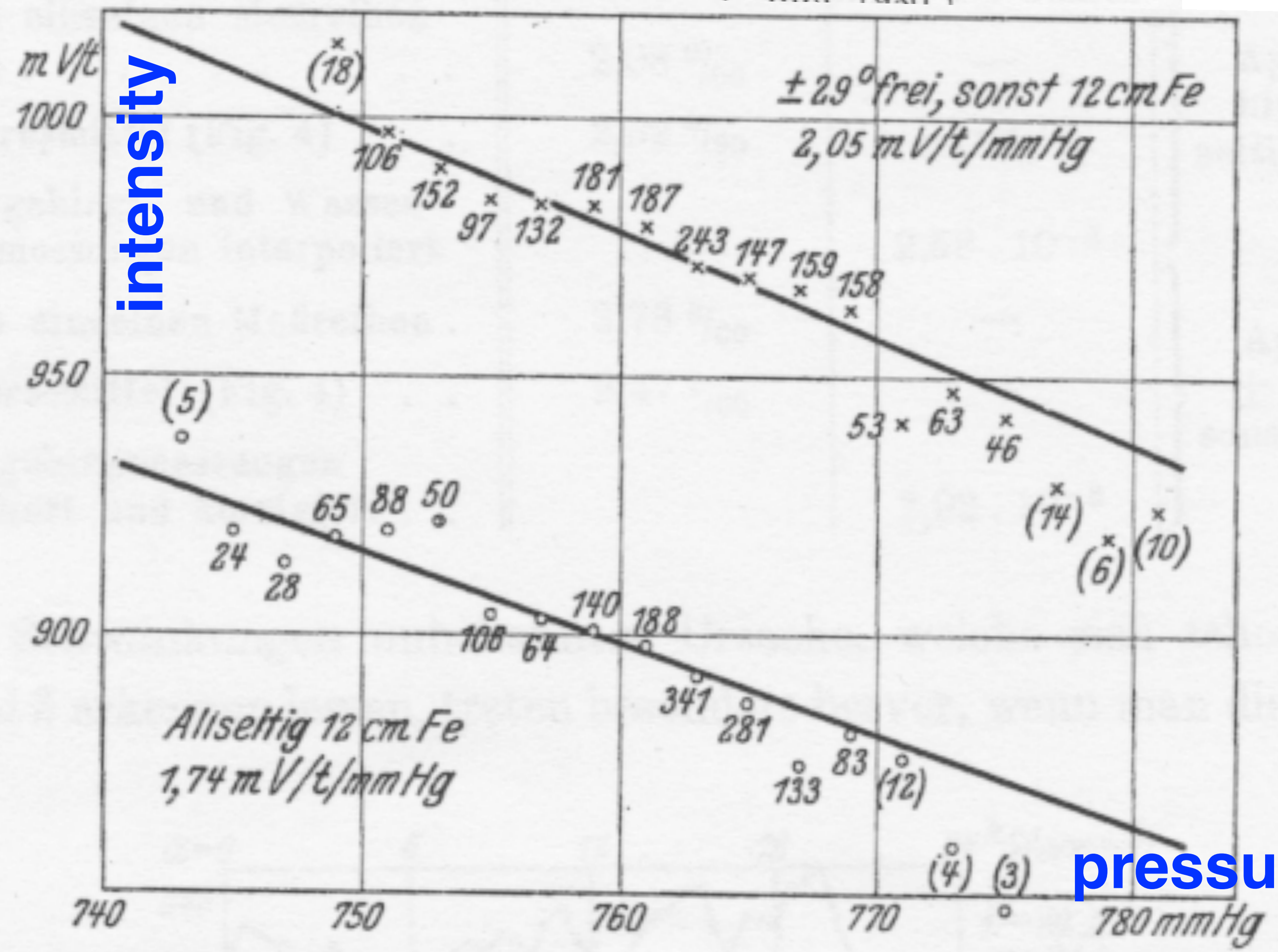

Fig. 4. Zusammenhang zwischen Barometerstand und Ionisation (Jahresmittel der Stundenwerte; die Zahlen geben die Anzahl der Stundenwerte an).

E. Steinke, Z. f. Physik 64 (1930) 48

Absorption in Lake Constance 1928

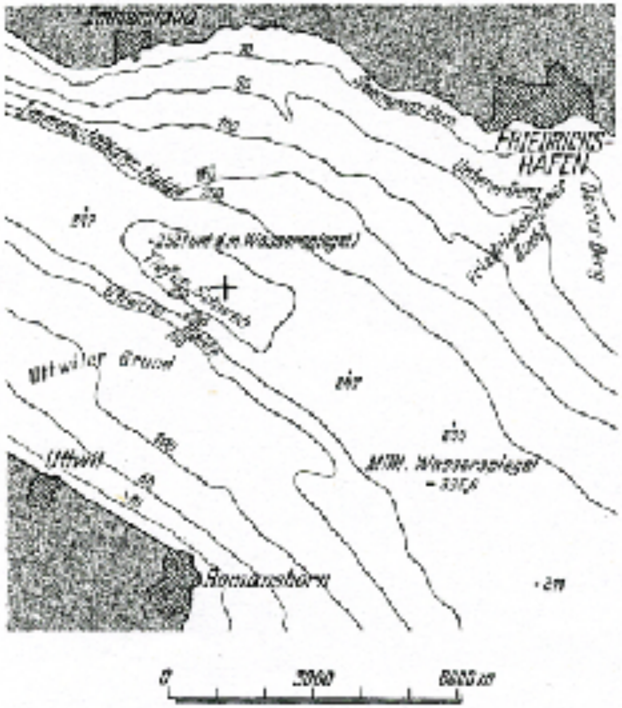

Fig. 5.

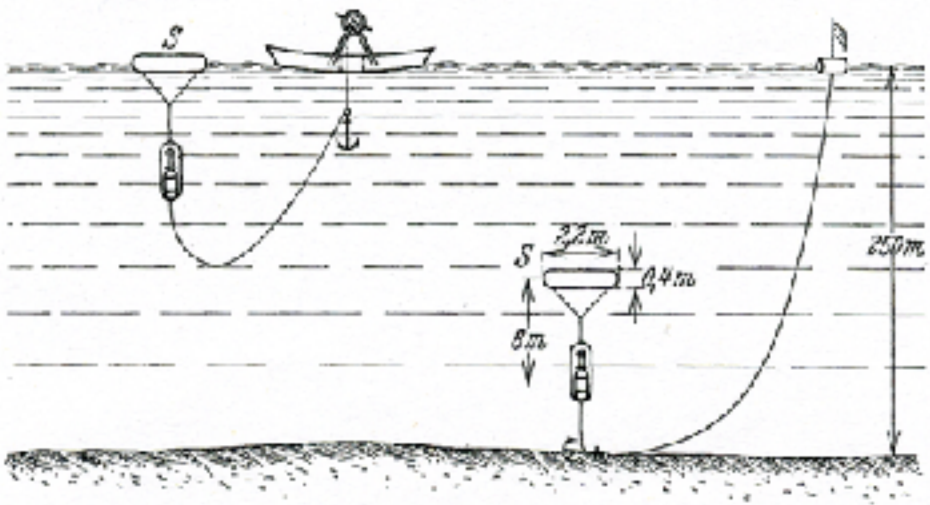

Fig. 6. Die „schwebende" Verankerung des Apparates.

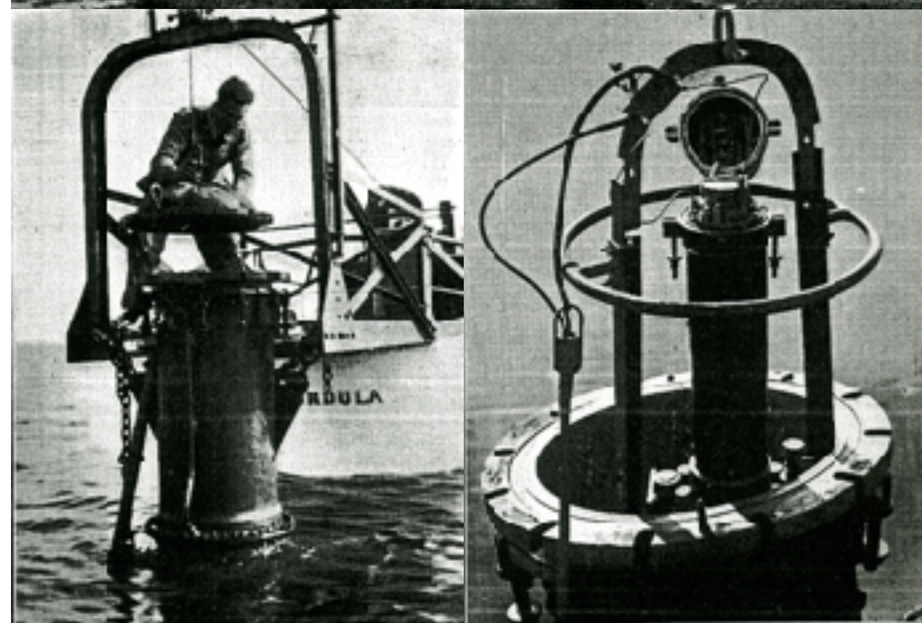

E. Regener Phys. Z. 34 (1933) 306

Absorption in Lake Constance 1928

Ionization chamber with electrometer read-out automatic each hour, up to 8 days

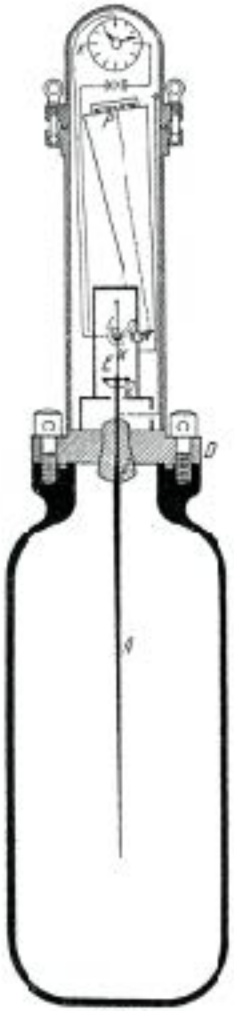

Fig 1.
Aufbau des wasserdichten Registrierapparates.

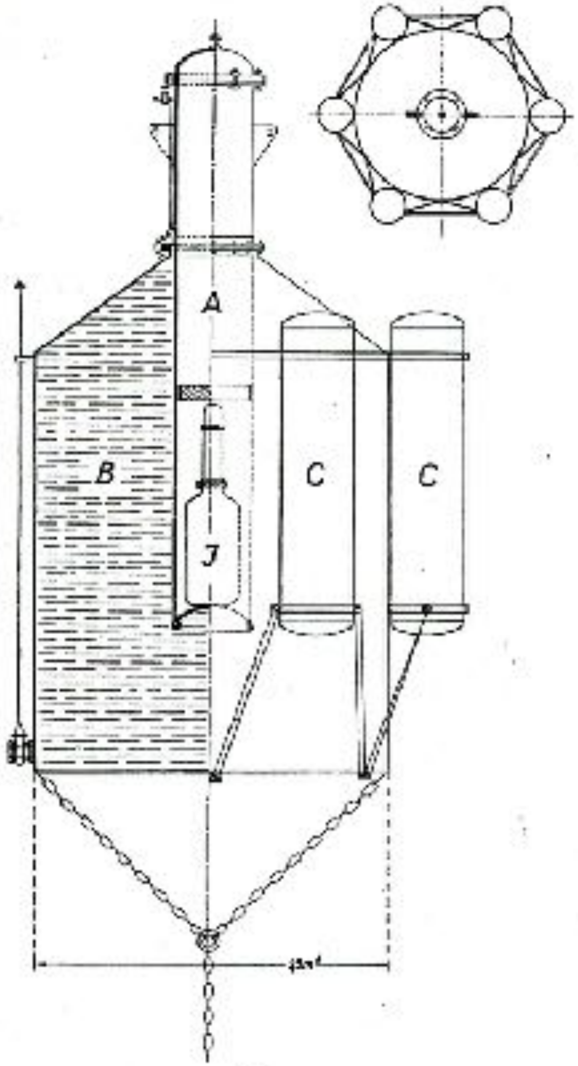

Fig. 1.

E. Regener Phys. Z. 34 (1933) 306

Absorption in Lake Constance 1928

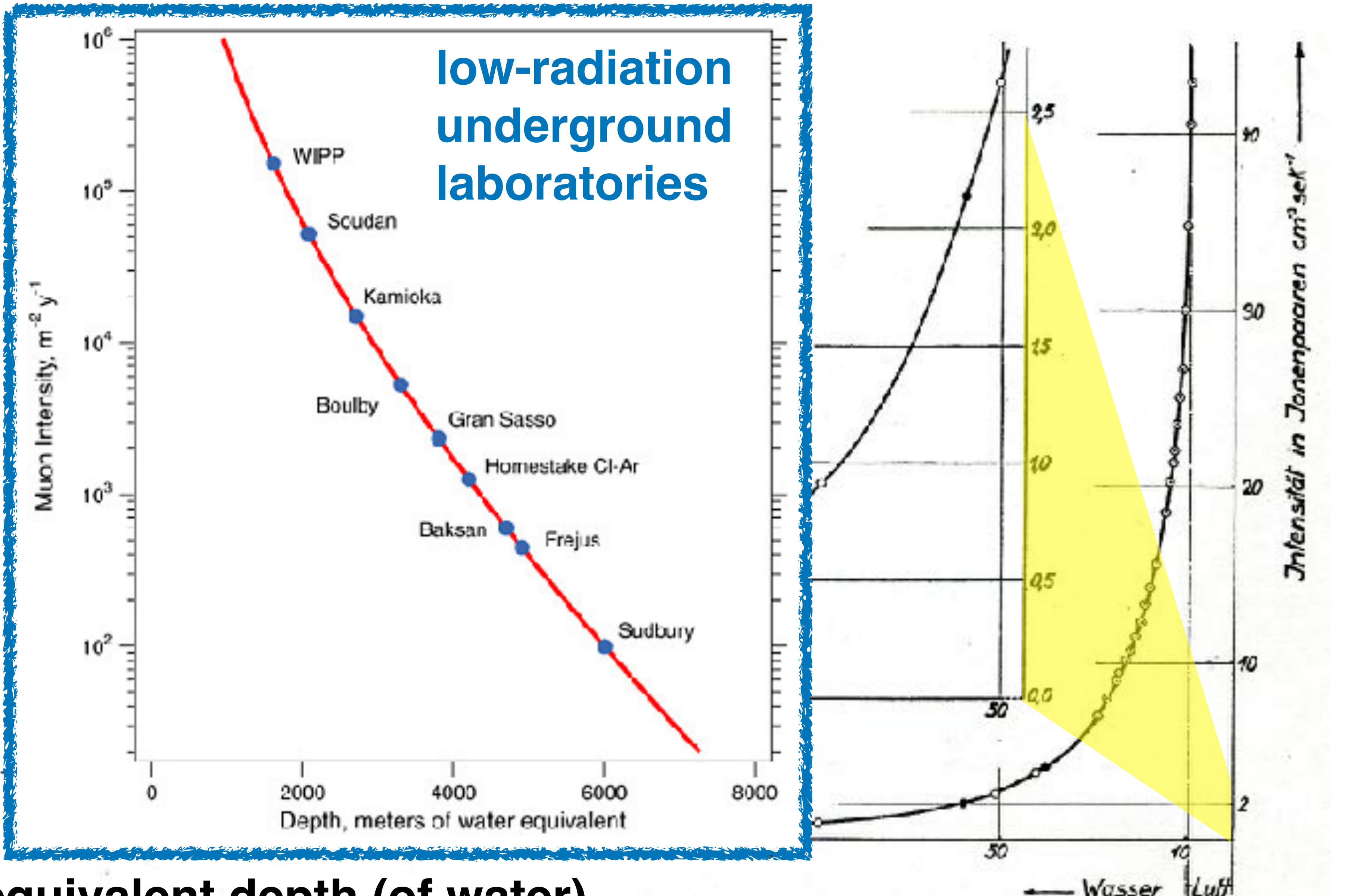

Fig. 6.

equivalent depth (of water) from top of the atmosphere

E. Regener Phys. Z. 34 (1933) 306

Three pioneers of Cosmic Ray research
Regener demonstrates his balloon electrometer
(Immenstaad/Lake Constance, August 1932).

Kolhörster
A new electrometer

derung zu danken, die ...

von Anh...

„We...

gebracht hat ...

1) Oskar Taussig ... ro-aeronautic research work (The First World Po... onference, London 1924), vgl. auch „Elektrotechnik ... Maschinenbau", Zeitschrift des Elektrotechnischen V... in Wien, Heft 46, 1924.

(E... gangen 28. August 1925.)

Ein neues Fadenelektrometer.

Von Werner Kolhörster.

Zu Messungen der durchdringenden Strahlung hatte ich für meine neuen Strahlungsapparate ein Fadenelektrometer konstruiert[1]), das ohne die bei derartigen Instrumenten notwendige Temperaturkompensation arbeitet. Da es sich auch für andere elektrostatische Messungen seiner Vorzüge und allgemeinen Verwendbarkeit halber als geeignet erwies, so seien hier einige Angaben über die Instrumente[2]) gemacht.

Prinzip: Als Gegenkraft gegen die elektrostatischen Abstoßungskräfte dient allein die Biegungselastizität der feinen Quarzfäden, die die Form vertikal stehender, frei tragender Schlingen haben und deren Enden in einigen Millimetern Abstand voneinander an einem Metallblech befestigt sind, das in den Isolator eingesetzt wird. Entsprechend den Ein- und Zweifadenelektrometern kann man Systeme mit einer oder zwei kongruenten Schlingen verwenden, die von einem Mikroskop mit Okularmikrometer am Scheitel der Schlingen abgelesen werden. Lädt man das System, so tritt keine merkliche Formänderung der Schlingen ein, diese bewegen sich vielmehr in der Horizon-

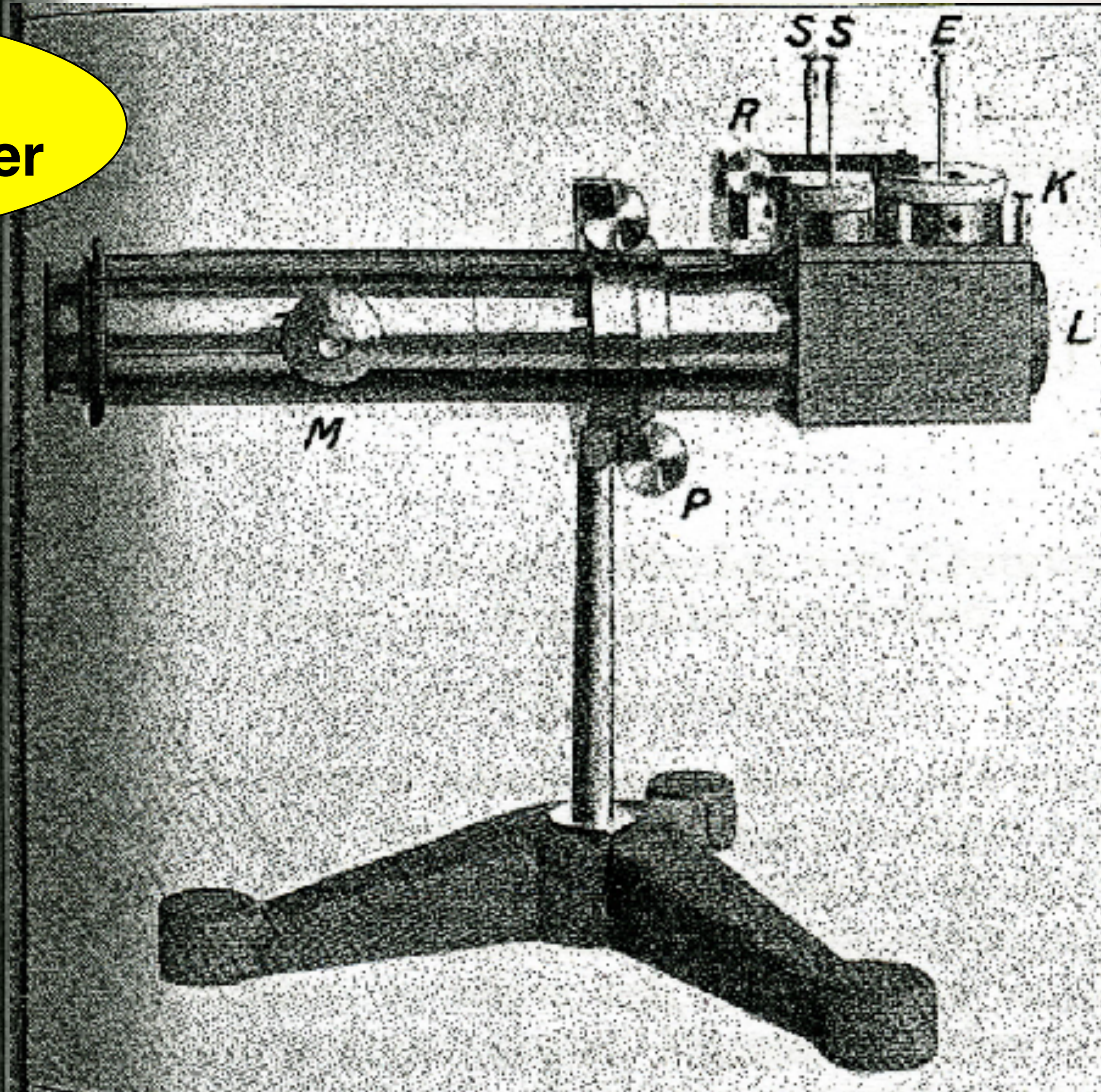

bildung zu verändern. Eine feinere Änderung läßt sich durch Verschwenken der Schneiden erzielen, die um die längere Rechteckseite drehbar, mehr oder weniger den Fäden genähert

Kohlhörster - balloon flight 13. May 1934

Abb.12 Vor dem Aufstieg

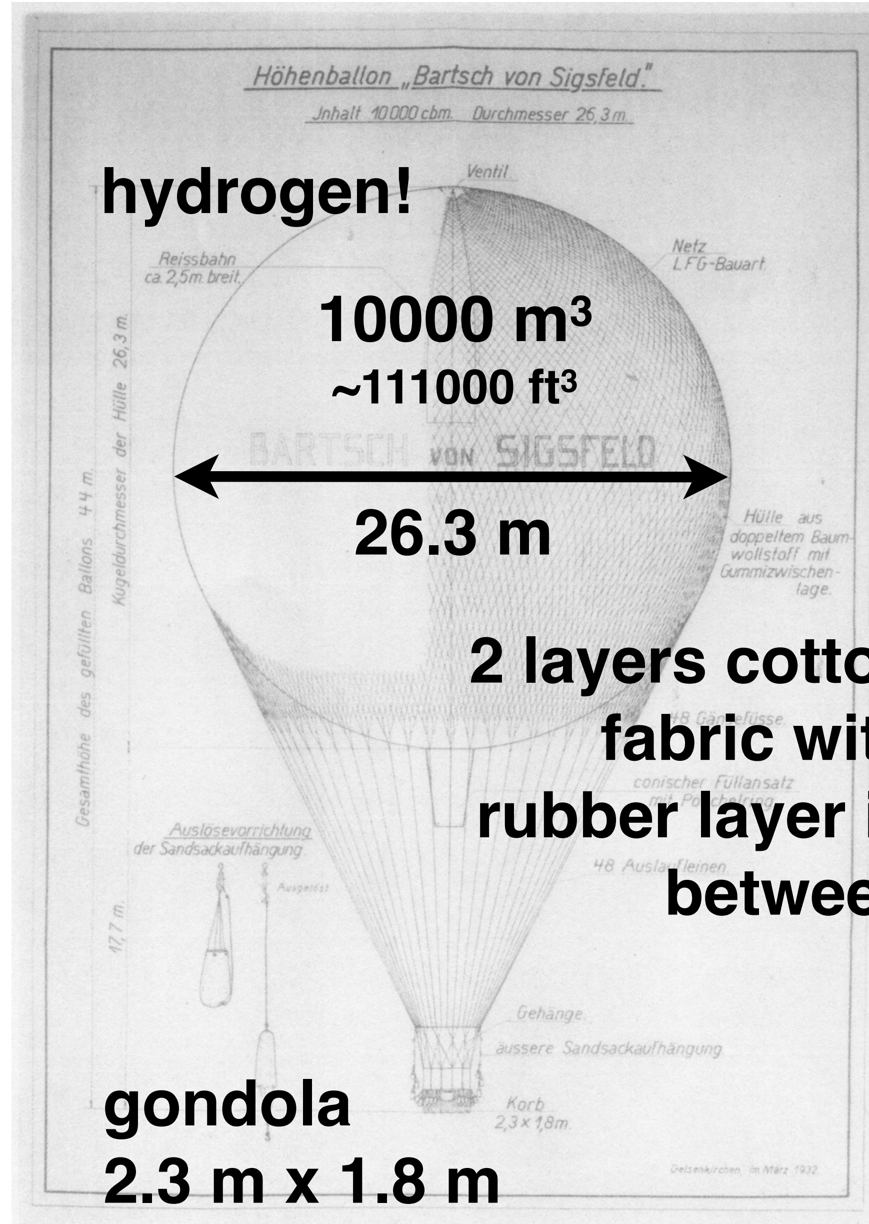

Abb.19 Höhenballon "Bartsch von Sigsfeld"
Füllung am 13.5.34 rd. 4400 m³.

Kohlhörster - balloon flight 13. May 1934

Dr. Schrenk

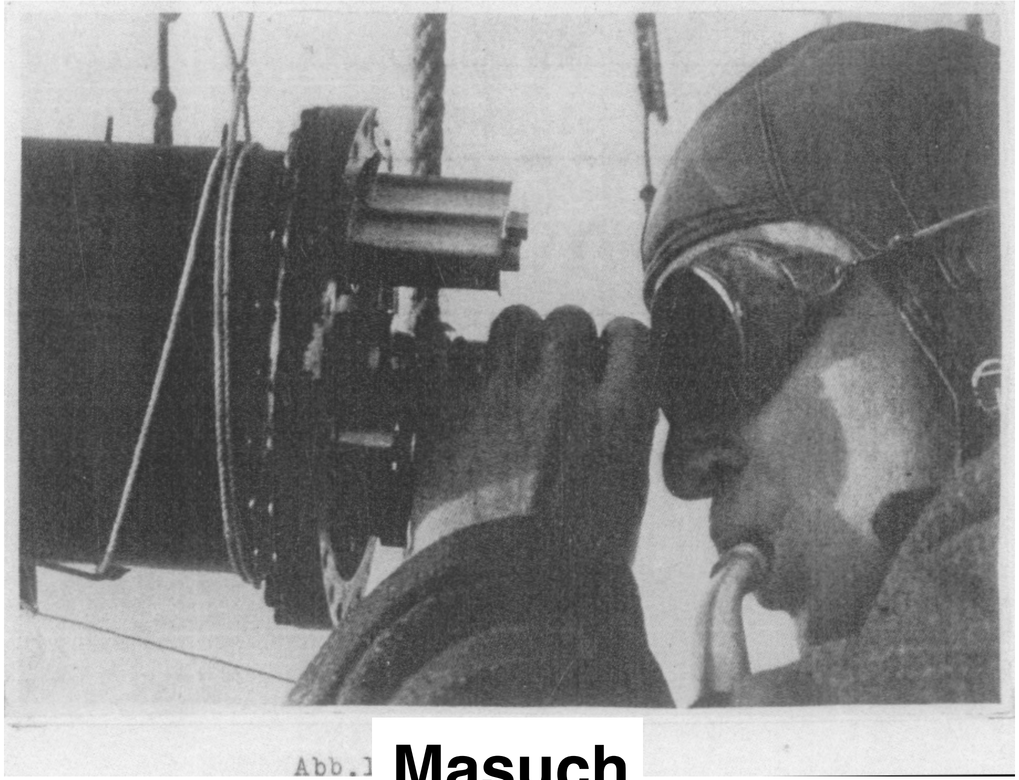

Masuch

Measurements of the cosmic-ray intensity (Höhenstrahlung) up to 12000 m

Fig. 19. Regener recovering a balloon payload from a farm house.

3) Die Firma Gebr. Junghans, Schramberg, hat uns freundlicherweise diese schönen Zählwerke hergestellt.

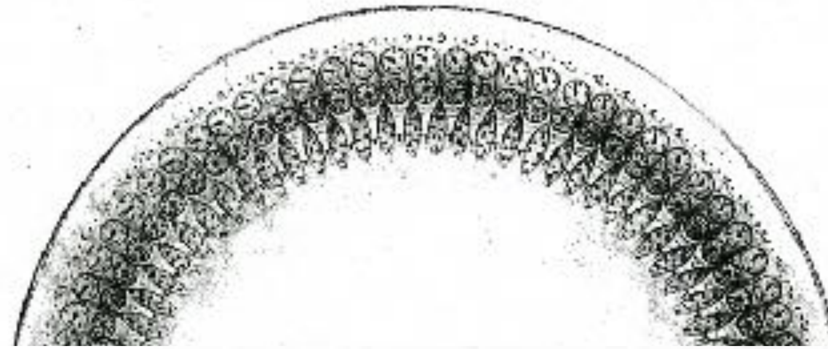

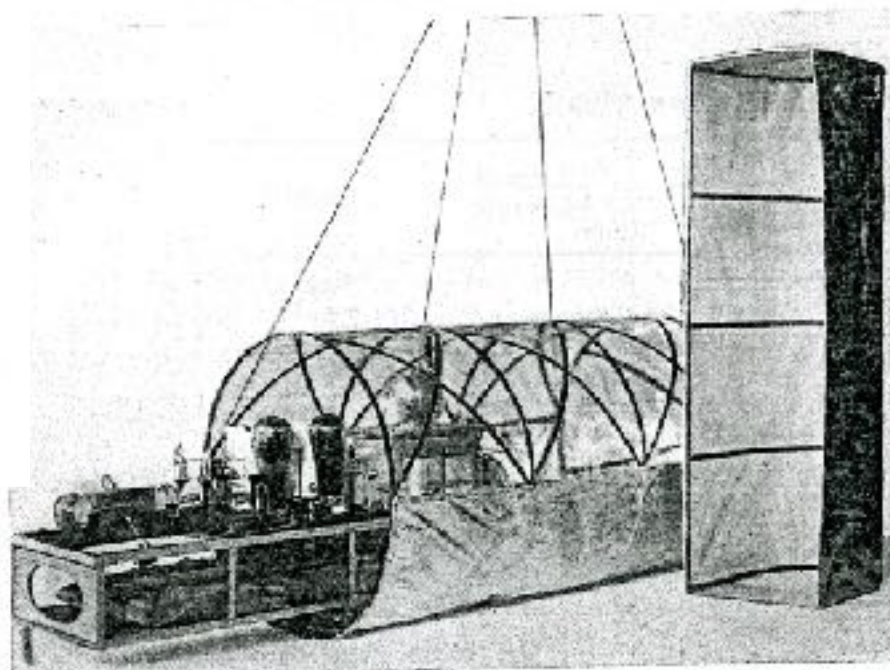

Fig. 6. Registrierapparat mit Schutzgondel.

coincidence technique

(Mitteilung aus der Physikalisch-Technischen Reichsanstalt.)

Das Wesen der Höhenstrahlung.

Von W. Bothe und W. Kolhörster.

Mit 8 Abbildungen. (Eingegangen am 18. Juni 1929.)

the nature of the „high-altitude radiation“

... ist die ... Höhen- ... hatten

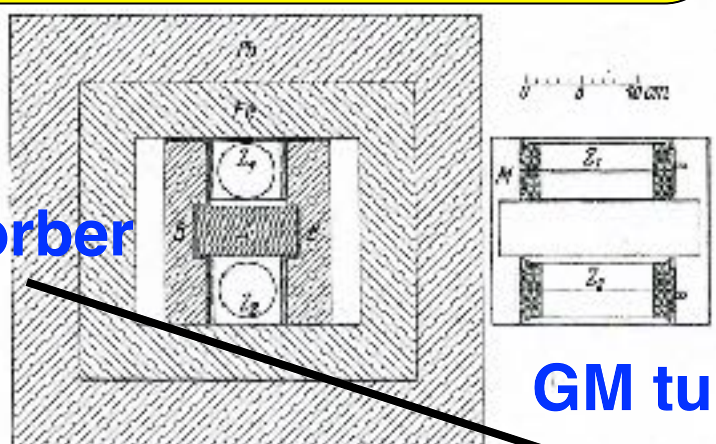

Fig. 1.

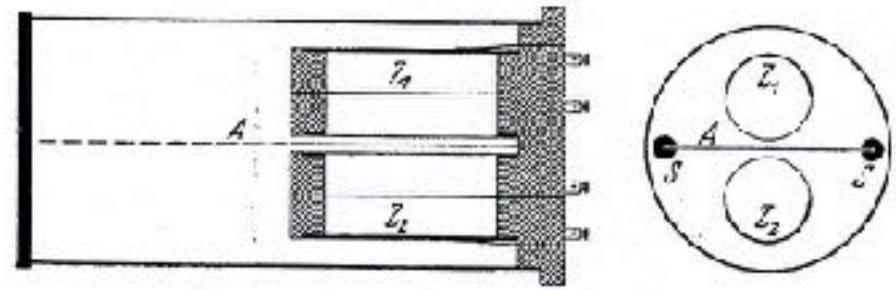

Fig. 2.

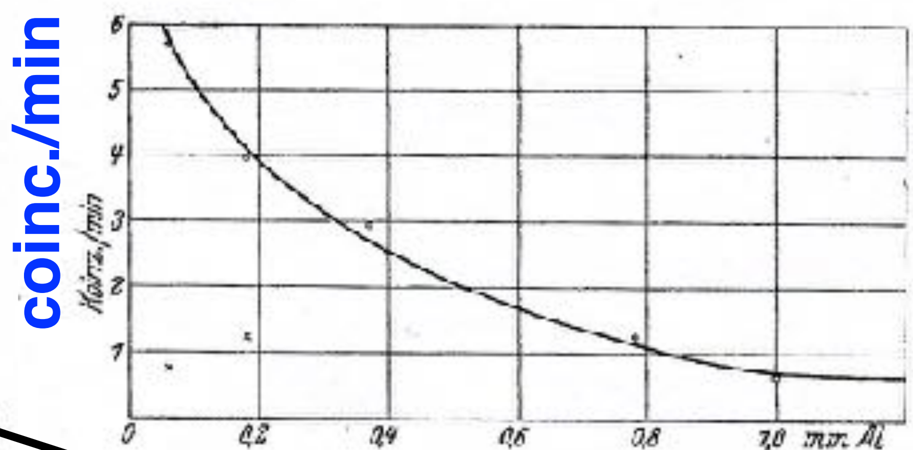

Fig. 3.

innen 5 cm Durchmesser und 10 cm Länge; sie waren anfangs aus 1 mm starkem Messing, später aus 1 mm starkem Zink hergestellt und an den Enden mit Ebonitstopfen verschlossen, welche die zentralen Drähte trugen. Diese waren nach dem Verfahren von Geiger und Müller präpariert. Die Zählrohre waren mit trockener, kohlensäure- und emanationsfreier Luft von 4 bis 6 cm Hg-Druck gefüllt. Sie wurden durch ein Messinggestell *M* getragen, welches so eingerichtet war, daß Absorberschichten bis zu 45 mm Dicke zwischen die Zählrohre gebracht werden konnten. Seitlich waren die Rohre durch Bleiklötze *B B* geschützt; diese hatten Nuten, in welche der Absorber eingriff. Die Dicke dieser Seitenblenden war stets so bemessen, daß ein Strahlenteilchen, welches etwa durch Streuung um den Absorber herum aus dem einen Zählrohr in das andere gelangen

W. Bothe
Nobel Prize 1954

W. Bothe & W. Kolhörster, Z. f. Phys. 56 (1929) 751

Dreifachkoinzidenzen der Ultrastrahlung aus vertikaler Richtung in der Stratosphäre *).

I. Meßmethode und Ergebnisse.

Von Georg Pfotzer in Stuttgart.

Mit 11 Abbildungen. (Eingegangen am 9. Juni 1936.)

Mit einer selbstaufzeichnenden Apparatur werden bei drei Registrierballon aufstiegen Dreifachkoinzidenzen der Ultrastrahlung aus vertikaler Richtung bi zu 10 mm Hg Luftdruck (29 km Höhe ü. M.) gemessen. Die Kurve der Zählroh koinzidenzen in Abhängigkeit vom Luftdruck zeigt ein Maximum bei 80 mm H und einen Buckel bei 300 mm Hg. Die Kurve kann gegen das Ende der Atmo sphäre extrapoliert werden.

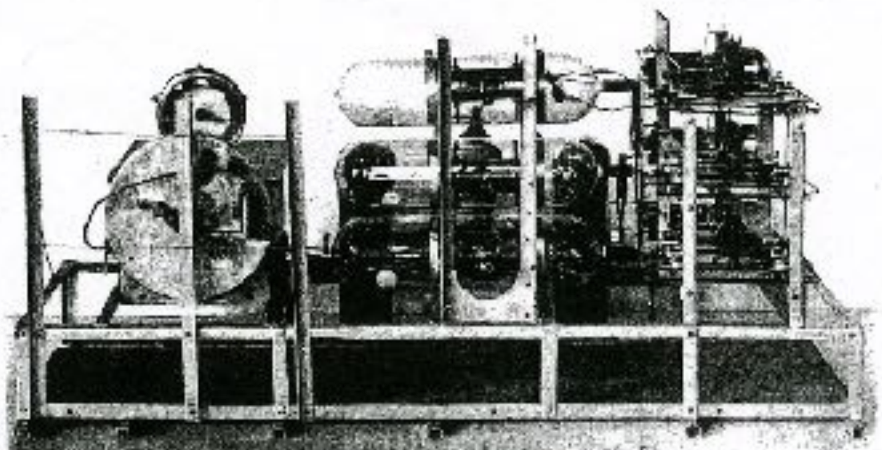

a

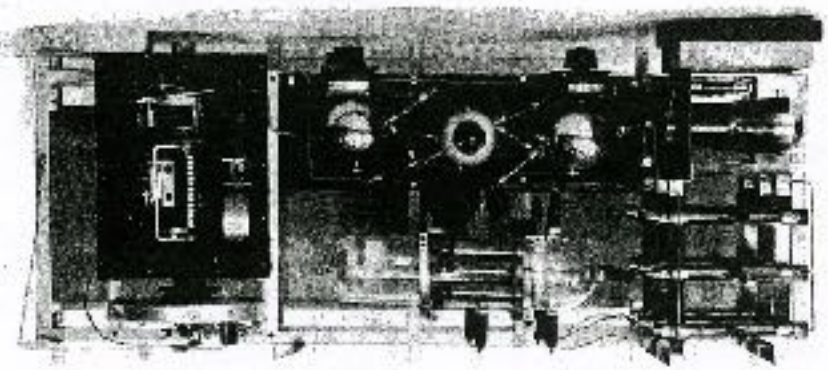

b

Fig. 6. Aufbau der Registrierapparatur. a) Von der Seite b) von oben gesehen.

Fig. 5. Launching of a balloon train from the courtyard of the institute.

b

Fig. 4. a) Aufstiegplatte (nat. Größe, Hälfte); b) Vergrößerter Ausschnitt.

3) Die Firma Gebr. Junghans, Schramberg, hat uns freundlicherweise diese schönen Zählwerke hergestellt.

G. Pfotzer, Z. f. Phys. 102 (1936) 23

Dreifachkoinzidenzen der Ultrastrahlung aus vertikaler Richtung in der Stratosphäre *).

I. Meßmethode und Ergebnisse.

Von Georg Pfotzer in Stuttgart.

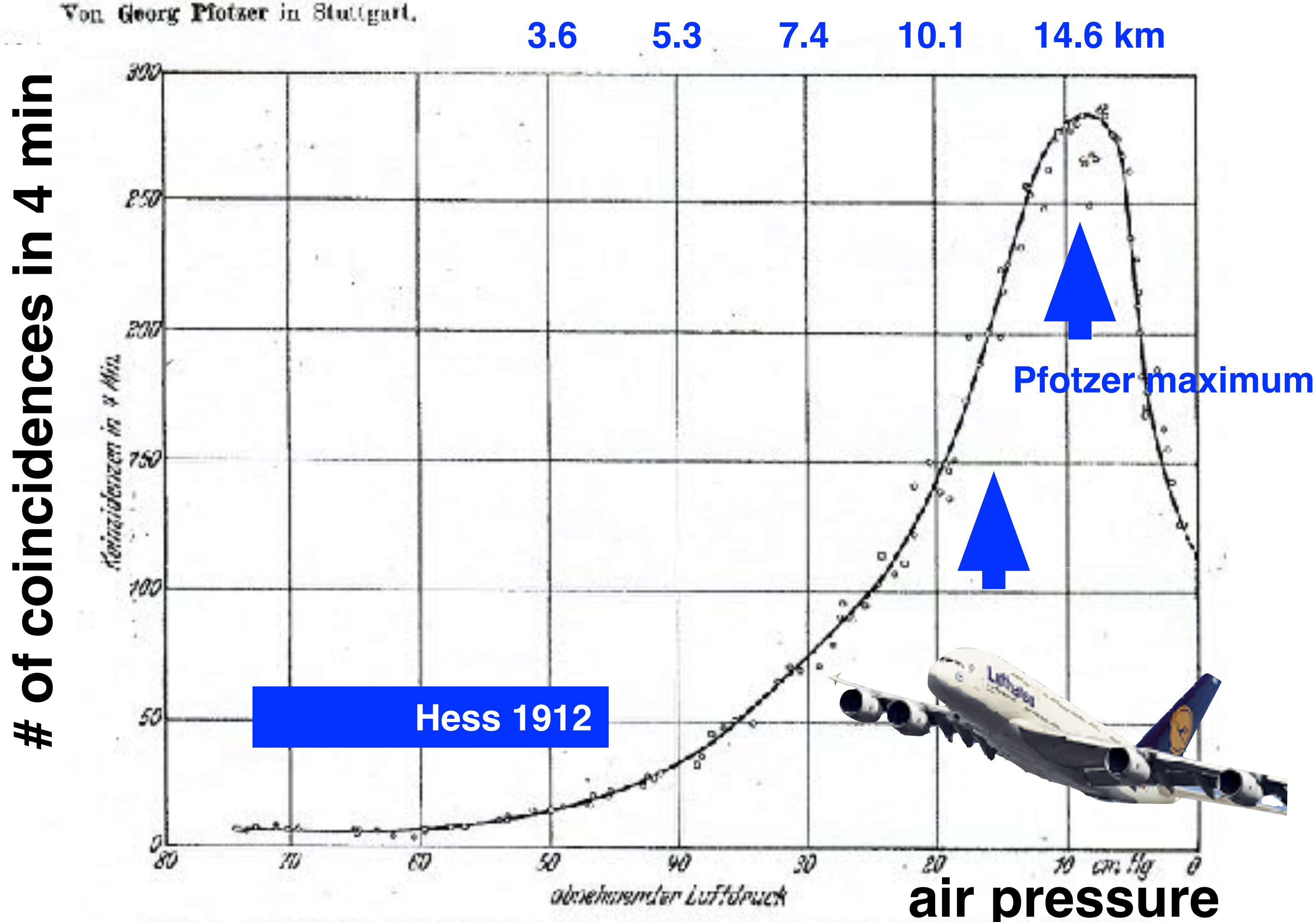

Fig. 1. Aus drei Aufstiegen gemittelte Kurve der Vertikalintensität der Ultrastrahlung in der Atmosphäre.

G. Pfotzer, Z. f. Phys. 102 (1936) 23

Latitude effect

Letters to the Editor

[The Editor does not hold himself responsible for opinions expressed by his correspondents. Neither can he undertake to return, nor to correspond with the writers of, rejected manuscripts intended for this or any other part of NATURE. *No notice is taken of anonymous communications.]*

Latitude Effect of Cosmic Radiation

ON the expedition organised by the Deutscher und Oesterreichischer Alpenverein in 1932 to the Andes of Peru, observations of cosmic rays were made at several heights up to 6,100m. and during the sea-voyage. From Bremen to Peru one apparatus worked during March and April 1932 on board the M.S. *Erfurt* of the Norddeutscher Lloyd line. On the return voyage in January and February 1933, three apparatuses were in full action from Peru through the Strait of Magellan to Hamburg on board the M.S. *Isis* of the Hamburg-Amerika line. The self-recording electrometers were constructed by Prof. E. Regener on the same principle as those used for his researches in Lake Constance[1] and in the upper atmosphere[2]. The electrometer wire is inside an ionisation chamber of 16 cm. diameter with 'deltametal' walls of 1 cm. thickness. The position of the wire is photographed every half-hour on a fixed photographic plate.

Instrument No. 1 was filled with carbon dioxide at 9·7 atmospheres pressure and 16° C. With a radium capsule, I found the temperature effect on ionisation to be + 0·13 per cent for every + 1° C. difference. The correction for barometric pressure was 0·29 per cent per millimetre of mercury. All data were reduced to 16° C. and 760 mm. pressure. The ionisation due to radioactivity in the chamber itself was allowed for as 0·8 volts per hour as found on the bottom of Lake Constance at a depth of 250 m. Eight hemispherical shells of iron were fitted round the chamber. The combined thickness of this iron wall was 10 cm.

In Fig. 1 are recorded the data of apparatus No. 1, the iron case of which was open on the upper side. The graph shows the intensity of cosmic radiation in volts per hour for different geomagnetic latitudes on the voyage from the Strait of Magellan to Hamburg. The geographical position of the geomagnetic north pole was taken to be 78° 32′ N. and 69° 08′ W. Each point of the curve corresponds to an average of a twenty hours' registration. The points give a smooth curve which shows the accuracy of the recording method employed. The intensity increases by about 12 per cent when going from the equatorial region to 55° N. geomagnetic latitude.

Apparatus No. 2 was wholly encased in the iron shell. Apparatus No. 3 worked without any iron shell. Every instrument shows substantially the same effect.

In general, the curves agree with the observations of Clay[3] and with those of A. H. Compton[4] made at about the same time. It is very interesting that the northern and southern parts of the curve are *not* symmetrical with respect to either the geomagnetic or the geographical equator. Considering the accuracy of our uninterrupted registration, this result is quite trustworthy.

From the fact that a latitude effect of 12 per cent of the radiation exists, it must be concluded that this part of the radiation consists of corpuscles before entering the earth's atmosphere. For the magnitude of this part of the radiation, reference should be made to the analysis of the components of cosmic rays by Regener[2] and Lenz[5].

A more detailed report of these observations and of the researches in the Andes will be published in the *Zeitschrift für Physik*.

H. HOERLIN.

Physikalisches Institut
der Technischen Hochschule,
Stuttgart. June 8.

[1] Regener, E., *Z. Phys.*, **74**, 433 ; 1932.
[2] Regener, E., *Phys. Z.*, **34**, 306 ; 1933.
[3] Clay, J., *Naturwiss.*, **20**, 687 ; 1932.
[4] Compton, A. H., *Phys. Rev.*, **43**, 387 ; 1933.
[5] Lenz, E., *Z. Phys.* ; in the press.

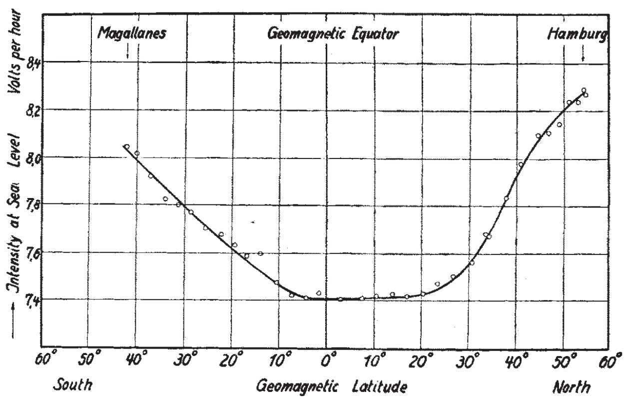

FIG. 1.

Clay: Latitude Effect

RESULTS OF THE DUTCH COSMIC RAY EXPEDITION 1933

II. THE MAGNETIC LATITUDE EFFECT OF COSMIC RAYS

A MAGNETIC LONGITUDE EFFECT

by J. CLAY, P. M. VAN ALPHEN and C. G. 'T HOOFT

Natuurkundig Laboratorium, Amsterdam

journey from Holland to Java
intensity variies with latitude

cosmic rays are charged particles

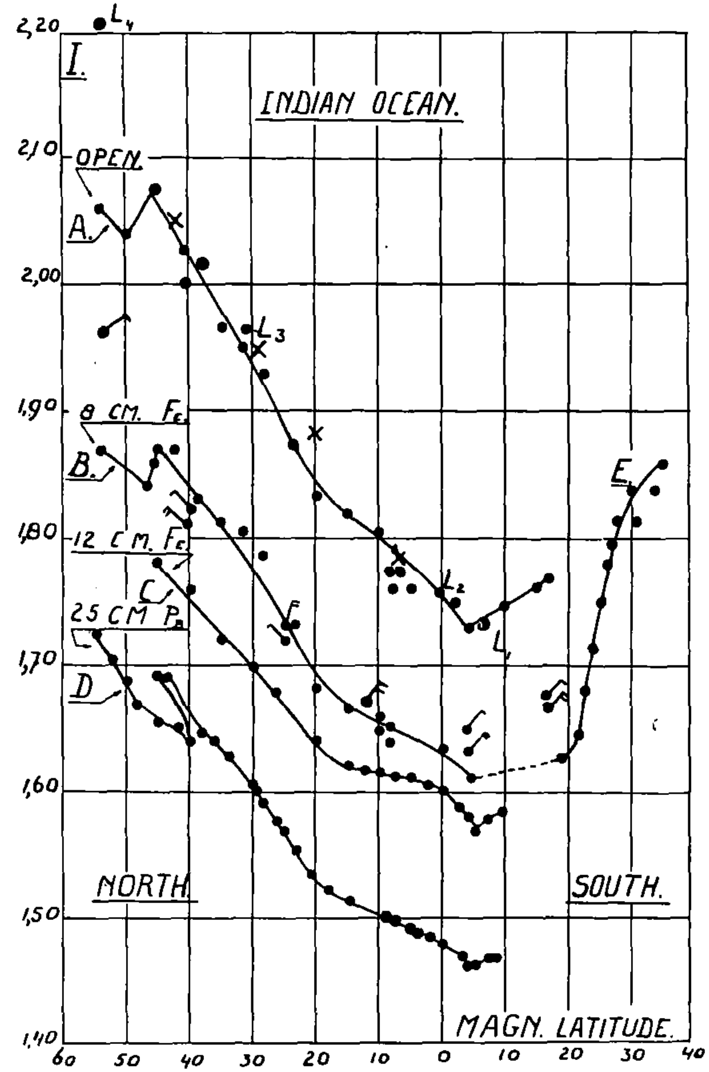

Fig. 1. Records of the variation of Cosmic Radiation with latitude on two different routes under different shielding with different instruments

× ---------- × results with instrument D open (Amsterdam—Batavia)

(L_1, L_2, L_3, L_4) results with instrument D_1 open (Batavia—Amsterdam)

Results 1928 and 1929.

J. Clay et al., Physica 1 (1934) 376; 2 (1935) 183

Compton: World-wide survey of intensity of radiation

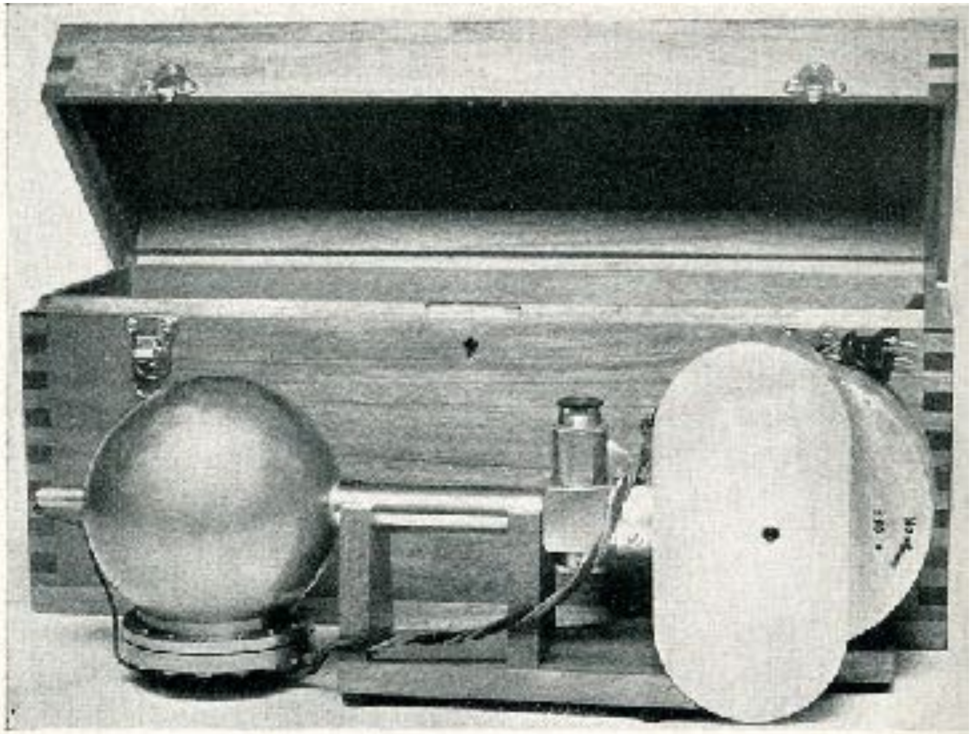

Fig. 24. The instrument used in this survey is usually shielded with lead and is placed in the box when used in most airplane flights.

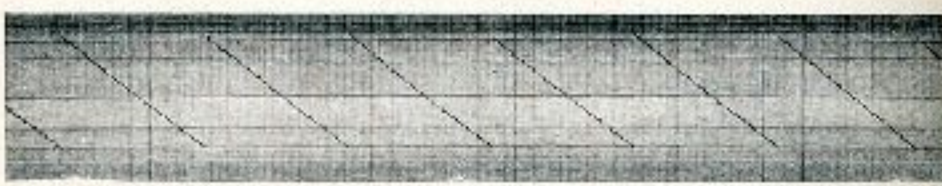

Fig. 27. Showing the type of record obtained at sea level in this world survey. Two of the horizontal lines give barometric and temperature records.

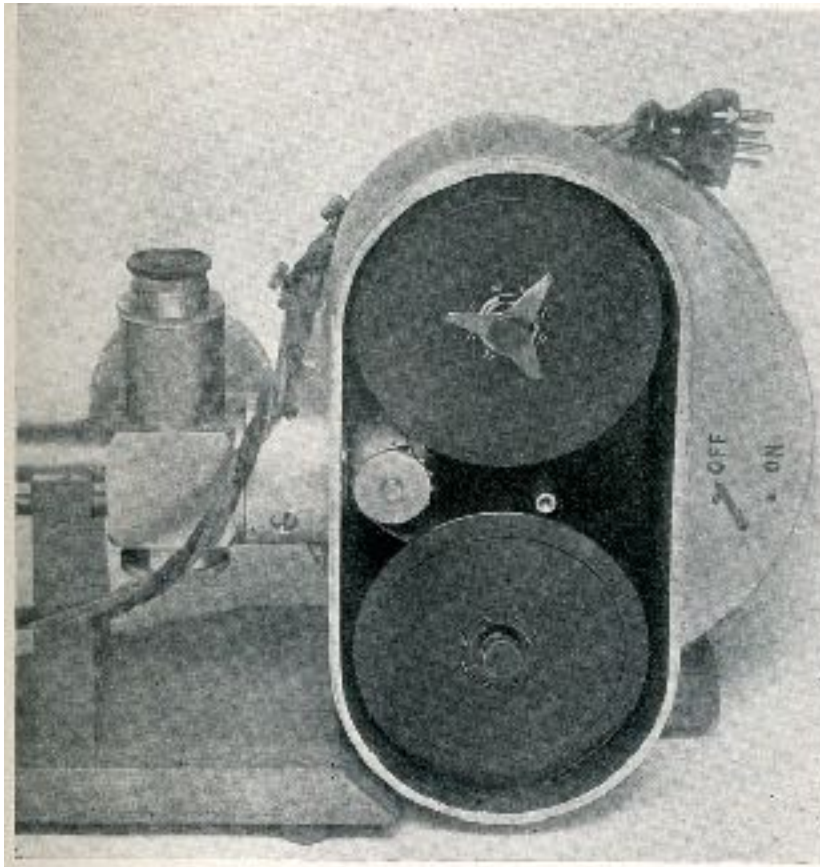

Fig. 25. The camera will take a one-hundred-foot reel of 35 mm motion picture film which is driven at a constant rate past the slit by a power clock. Changeable gears allow various rates of film speeds to be used, depending on the expected ionization.

~1930

THE
PHYSICAL REVIEW
A Journal of Experimental and Theoretical Physics
VOL. 43, NO. 6 MARCH 15, 1933 SECOND SERIES

A Geographic Study of Cosmic Rays

ARTHUR H. COMPTON, *University of Chicago*

(Received January 30, 1933)

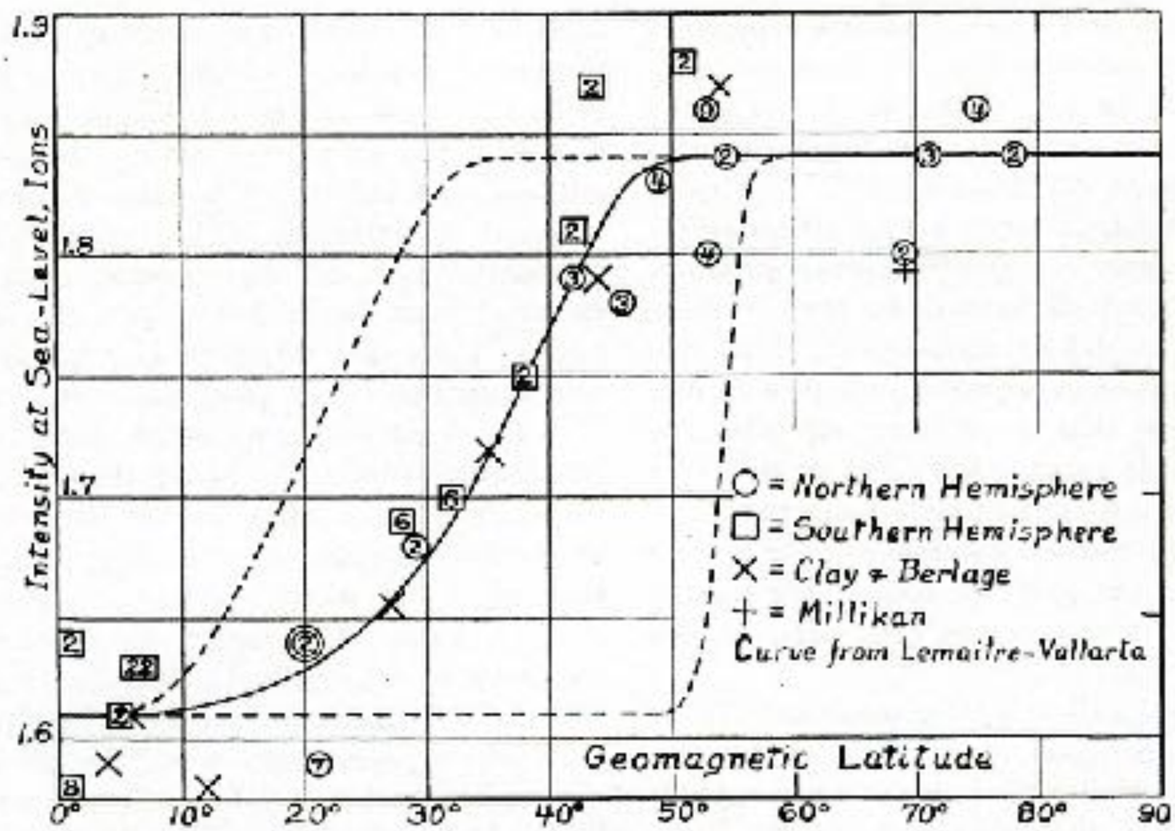

FIG. 7. Intensity *vs.* geomagnetic latitude at sea level, including data of Clay and Millikan.

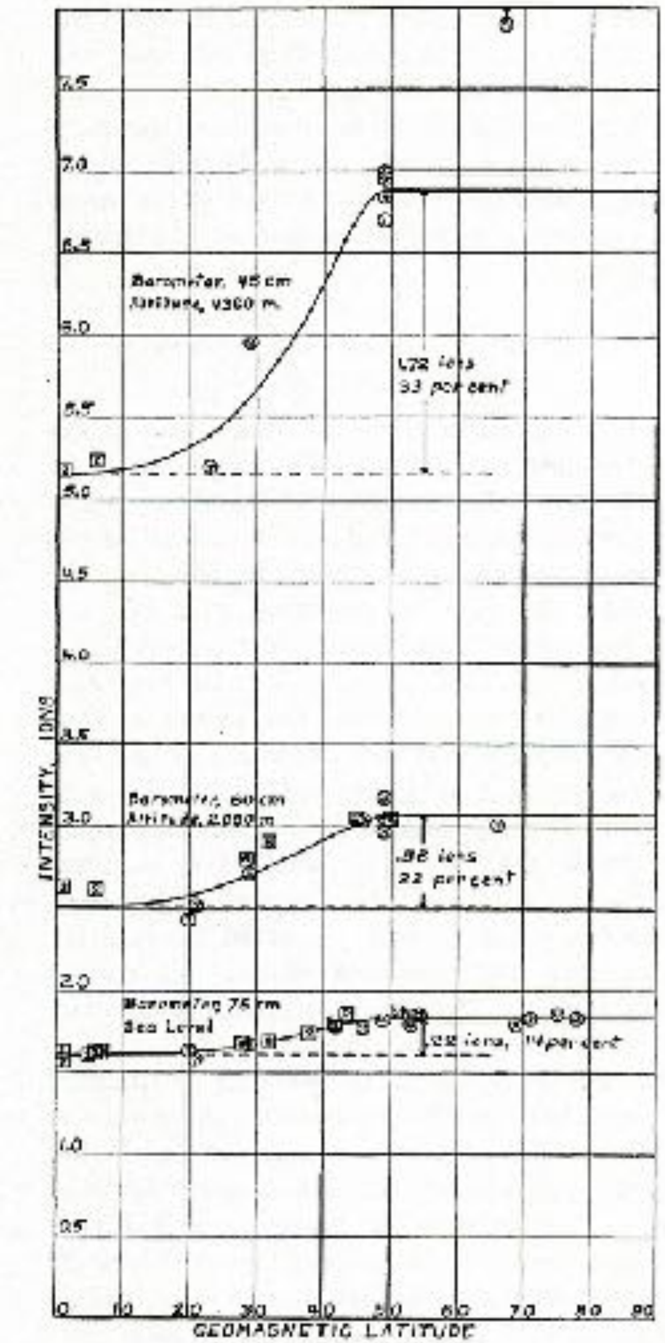

FIG. 6. Intensity *vs.* geomagnetic latitude for different elevations.

1931-34 A.H. Compton 12 expeditions → ~100 locations

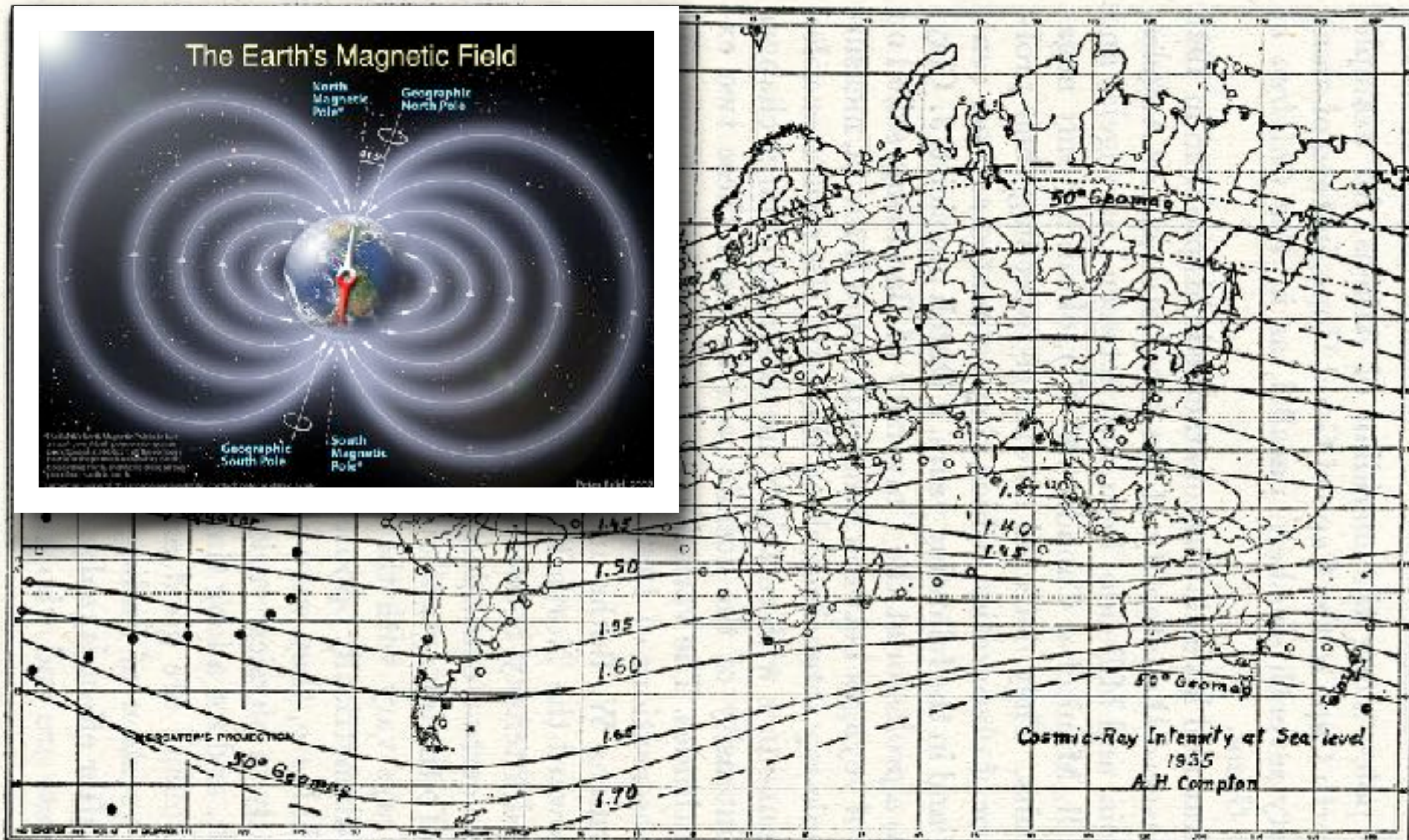

FIG. 6.—Compton's world map of isocosms. Note the parallelism of these lines of equal cosmic-ray intensity and the dotted curves of geomagnetic latitude (50° N. and S.).

→ **cosmic rays are charged particles**

~1937 East-West Effect of Cosmic-Ray Intensity

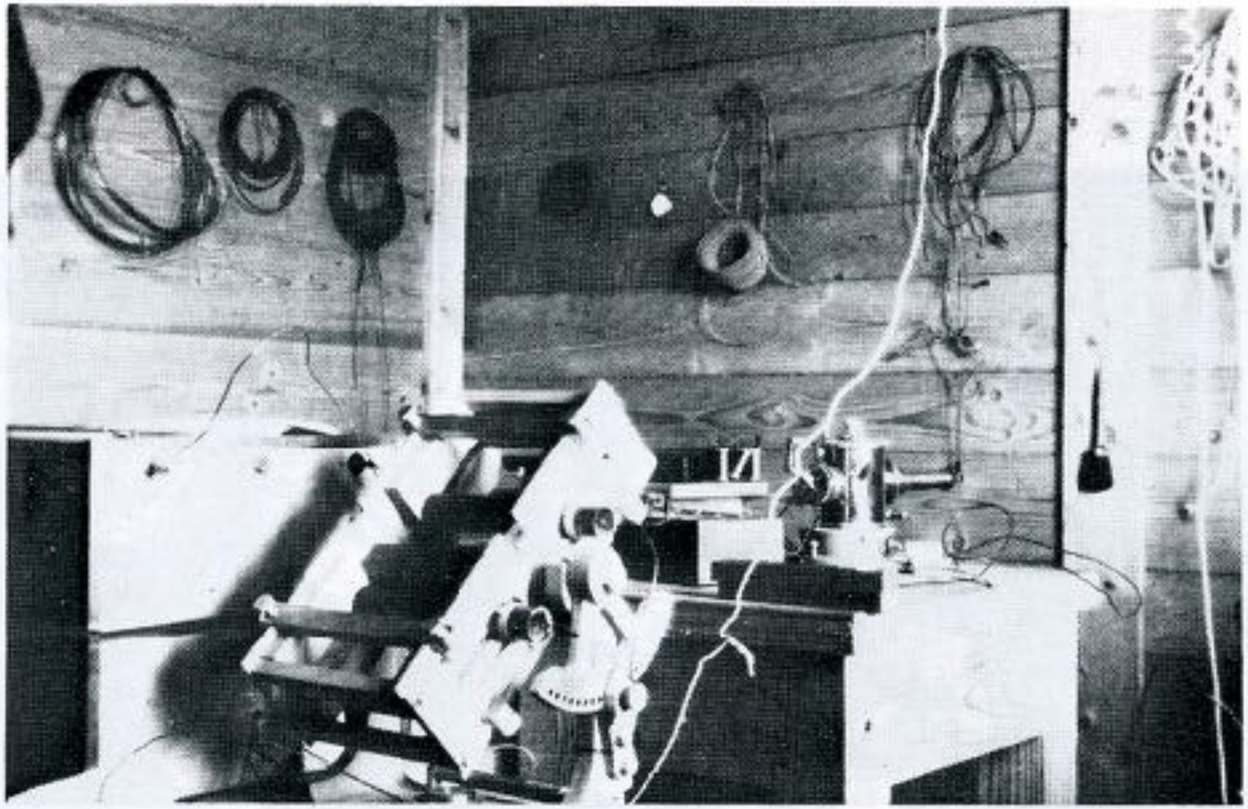

Fig. 14. The equipment for the E-W experiment.

Rossi and others

higher intensity from the west

➡ cosmic rays are mostly positively charged end 31 Jan

~1930 „elementary particles“:

		charged	neutral		
Rutherford	(1919)	p	n	(1932)	Chadwick
Thomson	(1897)	e^-	γ	(1905/26)	Einstein

Discovery of new particles in cosmic rays
~1930 – 1950
birth of elementary particle physics

cloud chamber
C.T.R. Wilson
Nobel Prize 1927

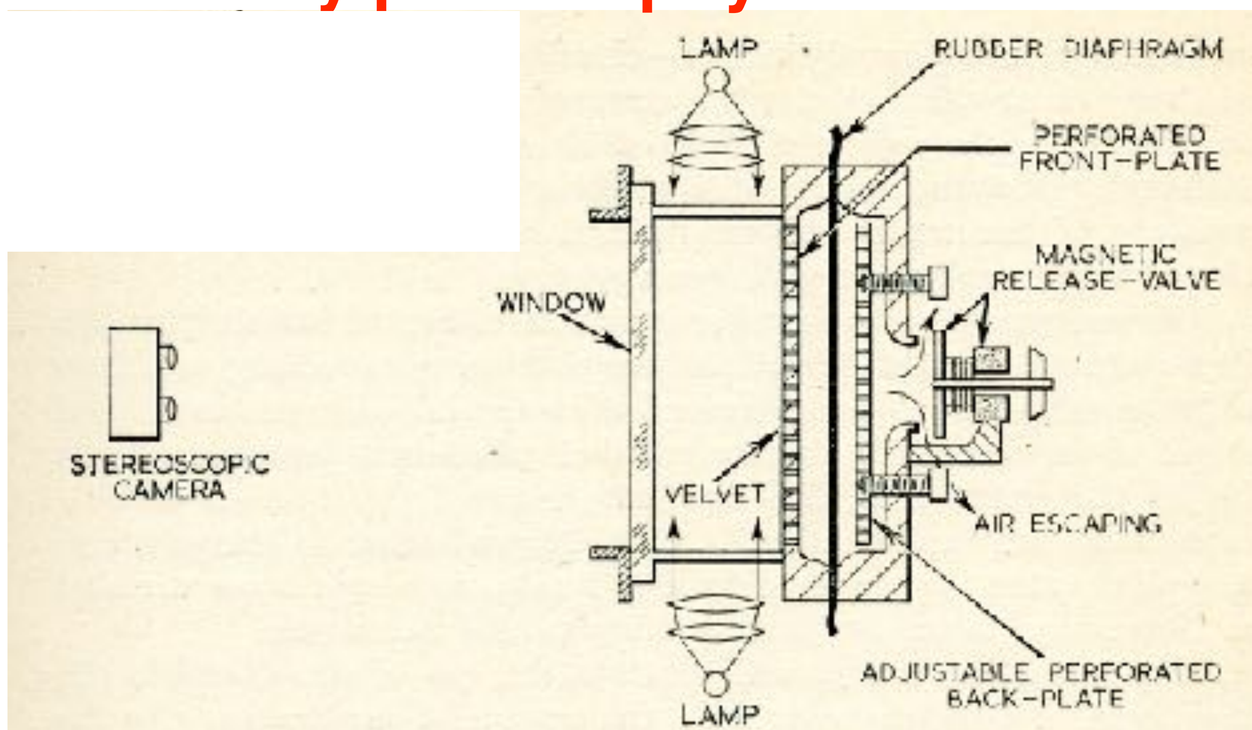

MARCH 15, 1933 PHYSICAL REVIEW VOLUME 43

Nobel Prize 1936

The Positive Electron e^+

CARL D. ANDERSON, *California Institute of Technology, Pasadena, California*

(Received February 28, 1933)

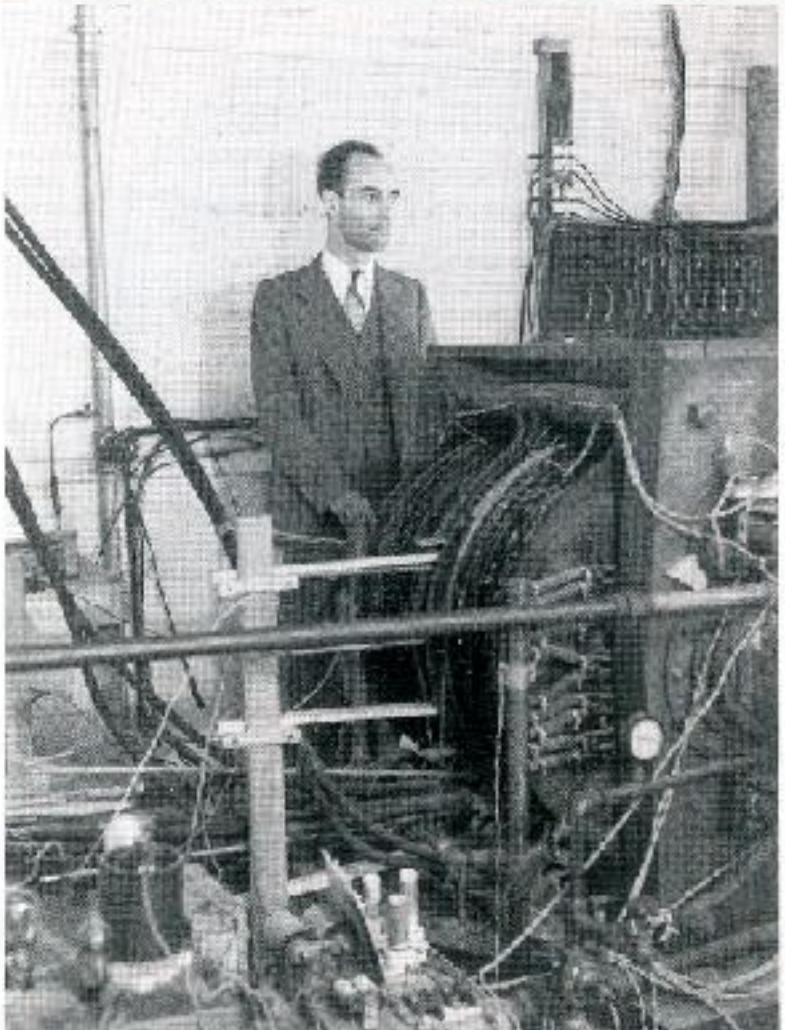

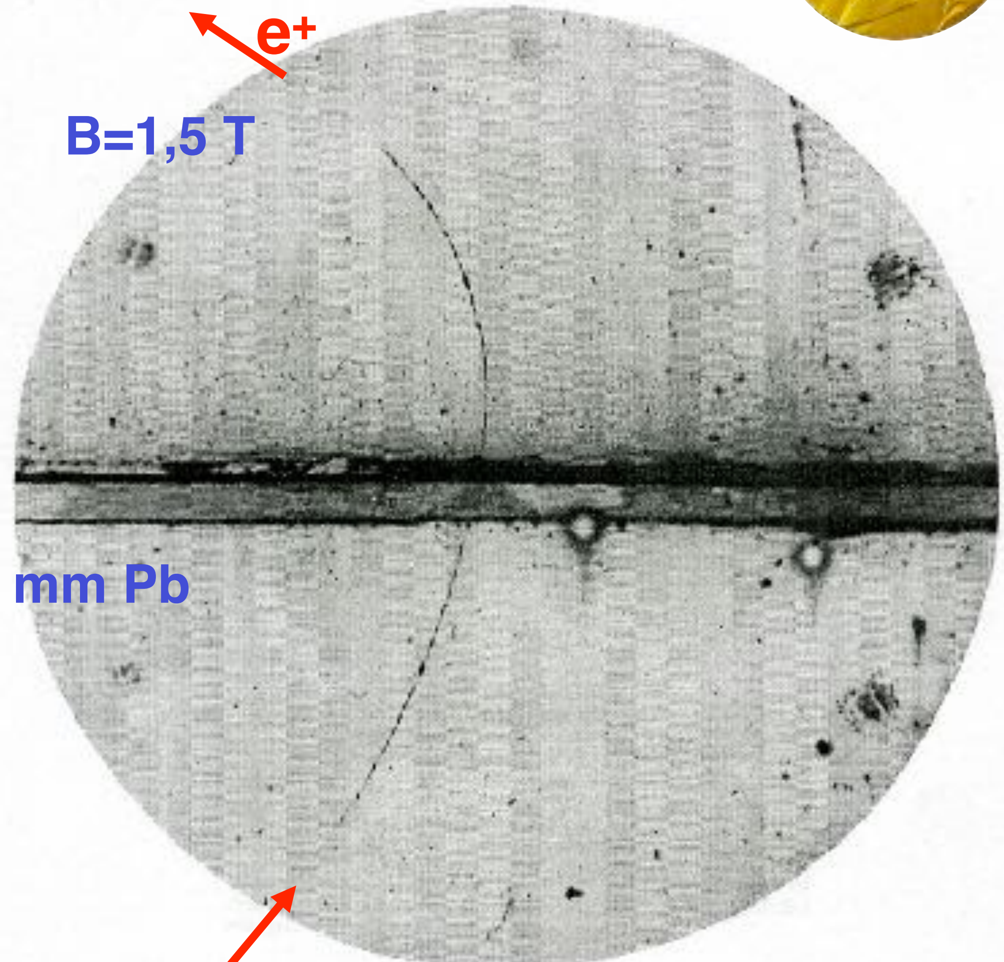

FIG. 1. A 63 million volt positron ($H\rho = 2.1 \times 10^5$ gauss-cm) passing through a 6 mm lead plate and emerging as a 23 million volt positron ($H\rho = 7.5 \times 10^4$ gauss-cm). The length of this latter path is at least ten times greater than the possible length of a proton path of this curvature.

P.M.S. Blackett
Nobel Prize 1948

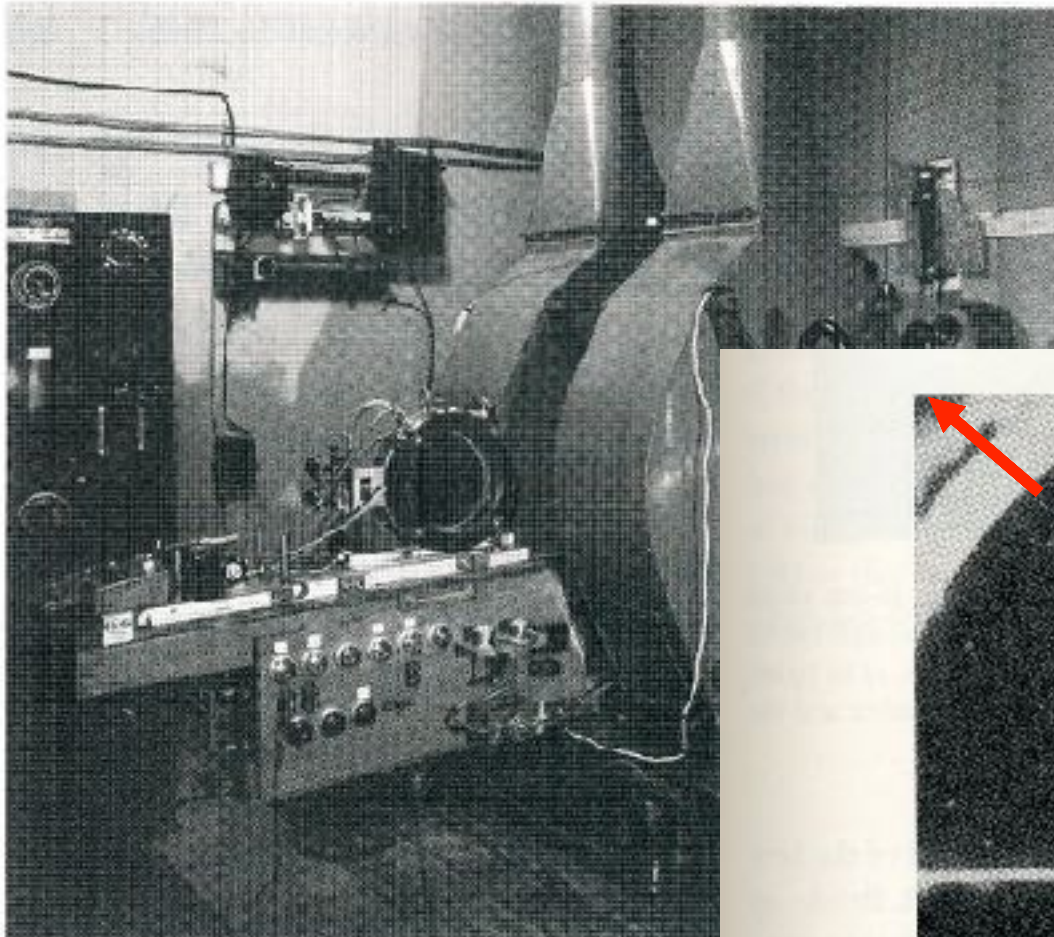

1933 Blackett & Occhialini

10 t electromagnet
30 cm cloud chamber

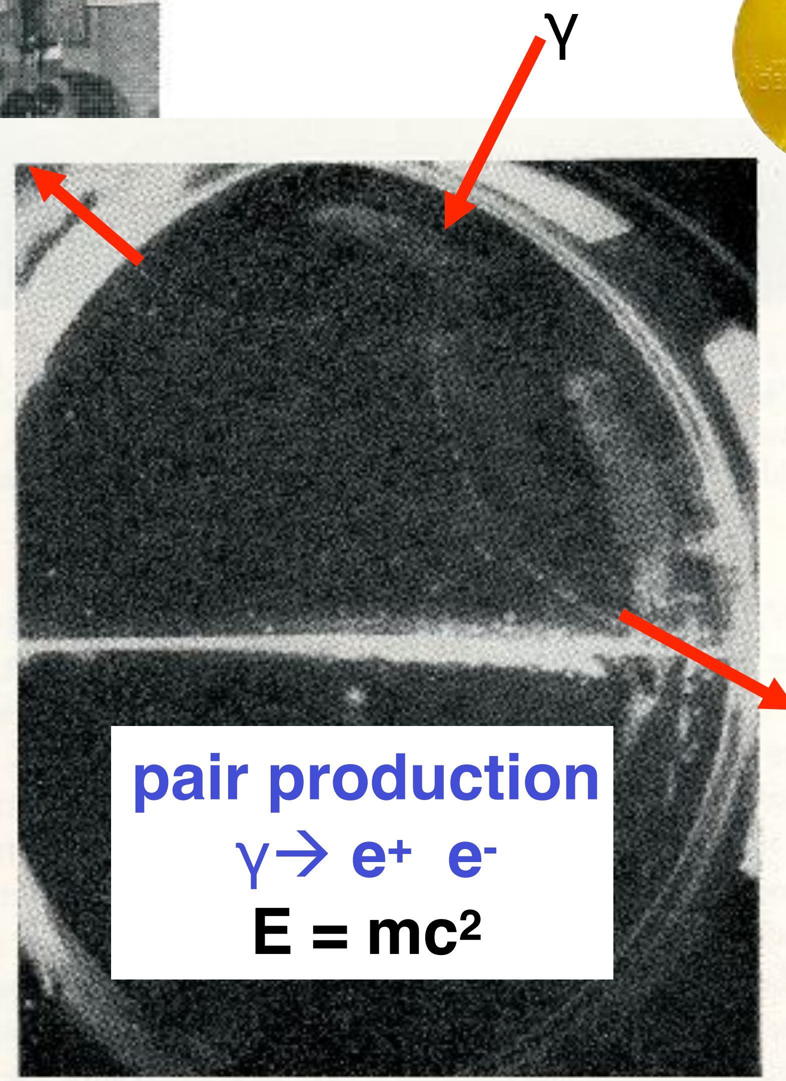

Fig. 9. Pair of positive and negative electrons produced by gamma rays. (Chadwick, Blackett, and Occhialini, 1934)

Electromagnetic Cascades B. Rossi 1933

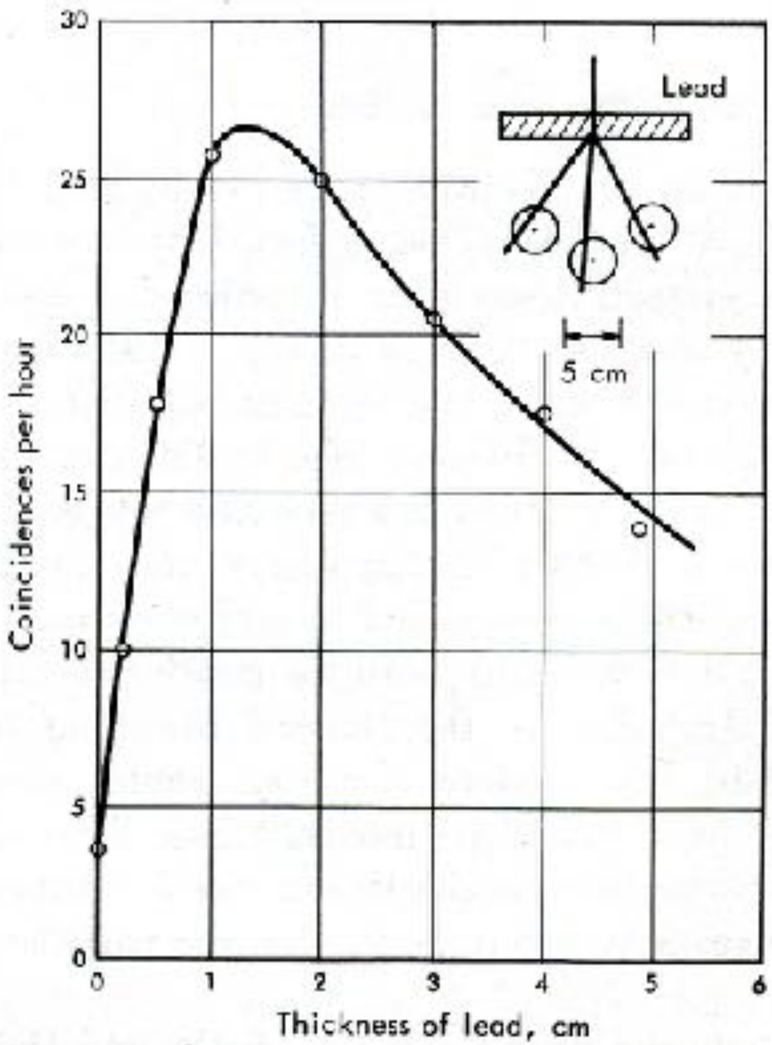

Fig. 7-1 Shower curve. The number of coincidences per hour is plotted as a function of the thickness of lead above the counters. The experimental arrangement is shown schematically in the inset. The circles are experimental points. (This figure is based on one appearing in a paper by the author in *Zeitschrift für Physik*, vol. 82, p. 151, 1933.)

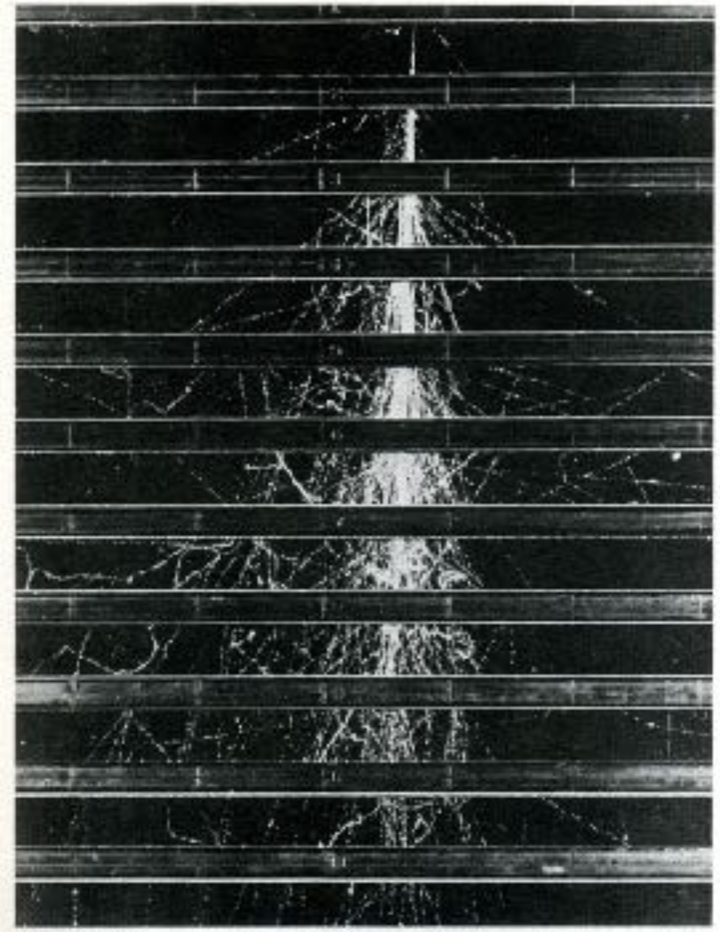

Fig. 7-5 A shower developing through a number of brass plates 1.25 cm thick placed across a cloud chamber. The shower was initiated in the top plate by an incident high-energy electron or photon. The photograph was taken by the MIT cosmic-ray group.

$\gamma \rightarrow e^+ e^-$

$e^{+/-} \rightarrow \gamma$

Discovery of the Muon

1937 Anderson & Neddermeyer: *μ* in cloud chamber

$m_\mu \sim 200\ m_e$

1939 B. Rossi: life time

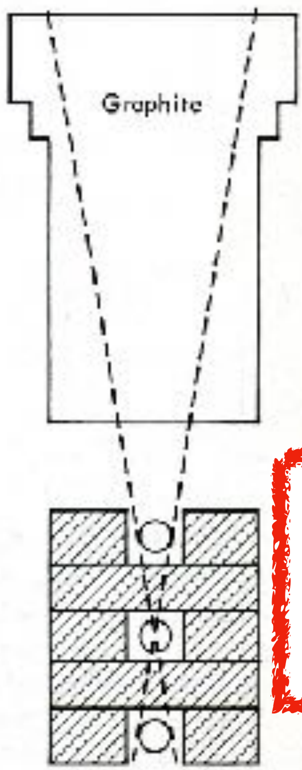

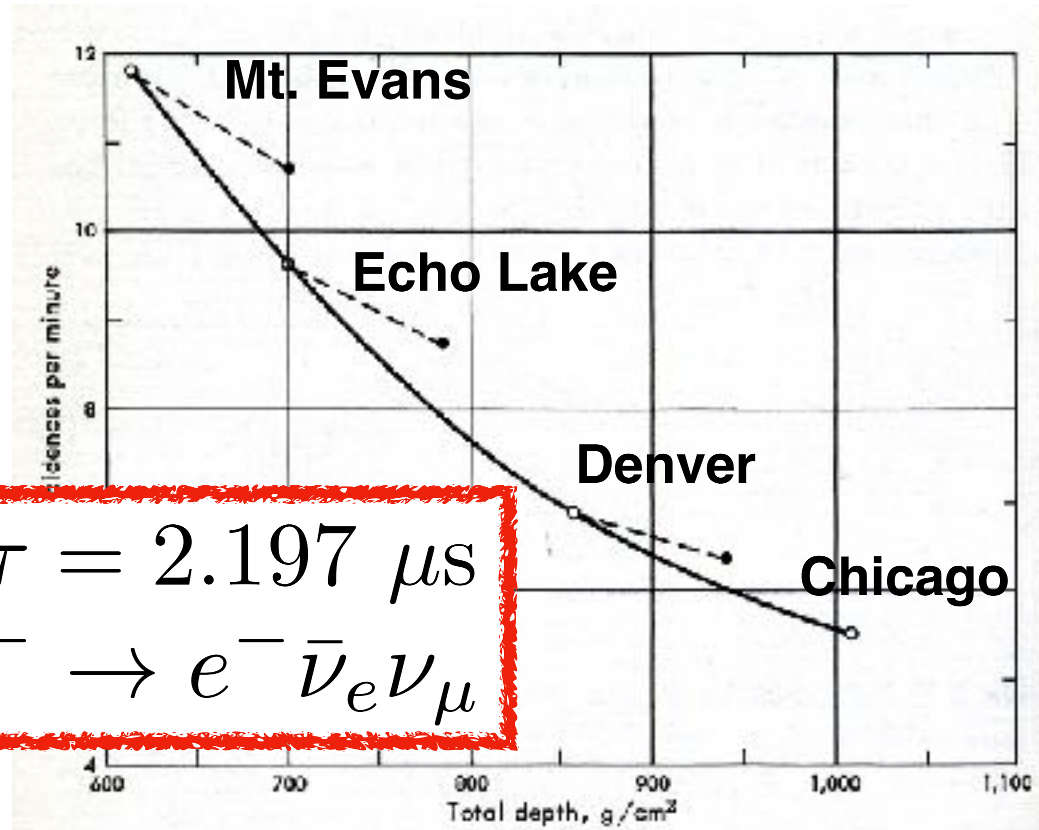

PDG: $\tau = 2.197\ \mu s$

$$\mu^- \rightarrow e^- \bar{\nu}_e \nu_\mu$$

➡ life time $\tau \sim 2\ \mu s$

$\mu \rightarrow e + \ldots$

P. Auger
Jungfraujoch

Measuring Cosmic Rays in the Swiss Alps

The author (*left*) and his collaborator, P. Ehrenfest, set up their apparatus in the Jungfraujoch.

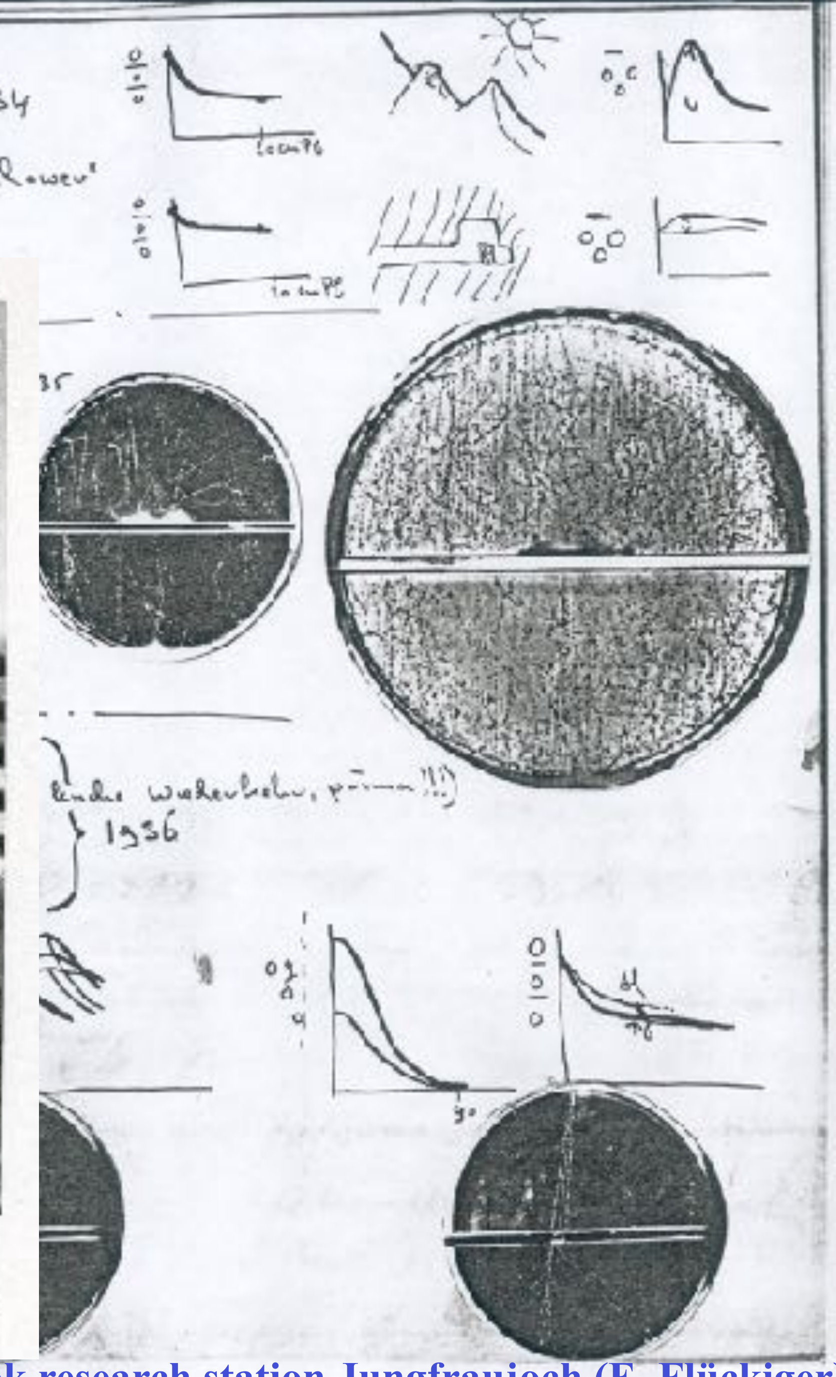

P. Auger et al., Comptes renduz 206 (1938) 1721

Guest book research station Jungfraujoch (E. Flückiger)

Kurze Originalmitteilungen.

Für die kurzen Originalmitteilungen ist ausschließlich der Verfasser verantwortlich.

Gekoppelte Höhenstrahlen.

Bei Bestimmungen der Zufallskoinzidenzen hoch aufl[...] der Zählrohrverstärkeranordnungen (bis $5 \cdot 10^{-7}$ sec) ergab sich eine wesentlich größere Anzahl, als nach den elektrischen Konstanten der Anordnung zu erwarten war, ferner ihre Anzahl abhängig vom gegenseitigen Abstand der Zählrohre, wie z. B. für Zählrohre von 430 qcm wirksamer Oberfläche (90 · 4,8) und $\tau = 5 \cdot 10^{-6}$ sec Tabelle 1 zeigt.

Tabelle 1. Anzahl der zusätzlichen Koinzidenzen je Stunde in Abhängigkeit vom gegenseitigen Abstand der ungepanzerten Zählrohre.

Rohrabstand in m:	1,25	3,75	5,00	7,50	10,00	20,00	75,00
Im Experimentierraum	13,3 ± 2,1	13,3 ± 1,3	13,1 ± 1,3	9,3 ± 1,2	0,4 ± 0,8	—	—
Im Freien	37,5 ± 4,4	—	21,5 ± 2,1	—	10,0 ± 2,2	2,5 ± 1,5	0,7 ± 1,3

Mit zunehmendem Abstand der Zählrohre voneinander nimmt die Anzahl der Zufallskoinzidenzen zunächst dauernd ab, bis sich bei über 10,0 m Abstand (Beobachtungen im Experimentierraum) konstante Werte einstellen und überschüssige Koinzidenzen nicht mehr nachweisbar sind. Wurde ein Bleipanzer ($10 \cdot 10 \cdot 40$ cm³) so zwischen die Zählrohre gebracht, daß er den Durchgang ein und desselben Strahles durch die beiden horizontal liegenden Rohre hinderte, so änderte sich wesentlich nichts, wie ja nach der Richtungsverteilung der Höhenstrahlen zu erwarten ist. Wohl aber machten sich die zusätzlichen Koinzidenzen nicht mehr bemerkbar, wenn die Rohre allseitig durch 10 cm Blei geschirmt wurden. Dann erhielt man auch bei nahe aneinanderliegenden Rohren dieselben konstanten Werte für τ wie bei über 10 m Abstand ungepanzert. Die zusätzlichen Koinzidenzen mußten demnach von Strahlen herrühren, die durch 10 cm Blei weitgehend absorbiert werden. Bei starker Erhöhung der Stoßzahlen durch radioaktive Bestrahlung wird der Einfluß der Höhenstrahlen unwirksam. Dann ergab sich ebenfalls bei kleinerem Zählrohrabstande (5 m) der Wert des Auflösungsvermögens, der 1. nach den elektrischen Daten, 2. nach den Bestimmungen mit allseitigem Panzer und 3. nach den Messungen über 10 m Abstand ungepanzert das wahre Auflösungsvermögen der Anordnung darstellt.

Nur bei statistisch verteilten und voneinander unabhängigen Einzelstößen N_1 und N_2 der beiden Zählrohre gilt die Beziehung $K_z = 2 N_1 N_2 \tau$ zur Bestimmung des Auflösungsvermögens τ. Es müssen also bei ungeschirmten und zu nahe

wird sich also um Sekundärs[...] um Schauer, handeln. Das zeigen auch folgende Versuche mit einer 3fachen Koinzidenzapparatur, deren Auflösungsvermögen mit einer besonderen Anordnung zu $5 \cdot 10^{-6}$ sec bestimmt worden war. Bei Aufstellung der Zählrohre horizontal und radial auf einem Kreise ist dann überhaupt keine meßbare Anzahl von Zufallskoinzidenzen zu erwarten (höchstens 10^{-4} Koi/Std.). Es ergaben sich aber bei Zählrohren von 216 qcm wirksamer Fläche

Ungepanzert . . . . . . 2,7 ± 0,4 Koi/Std.
1 Rohr gepanzert . . . . 0,7 ± 0,1 Koi/Std.
3 Rohre gepanzert . . . . 0,08 ± 0,02 Koi/Std.

Strahlen im Schauer. Unter der Decke des Experimentierraumes sind diese Sekundärstrahlen über eine Fläche von mindestens 60 qm sicher n[...]

Sollten sie bevorzugt in
würden nach der Geometri
bis zu 80° aus ihrer ursp
worden sein. Indessen ist
von nur 1 cm Blei und d
Strahlen von $\mu_{Pb} = 0{,}12$ cm
überwiegend in der Atmosp
Boden erzeugt werden. D
bierende als strahlenauslös
Freien eine größere Anzahl
dingungen zu erwarten ist.
mit der 2-fach-Koinzidenz
die zusätzlichen Koinziden
20 m sicher beobachtet we
strahlen im Freien sogar b
(Tabelle 1). Selbst bei 75 m
Überschuß vorhanden, der
reihen sichergestellt werde

Aus dem niedrigen Abso
daß selbst Schauerstrahlen
dem Boden entstehen, dies
würden dann über eine
Da für solche Schauer tro
die räumliche Dichte der S
ordentlich gering sein kan
wenn sie als zusätzliche Ko

Dresden kurz berichte[...]

Berlin, Institut für Höh[...]tät Berlin, den 25. Augus[...]

W. KOLHÖRS[...]

Neue Messungen der Fluo[...] grüne[...]

Ein günstiges Versuchsobjekt für quantitative Messungen ist die Meeresalge Ulva lactuca[1]. Sie besteht aus blattartigen

[1] Das Versuchsmaterial verdanken wir dem Entgegenkommen der Staatlichen Biologischen Anstalt auf Helgoland.

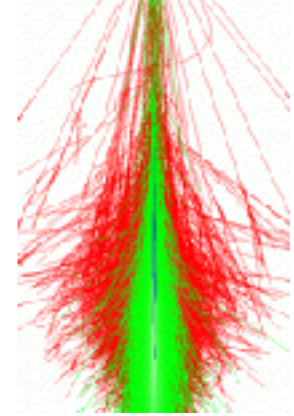

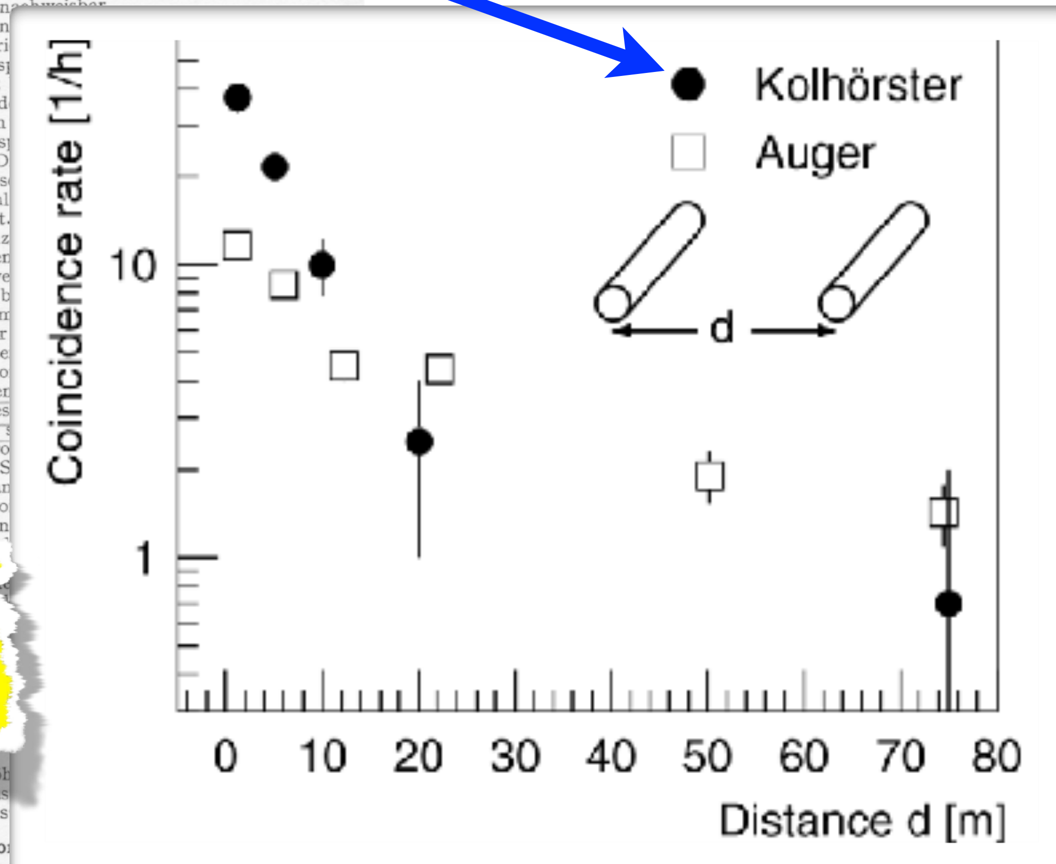

P. Auger et al., Comptes renduz 206 (1938) 1721

W. Kolhörster et al., Naturwiss. 26 (1938) 576

Extensive Air Shower

Proton 10^{15} eV:
on ground
10^{6} particles
80% photons
18% electr./positr.
1.7% muons
0.3% hadrons

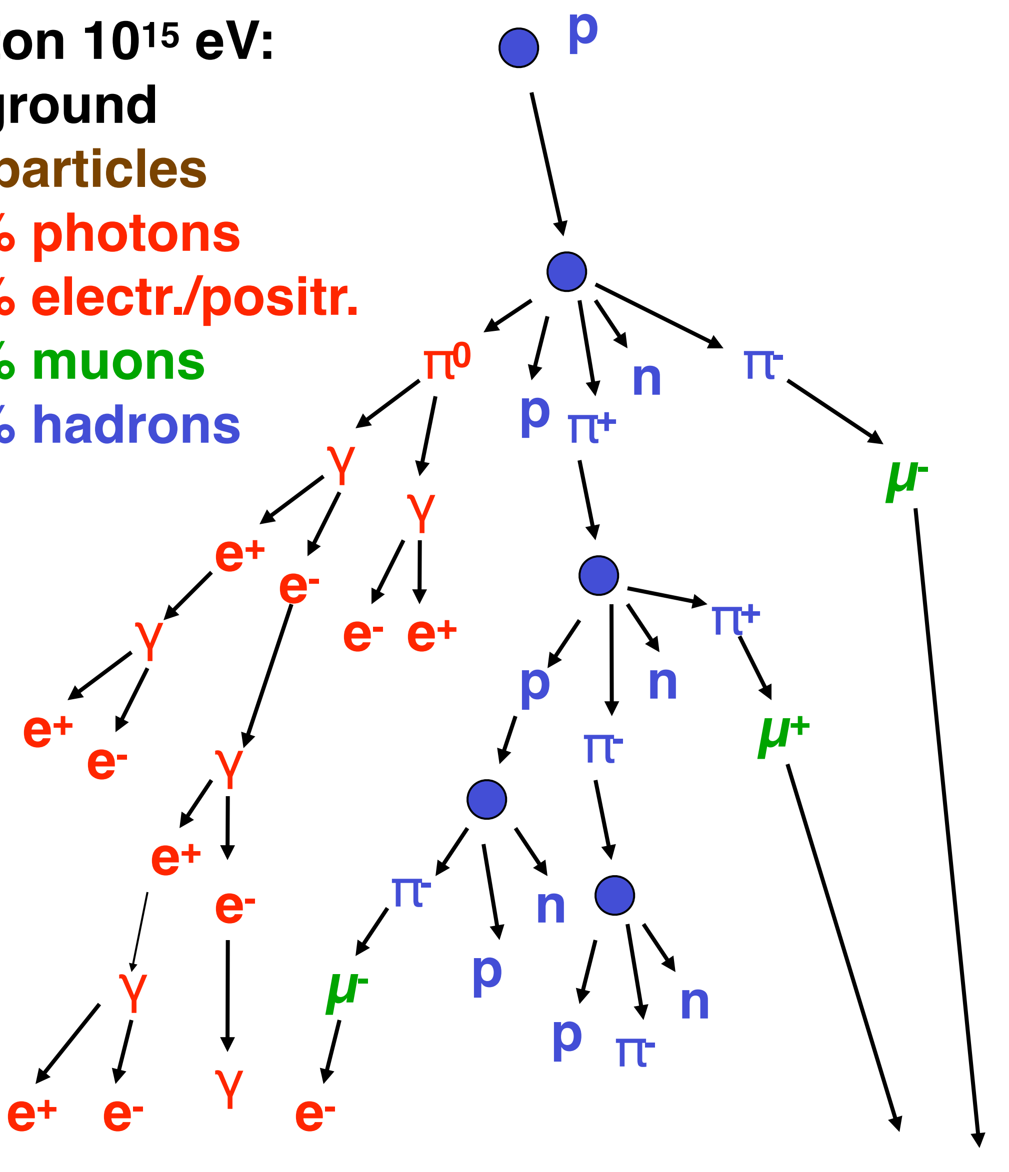

electromagnetic **hadronic** **muonic**
shower component

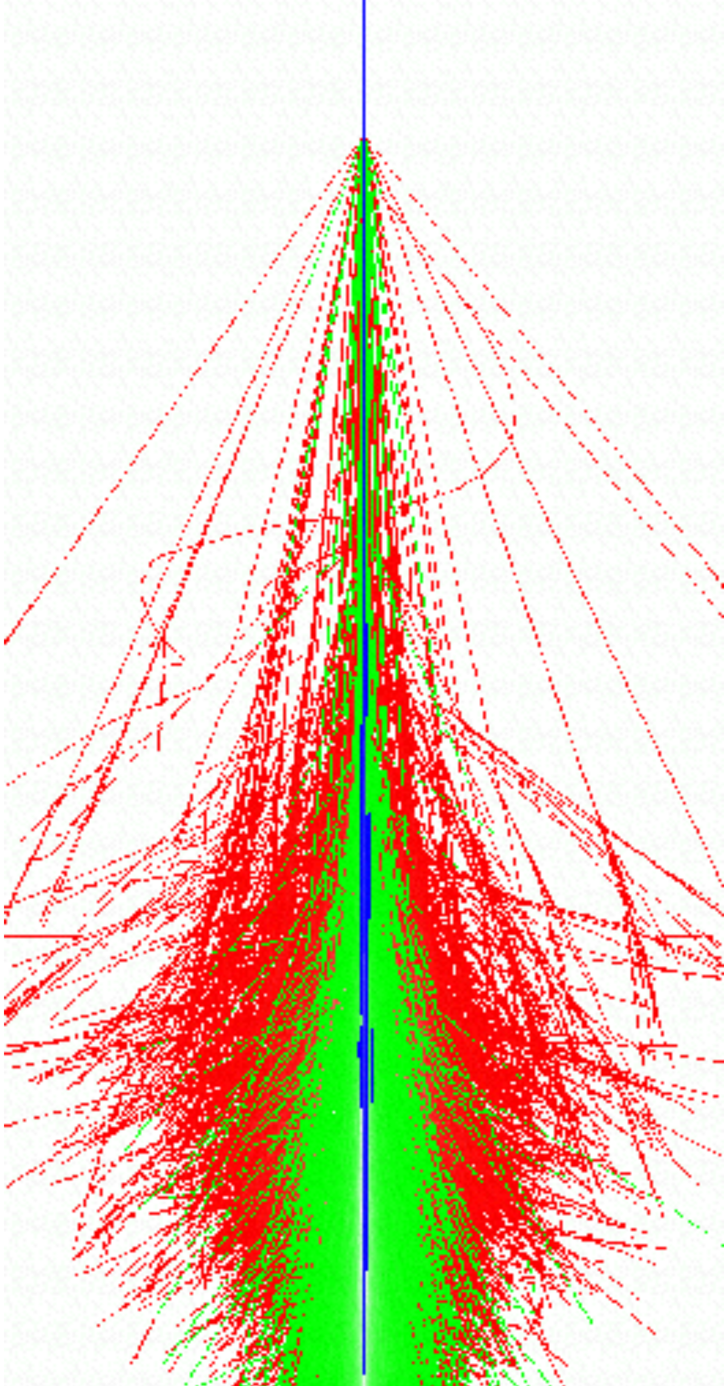

~ 1950 large detector arrays to measure extensive air showers

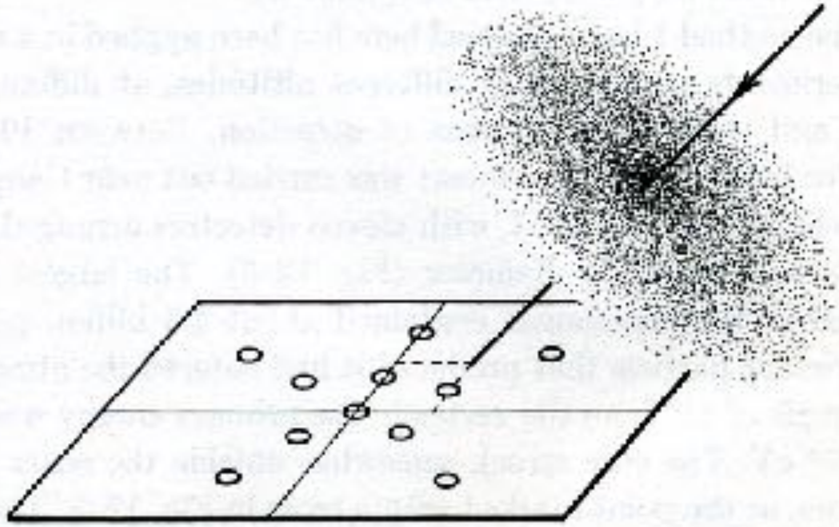

Fig. 12-4 Shower disk approaching detectors (represented by circles on a horizontal plane).

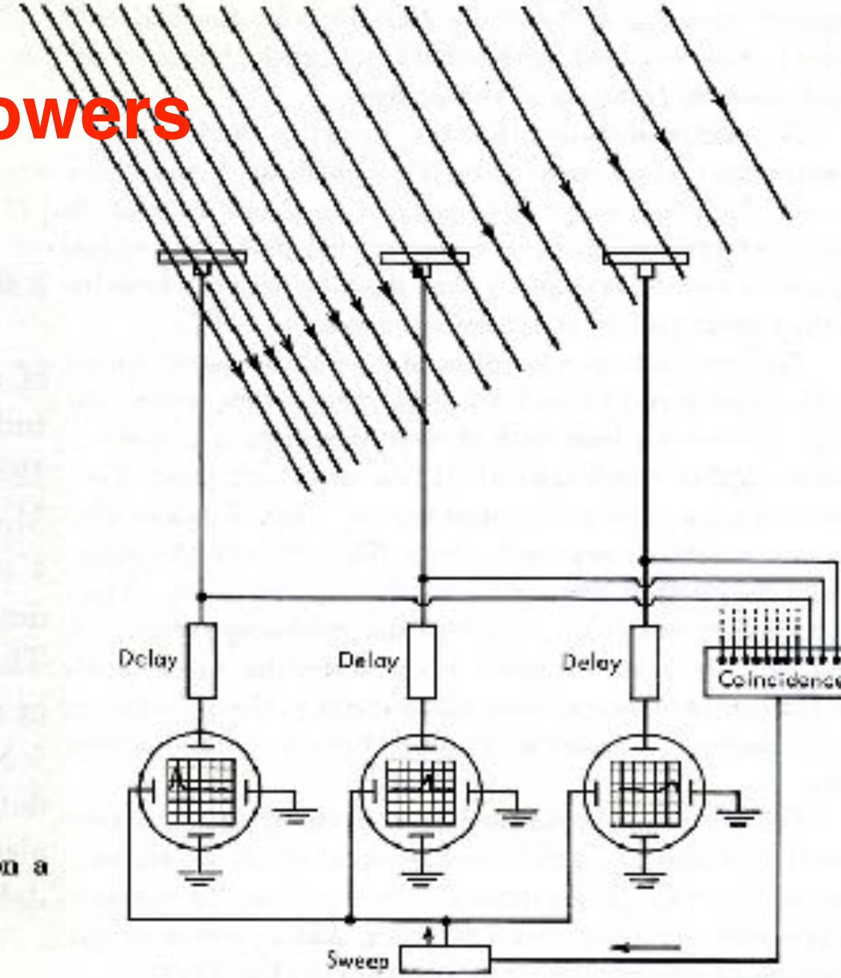

Fig. 12-3 Experimental arrangement used by the MIT cosmic-ray group to study air showers. Fluorescent plastic disks (thin rectangles at top) emit flashes of light when struck by charged particles. At the center of each disk is a photomultiplier tube that converts the light into an electrical pulse; the amplitude of the pulse is proportional to the brightness of the flash. Pulses travel to cathode-ray oscilloscopes (circles) through transmission lines containing delay circuits, which equalize the lengths of the electrical paths. Horizontal sweeps of all oscilloscope screens (grids) are triggered at the same time whenever three or more pulses pass through the coincidence circuit simultaneously. The amplitudes of the "spikes" (that is, the heights of the vertical deflections in the oscilloscope traces) indicate the numbers of particles striking the corresponding detectors. The positions of the spikes in the horizontal traces show the relative arrival times of the particles.

B. Rossi

VOLUME 10, NUMBER 4 PHYSICAL REVIEW LETTERS 15 FEBRUARY 1963

EVIDENCE FOR A PRIMARY COSMIC-RAY PARTICLE WITH ENERGY 10^{20} eV†

John Linsley
Laboratory for Nuclear Science, Massachusetts Institute of Technology, Cambridge, Massachusetts
(Received 10 January 1963)

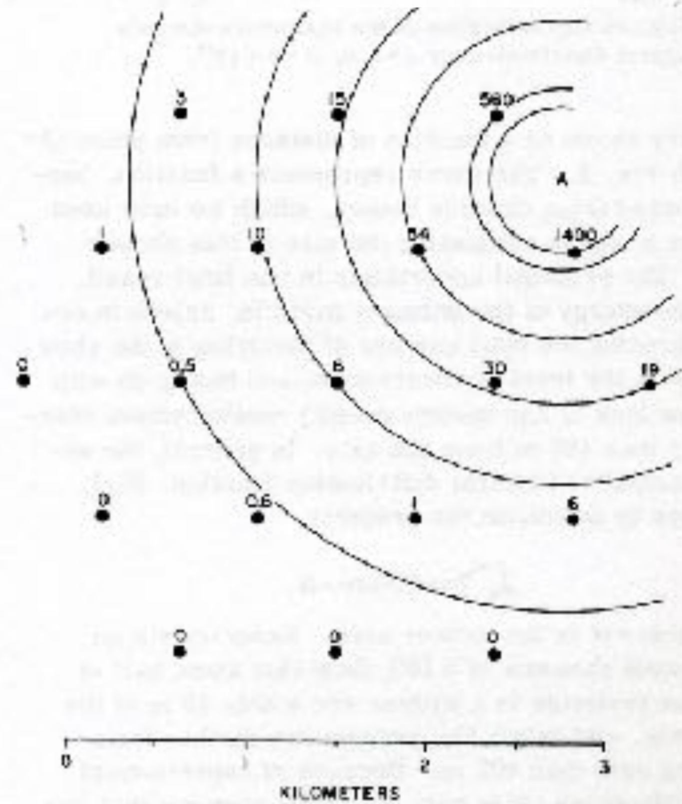

FIG. 1. Plan of the Volcano Ranch array in February 1962. The circles represent 3.3-m^2 scintillation detectors. The numbers near the circles are the shower densities (particles/m^2) registered in this event, No. 2-4834. Point "A" is the estimated location of the shower core. The circular contours about that point aid in verifying the core location by inspection.

1943

The University of Chicago

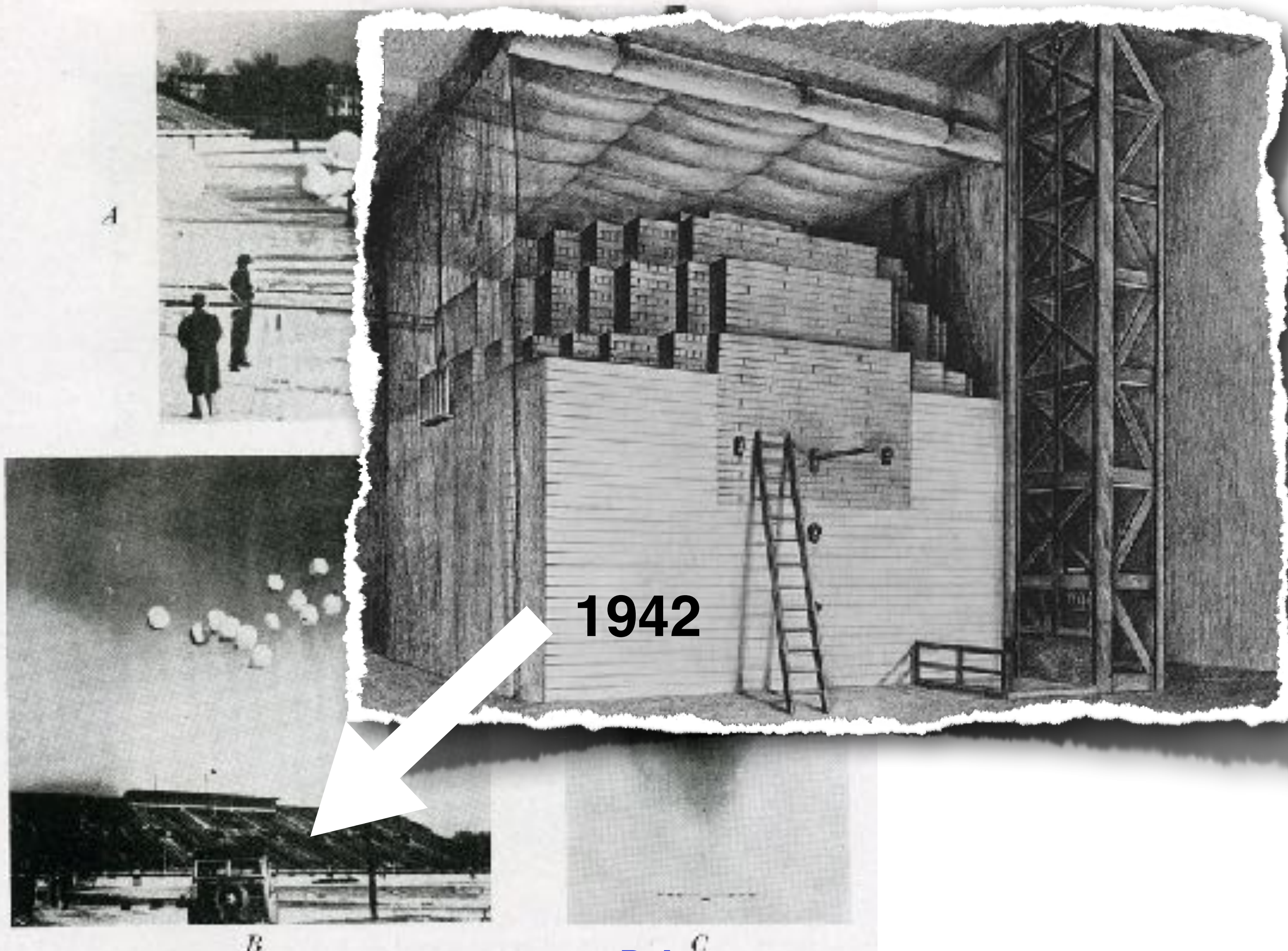

P. Auger

BALLOON FLIGHT OF JANUARY, 1943, CONDUCTED BY THE AUTHOR, SCHEIN, AND ROGOZINSKI FOR THE MEASUREMENT OF EXTENSIVE (OR AUGER-) SHOWERS IN THE STRATOSPHERE

A. The balloons are assembled on Stagg Field at the University of Chicago, Chicago, Illinois. In the foreground can be seen the long frame which was required for the wide separation of the cosmic-ray counters.

B. The large cluster of balloons as it is about to be released.

C. The balloon train sails into the sky after its release. Suspended below the balloons is the frame supporting the counters and recording apparatus.

Fig. 1. Participants at the Cosmic Ray Conference (Symposium on Cosmic Rays, 1939) convened at the University of Chicago in the summer of 1939. The identification of participants is given by numbers in the over lay of this photograph as follows:

1. H. Bethe
2. D. Froman
3. R. Brode
4. A.H. Compton
5. E. Teller
6. A. Baños, Jr.
7. G. Groetzinger
8. S. Goudsmit
9. M.S. Vallarta
10. L. Nordheim
11. J.R. Oppenheimer
12. C.D. Anderson
13. S. Forbush
14. Nielsen (of Duke U.)
15. V. Hess
16. V.C. Wilson
17. B. Rossi
18. W. Bothe
19. W. Heisenberg
20. P. Auger
21. R. Serber
22. T. Johnson
23. J. Clay (Holland)
24. W.F.G. Swann
25. J.C. Street (Harvard)
26. J. Wheeler
27. S. Neddermeyer
28. E. Herzog (?)
29. M. Pomerantz
30. W. Harkins (U. of C.)
31. H. Beutler
32. M.M. Shapiro+
33. M. Schein*
34. C. Montgomery (Yale)
35. W. Bostick+
36. C. Eckart
37. A. Code+
38. J. Stearns (Denver?)
39. J. Hopfield
40. E.O. Wollan*
41. D. Hughes+
42. W. Jesse*
43. B. Hoag
44. N. Hillberry+
45. F. Shonka+
46. P.S. Gill+
47. A.H. Snell
48. J. Schremp
49. A. Haas? (Vienna)
50. E. Dershem*
51. H. Jones+

*Then research associate of Compton.

+Then graduate student of Compton.

ICS

Number 3-4

C RAYS

CAGO

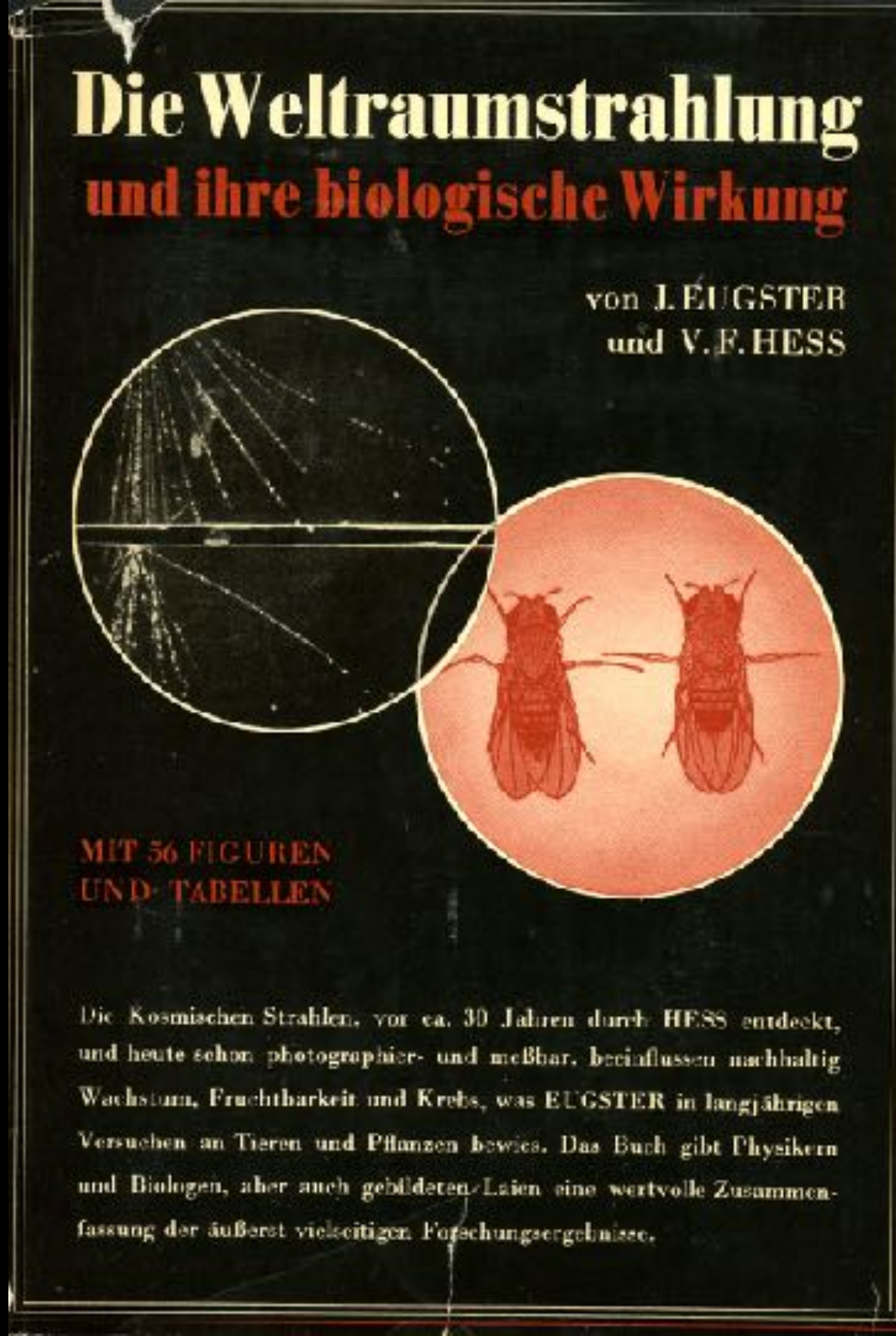
Die Weltraumstrahlung
und ihre biologische Wirkung
von J. EUGSTER
und V. F. HESS
MIT 56 FIGUREN
UND TABELLEN
Die Kosmischen Strahlen, vor ca. 30 Jahren durch HESS entdeckt, und heute schon photographier- und meßbar, beeinflussen nachhaltig Wachstum, Fruchtbarkeit und Krebs, was EUGSTER in langjährigen Versuchen an Tieren und Pflanzen bewies. Das Buch gibt Physikern und Biologen, aber auch gebildeten Laien eine wertvolle Zusammenfassung der äußerst vielseitigen Forschungsergebnisse.

1939

emulsion chambers at high-altitude lab above Innsbruck (Austria)

Disintegration Processes by Cosmic Rays with the Simultaneous Emission of Several Heavy Particles

Disintegration Processes by Cosmic Rays with the Simultaneous Emission of Several Heavy Particles

ON photographic plates which had been exposed to cosmic radiation on the Hafelekar (2,300 m. above sea-level) near Innsbruck for five months, we found, apart from the very long tracks (up to 1,200 cm. in length) which have been reported recently in a note in the Wiener Akademie-Berichte, evidence of seve processes described below.

From a single point within the emulsion seve tracks, some of them having a considerable leng take their departure. We observed four cases w three particles, four with four and 'stars' with s seven, eight and nine particles, one of each kind.

The longest track corresponded to a range in (15°, 760 mm. Hg) of 176 cm. The ionization p duced by the particles is different in the differ cases. Most of the tracks show much larger me grain-distances than α-particles and slow protons.

In Fig. 1 a 'star' with eight tracks is reproduce On account of the rather steep angles at which so of the particles cross the emulsion-layer (appro mately 70 μ thick) it is not possible to have all t tracks of a 'star' in focus simultaneously. Fig. shows a sketch of the same 'star'. Measurement the tracks gives the results in the accompanyi table.

Track	Length in cm. of air (15°, 760 mm.)	Number of grains	Position of the end of the track
A	30·0 cm.	113	Within the emulsion
B	11·0 ,,	15	,, ,, ,,
C	44·6 ,,	71	Glass
D	6·2 ,,	11	,,
E	7·0 ,,	22	,,
F	1·2 ,,	5	Within the emulsion
G	13·6 ,,	67	Surface of the emulsion
H	23·9 ,,	58	Glass

Centre of the 'star' 25 μ under the surface of the emulsion.

We believe that the process in question is a disintegration of an atom in the emulsion (probably Ag or Br) by a cosmic ray. The striking feature about it is the simultaneous emission of so many heavy particles with such long ranges, which excludes any confusion with 'stars' due to radioactive contamination. A similar configuration of tracks by chance is equally out of question. Brode and others[1]

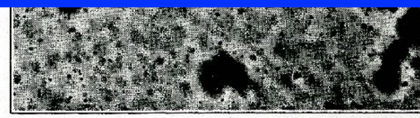

FIG. 1.

observed a single case of a disintegration with three heavy particles in a Wilson cloud chamber. The phenomenon which Wilkins believes was a shower of protons is perhaps a similar process, but he did not observe a centre[2].

M. BLAU.
H. WAMBACHER.
Radium Institut
u. 2 Physik. Institut,
Wien.
Aug. 25.

TRACK. AN INTERRUPTED LINE MEANS THAT THE TRACK IS TOO LONG TO BE REPRODUCED ON THE SAME SCALE. THE ARROWS INDICATE THE DIRECTION FRO THE SURFACE OF THE EMULSION TO THE GLAS

The total energy involved in the process cannot as yet be calculated as most of the particles do not end in the emulsion.

We hope to give further details before long in the Wiener Akademie-Berichte.

M. BLAU.
H. WAMBACHER.
Radium Institut
u. 2 Physik. Institut,
Wien.
Aug. 25.

[1] Brode, R. L., and others, *Phys. Rev.*, 50, 581 (October, 1936).
[2] Wilkins, *Nat. Geog. Soc.*, Stratosphere Series, No. 2, 37 (1936).

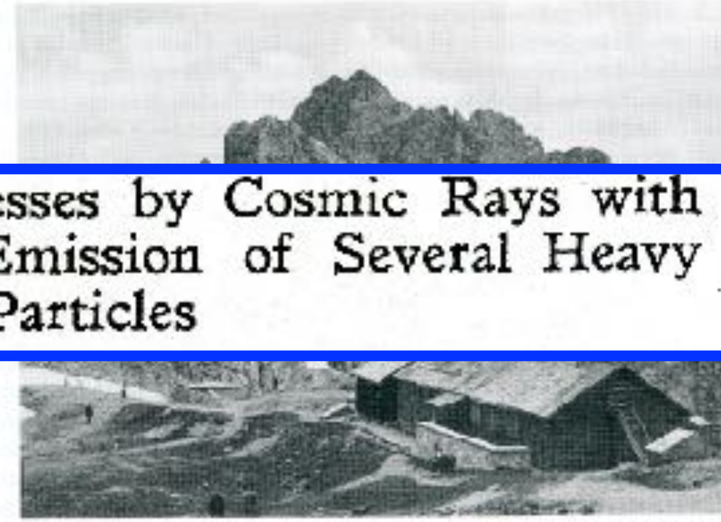

Die "Station für Ultrastrahlenforschung" auf dem Hafelekar bei Innsbruck (2300 m), 1950, vor dem späteren Ausbau.

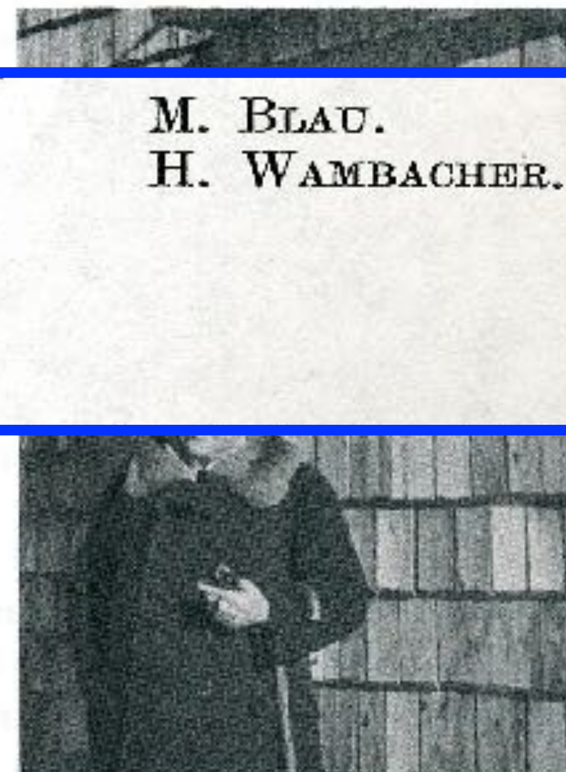

JANUARY, 1941 REVIEWS OF MODERN PHYSICS VOLUME 13

Tracks of Nuclear Particles in Photographic Emulsions

MAURICE M. SHAPIRO
Ryerson Laboratory, University of Chicago, Chicago, Illinois

CONTENTS

1947 Discovery of the Pion

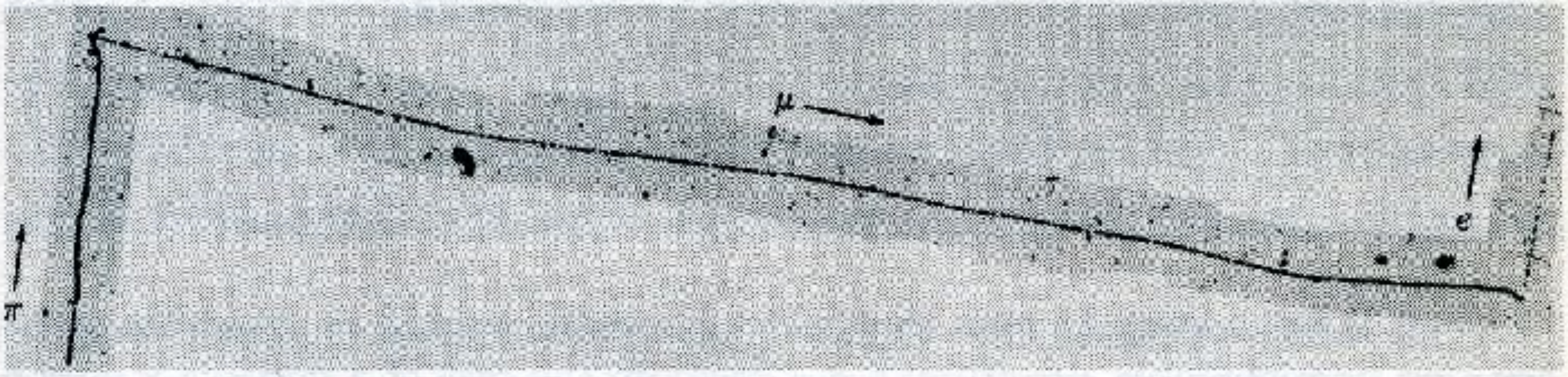

Fig. 9-4 Photomicrograph of tracks in a nuclear emulsion, showing a π meson (π) that comes to rest and decays into a μ meson (μ). The μ meson in turn comes to rest and decays into an electron (e). (From R. H. Brown, U. Camerini, P. Fowler, H. Muirhead, C. F. Powell, and D. M. Ritson, *Nature*, vol. 163, p. 47, 1949.)

C.F. Powell
Nobel Prize 1950

$m_\pi \sim 280\ m_e$

Pion: nuclear interaction
decay $\pi^{+/-} \rightarrow \mu^{+/-} \rightarrow e^{+/-}$
$\pi^0 \rightarrow \gamma\gamma$

End 1940s plastic balloons

Fig. 1. Inflation of balloon of polyethylene just after dawn. The balloon has a total length of about 120 ft. and most of the fabric is on the ground. Such a balloon can in favourable conditions give level flight at about 90,000 ft. for many hours with a load of 40 kg.

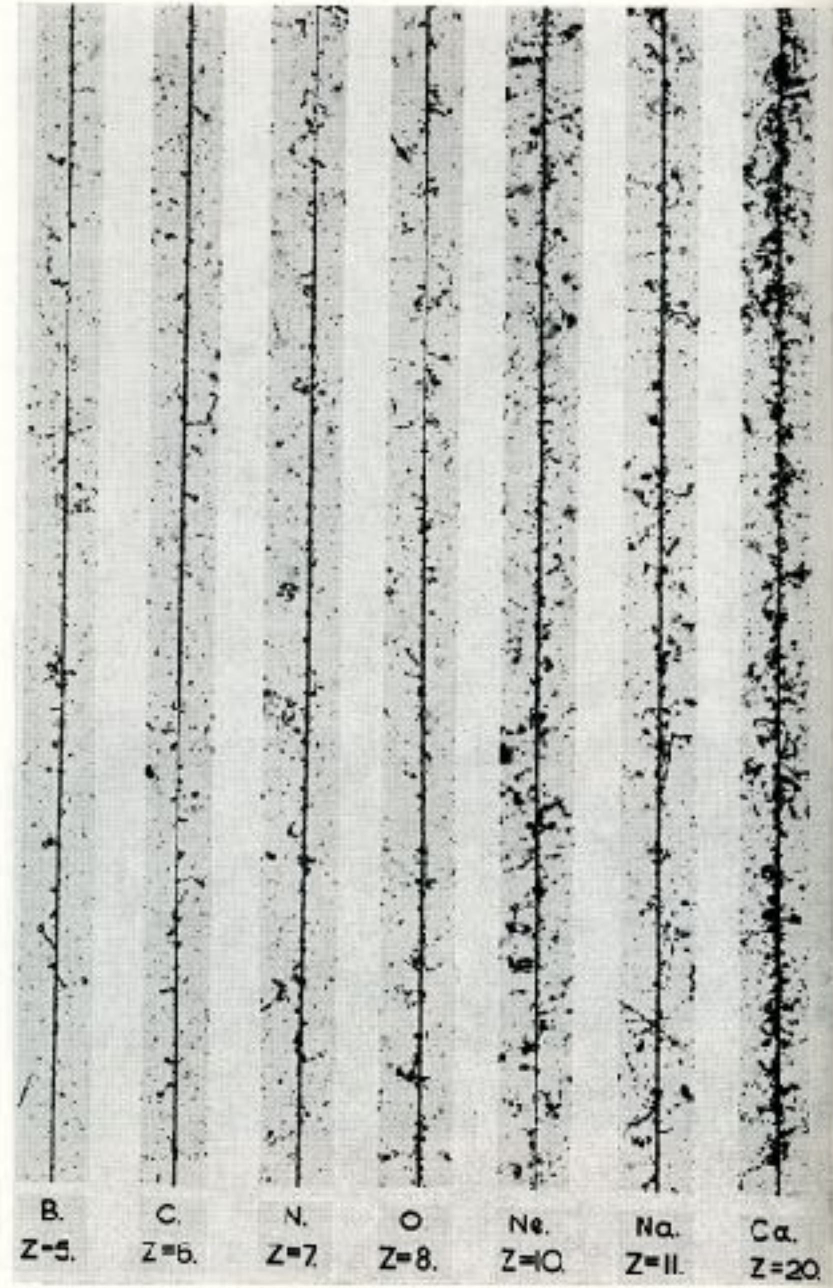

Fig. 2. Examples of the tracks in photographic emulsions of primary nuclei of the cosmic radiation moving at relativistic velocities.

1941 protons (M. Schein)

1948 heavy nuclei (Brandt & Peters)

PHYSICAL REVIEW VOLUME 73, NUMBER 3 FEBRUARY 1, 1948

The Cosmic-Ray Counting Rate of a Single Geiger Counter from Ground Level to 161 Kilometers Altitude

J. A. VAN ALLEN AND H. E. TATEL*
Applied Physics Laboratory, Johns Hopkins University, Silver Spring, Maryland

(Received October 16, 1947)

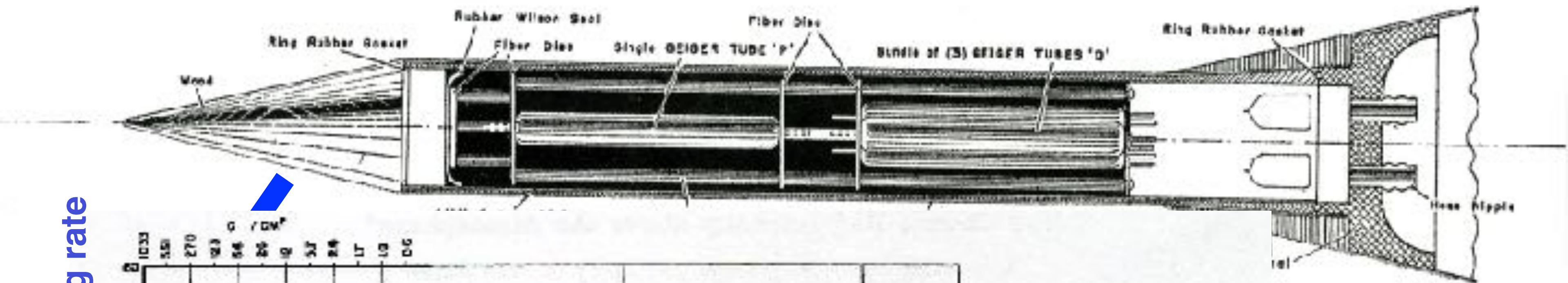

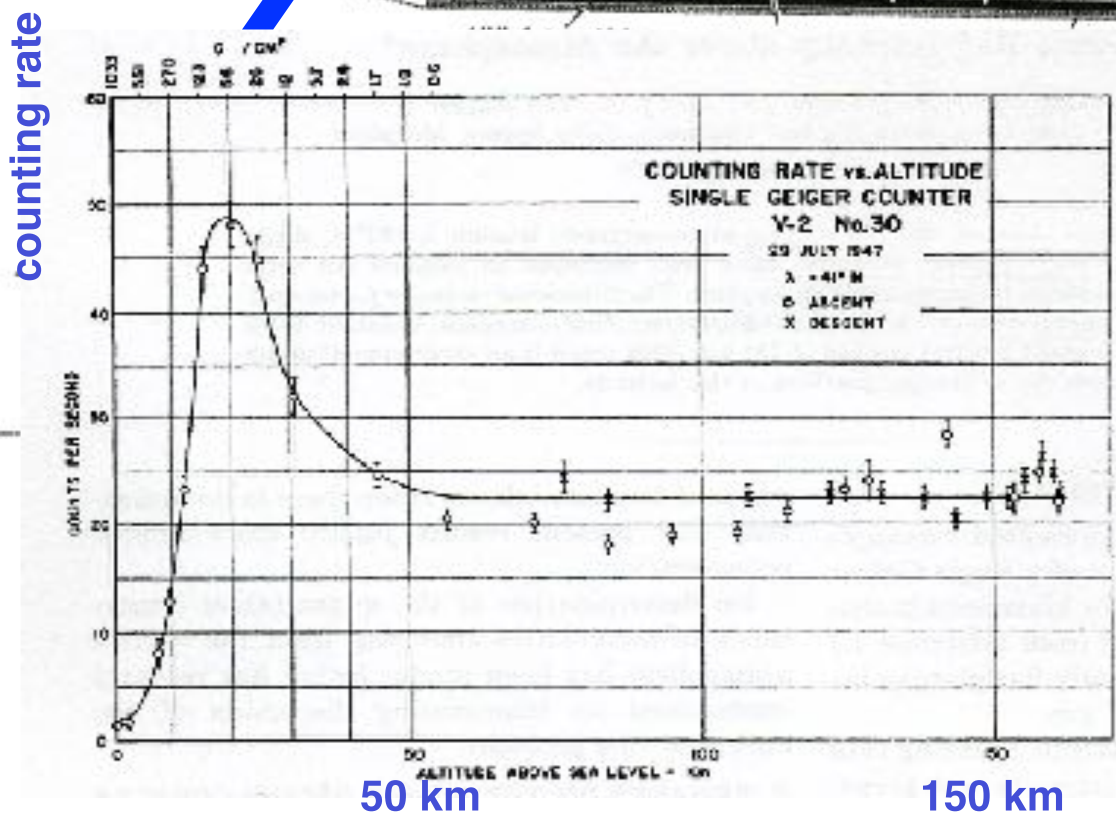

FIG. 1. Counting rate of a single Geiger counter as a function of altitude.

Intensity vs. height

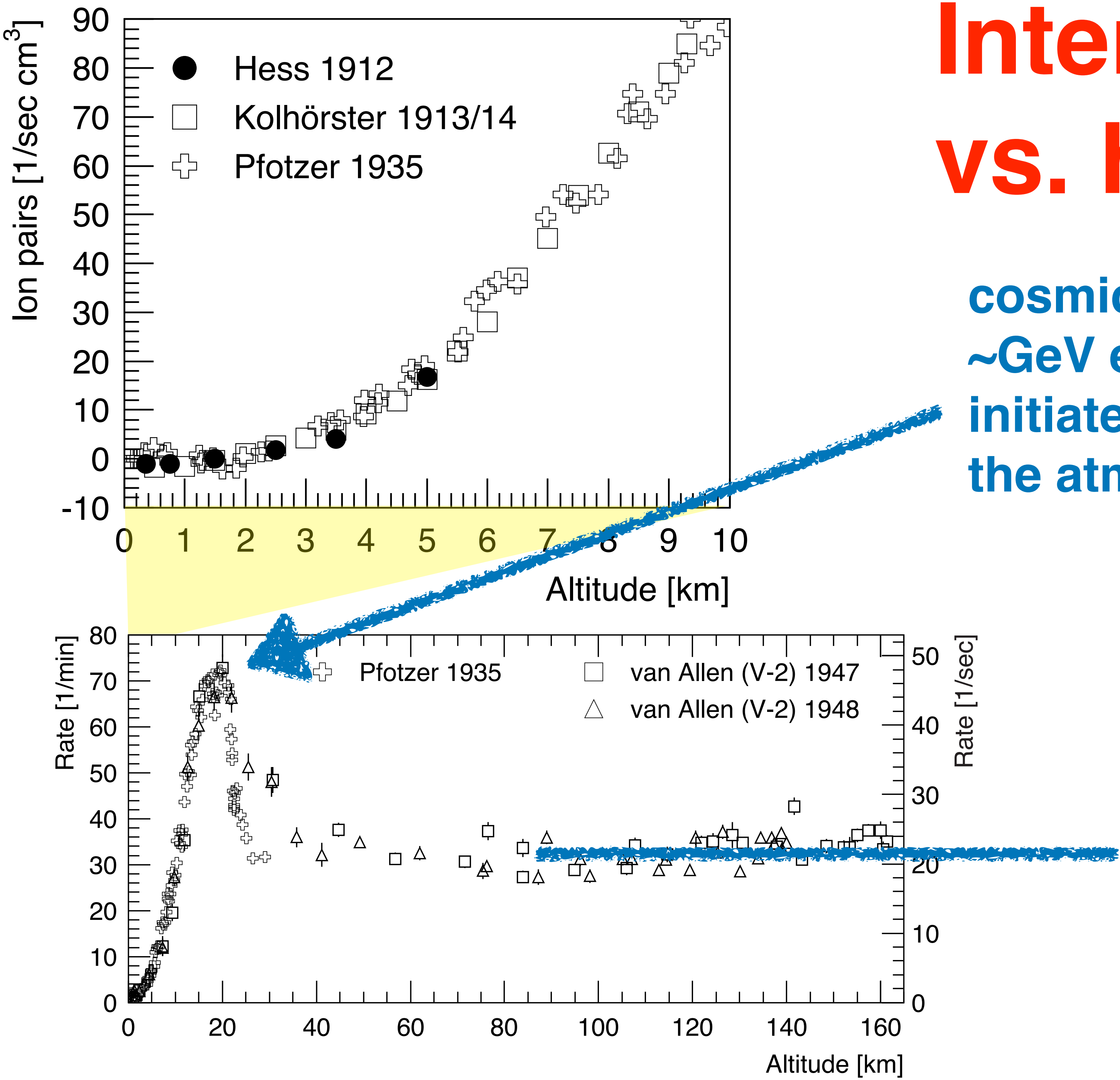

cosmic rays with ~GeV energies initiate cascades in the atmosphere

(galactic) cosmic rays

Faculty of Science
Physics and Astronomy

Academic year 2019 - 2020
May 12, 2020

Cosmic-Ray Detection on Board of a REXUS Rocket

JOCHEM BEURSKENS

SUPERVISORS: **JÖRG R. HÖRANDEL, BJARNI PONT**

Radboud University

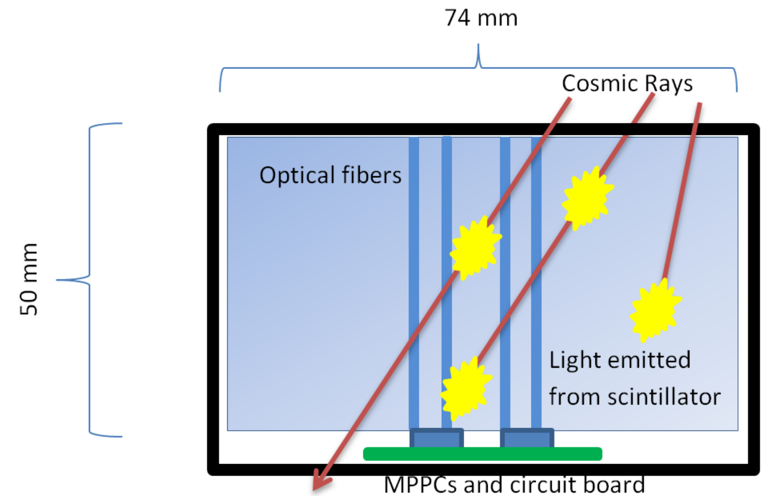

Figure 1.6: A schematic view of an intersection of the CubeSat cosmic-ray detector. Some cosmic-rays pass through the scintillator, but others are absorbed. Light emitted by the scintillator can then be detected by the light sensitive MPPCs at the bottom. The optical fibers increase the amount of light that is guided towards the MPPCs, thereby decreasing the amount of energy absorbed that remains undetected. The black outer rim represents the tape that covers the entirety of the cosmic-ray sensor, so that no outside light sources can cause misfires in the MPPCs.

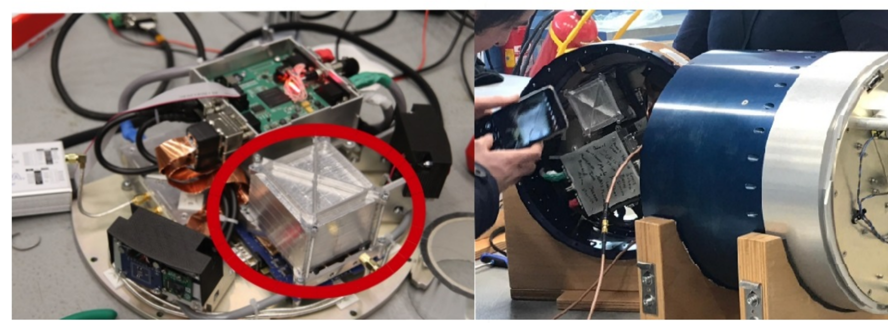

Figure 2.3: The PR3 module, without the outer rim. The circled gray box is the CubeSat cosmic-ray detect
And the PR3 module in the rocket.

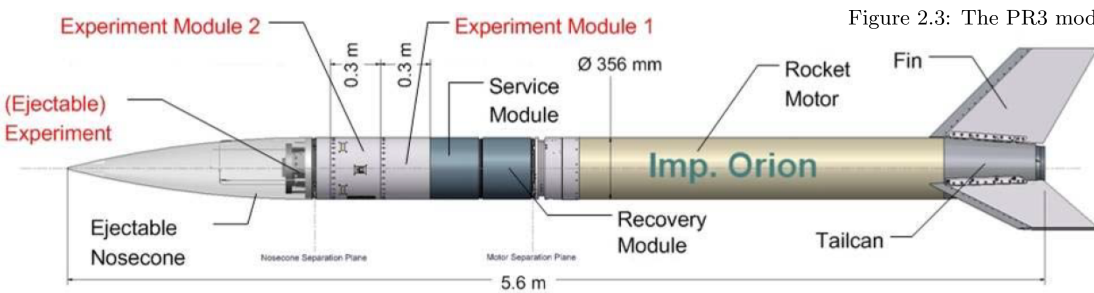

Figure 2.1: A typical configuration of a REXUS sounding rocket [4].

Faculty of Science
Physics and Astronomy

Academic year 2019 - 2020
May 12, 2020

Cosmic-Ray Detection on Board of a REXUS Rocket

Jochem Beurskens

Supervisors: Jörg R. Hörandel, Bjarni Pont

Radboud University

3.2.2 Counts and Altitudinal Profile

Using the altitude data, from the combination of REXUS 25 and REXUS 26, together with the measured counts for the cosmic radiation a cosmic-ray count rate versus altitude graph is reconstructed. This is done in order to get a look at the shape of the Pfotzer maximum, from which the ratio of high and low energy particles can roughly be estimated.

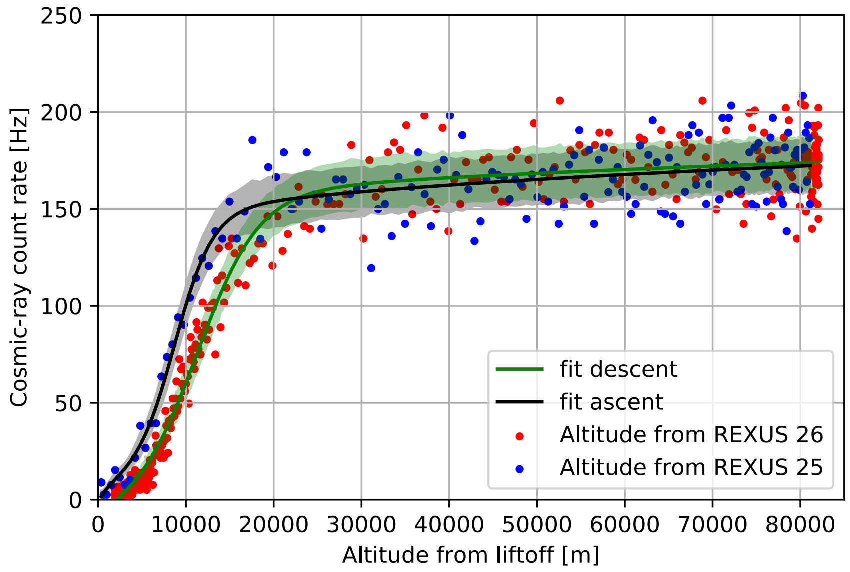

Figure 3.5: Altitude versus count rate. As the GPS data for the REXUS 25 flight cut-off around 80 km altitude this part of the flight has been fitted separate from the descent part of the flight, which was mainly made with GPS data from REXUS 26. A square root of N error for both the ascent and descent fit is added as the shaded areas.

PHYSICAL REVIEW VOLUME 78, NUMBER 6 JUNE 15, 1950

Stars and Heavy Primaries Recorded during a V-2 Rocket Flight

HERMAN YAGODA, HERVASIO G. DE CARVALHO,* AND NATHAN KAPLAN
Laboratory of Physical Biology, Experimental Biology and Medicine Institute, National Institutes of Health, Bethesda, Maryland

(Received February 23, 1950)

Plates flown to an altitude of 150.7 km in a V-2 rocket exhibit a differential star population of 5000±800 per cc per day and a flux of heavy primaries of about 0.03 per cm² per min. above the stratosphere. The star intensity is about 3.6 times greater than that recorded by plates exposed in the stratosphere, the increment being attributable to secondary star forming radiations created by interaction of cosmic-ray primaries with the massive projectile. The flux of heavy primaries is essentially of the same order of magnitude as reported for elevations of 28 km.

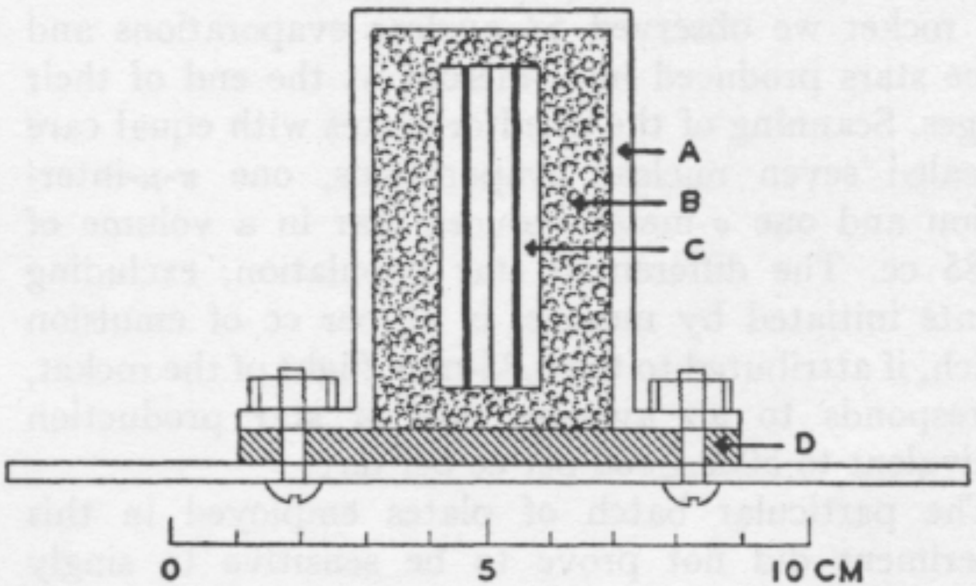

FIG. 1. Cross section of plate holder. A. Aluminum jacket 3 mm thick. B. Sponge rubber packing. C. Plates assembled with emulsion layers adjacent to each other. D. Rubber gasket.

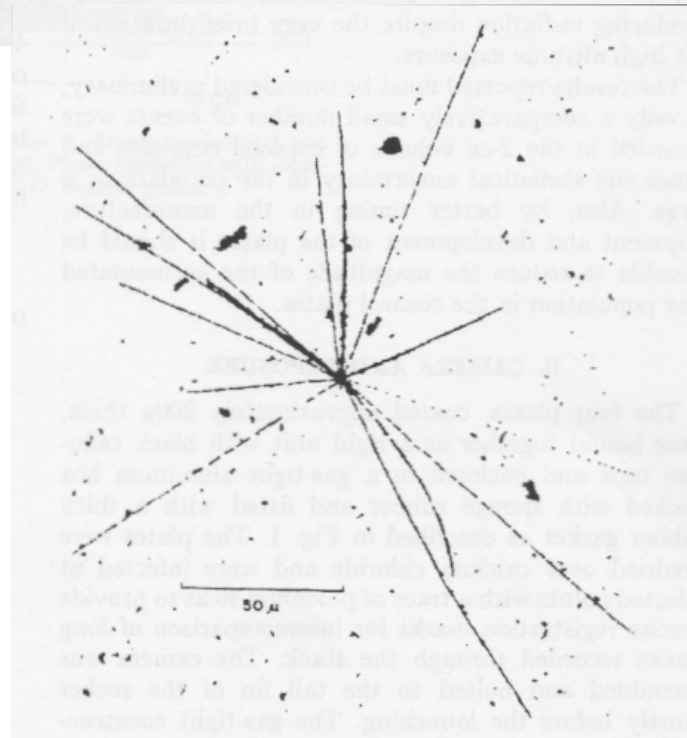

FIG. 3. Nuclear evaporation recorded in one of the rocket plates.

1953 Cosmic-Ray Conference

birth of particle physics

particles discovered in cosmic rays:

- **1932 e^+ Anderson**
- **1937 μ Anderson/ Neddermeyer**
- **1947 π Lattes, Occhialini, Powell**
- **1947 K Rochester, Butcher, Powell**
- **1951-53 hyperons**

$\Lambda \quad \Xi \quad \Sigma$

PHYSICAL REVIEW VOLUME 88, NUMBER 2 OCTOBER 15, 1952

Rocket Determination of the Ionization Spectrum of Charged Cosmic Rays at $\lambda = 41°$N

G. J. PERLOW,* L. R. DAVIS, C. W. KISSINGER, AND J. D. SHIPMAN, JR.
U. S. Naval Research Laboratory, Washington, D. C.

(Received June 30, 1952)

In a V-2 rocket measurement at $\lambda = 41°$N an analysis has been made of the various components of the charged particle radiation on the basis of ionization and absorption in lead. The ionization was determined by two proportional counters, the particle paths through which were defined by Geiger counters. With increasing zenith angle toward the north, the intensity is found to be substantially constant until the earth ceases to cover the under side of the telescope. The intensity of all particles with range ≥ 7 g/cm² is 0.079 ± 0.005 (cm² sec steradian)$^{-1}$. Of this an intensity 0.012 ± 0.002 is absorbed in the next 14 g/cm². The ionization measurement is consistent with $\frac{3}{4}$ of these soft particles being electrons of $<\sim 60$ Mev, the remainder being slow protons and alpha-particles. For the particles with greater range an ionization histogram is plotted, the smaller of the two ionization measurements for a single event being used to improve the resolution. The particles divide into protons, alpha-particles, and one carbon nucleus, with $N_p/N_\alpha = 5.3 \pm 1.0$. Their absorption is exponential with mean free path 440 ± 70 g/cm² Pb. Extrapolating to zero thickness, the total primary intensity is 0.070 ± 0.005 (cm² sec steradian)$^{-1}$ with 0.058 ± 0.005 as protons, 0.011 ± 0.002 as alpha-particles, and 0.001 ± 0.001 as $Z > 2$.

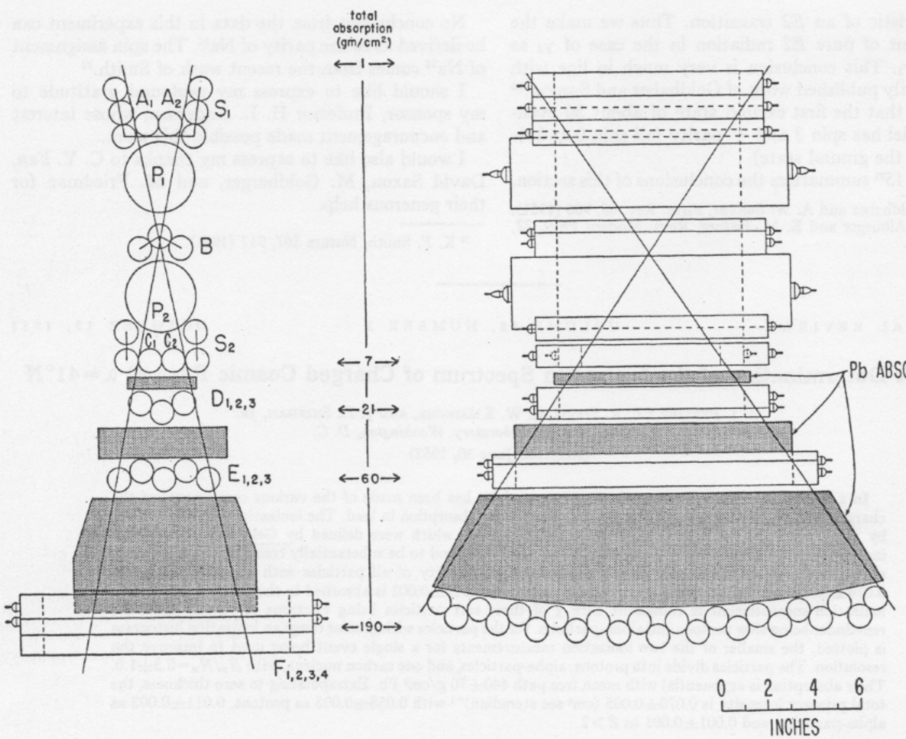

FIG. 1. Diagram of telescope.

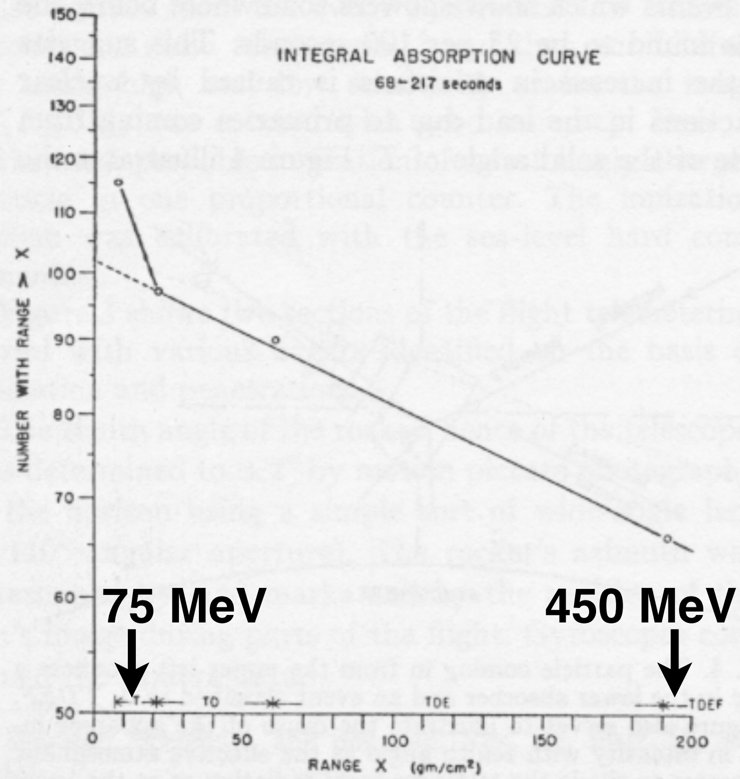

FIG. 6. Absorption in lead of the total radiation.

Van Allen Belts

KEY

1. Cosmic ray burst detector.
2. Vertical telescope.
3. and 4. Dynamotor power supply and flight batteries.
5. Magnetic orientor for determining direction of rocket axis with respect to earth's magnetic field.
6, 7, 8 and 10. Geiger counter coincidence circuits, telemetering circuits and radio telemetering transmitter.
9. Horizontal telescope.
11. 45° telescopes.
12. Photocell orientor to determine angle of rocket axis with the solar vector.
13. Coaxial cable to telemetering antenna 14.

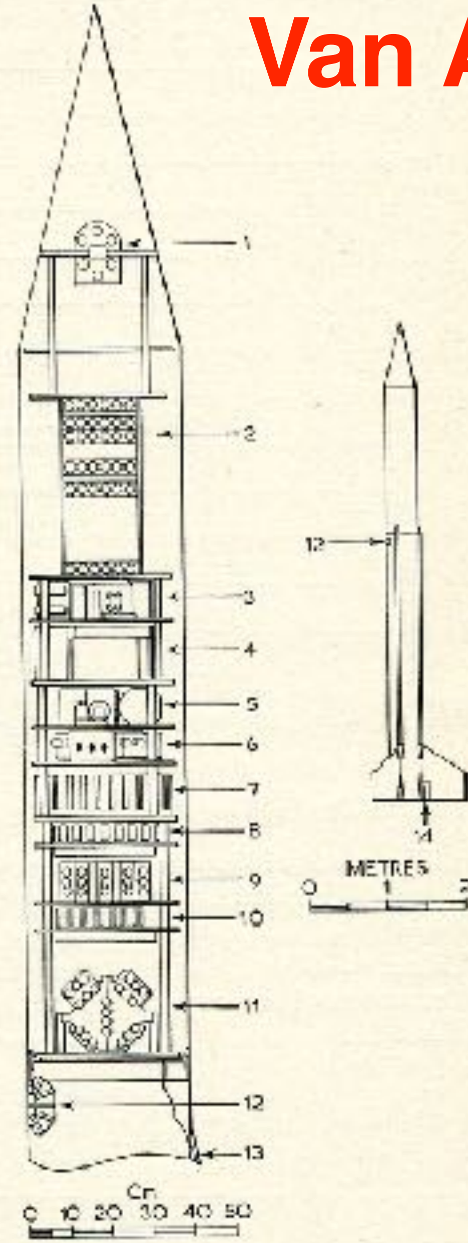

FIG. 32. EXPERIMENTAL ARRANGEMENT FOR AEROBEE ROCKET COSMIC RAY EXPERIMENTS OF VAN ALLEN AND SINGER.

(Reproduced from S. F. Singer, "Progress in Elementary Particle and Cosmic Ray Physics" Vol. IV., Ed. J. G. Wilson and S. A. Wouthuysen, North-Holland Publishing Co., 1958, by permission of the author and publisher).

Nature **183**, 430 - 434 (14 February 1959); doi:10.1038/183430a0

Van Allen Belts

Radiation Around the Earth to a Radial Distance of 107,400 km.

JAMES A. VAN ALLEN & LOUIS A. FRANK

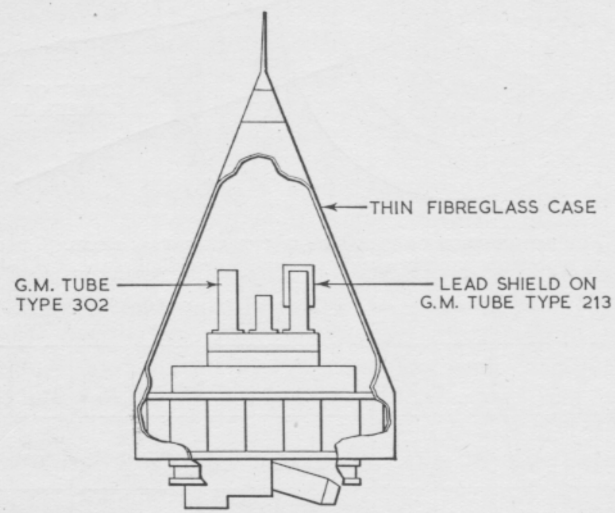

FIG. 71. THE ARRANGEMENT OF RADIATION DETECTORS IN PIONEER IV. (*After van Allen*).

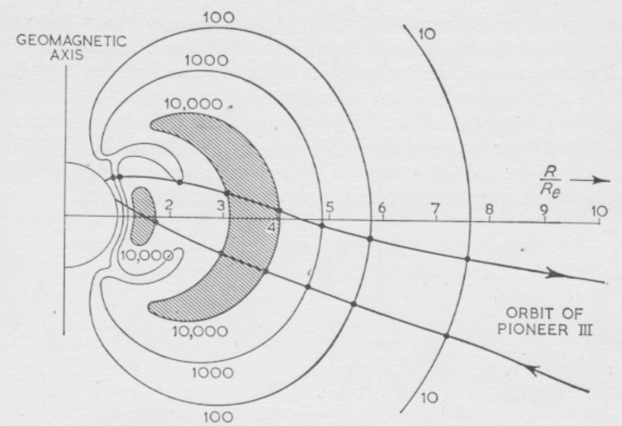

FIG. 69. THE DISTRIBUTION OF INTENSITY IN THE RADIATION BELTS. (6 DEC. 1958). The diagram represents a cross section through a meridian plane. R_e(∼6400 km) is the radius of the earth. (*After van Allen and Frank, Nature*, **183**, 430 (1959)).

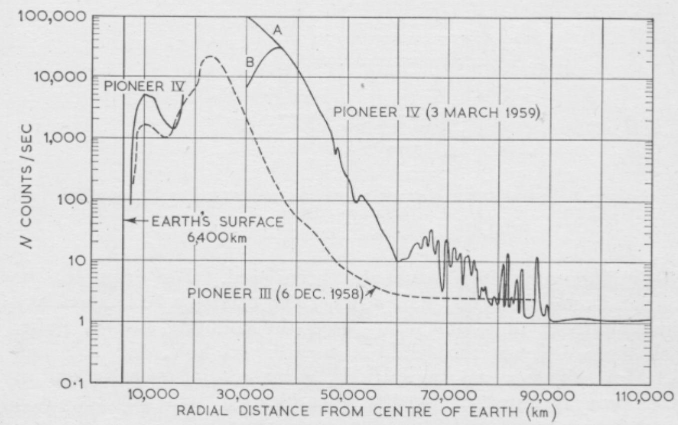

FIG. 70. A COMPARISON OF THE INTENSITIES OF RADIATION FOUND WITH NEARLY IDENTICAL COUNTERS IN PIONEER III AND PIONEER IV. The trajectories of the two probes were almost, but not quite, the same. At the peak of the second belt the readings of the intensity from Pioneer IV were ambiguous and followed either curve A or curve B. Curve A is more probable. (*After van Allen and Frank, Nature* **184**, 219 (1960)).

John Si

Preciss
measu
abunda
dE/dx vs
solid sta
space

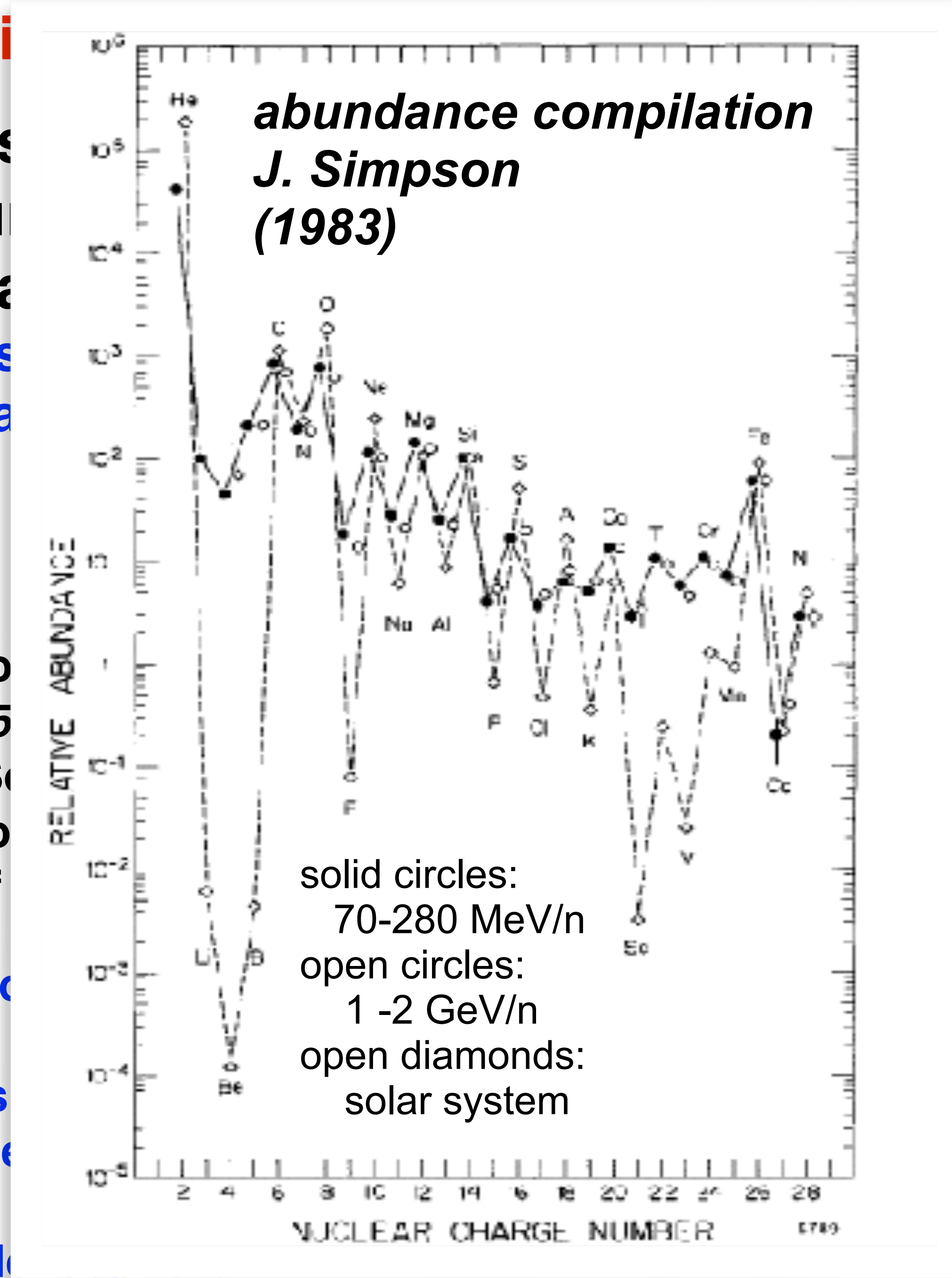

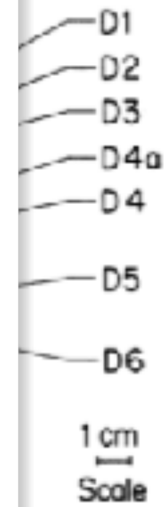

1958 PIONEER 2
1959 EXPLORER 6
subsequently, more than 20 o
including: ***IMP1-8; OGO 1,3,5***
PIONEER 5,6,7 **- S**
PIONEER 10,11 **- o**
ULYSSES **- out of**

- **Elemental composition of c**
- **Isotopic composition**
- **Measurement of anomalous**
- **Particles and fields in the He**
- **Planetary magnetospheres**
- **Solar modulation to outer H**

Formation of the chemical composition

Relative abundance of elements at Earth

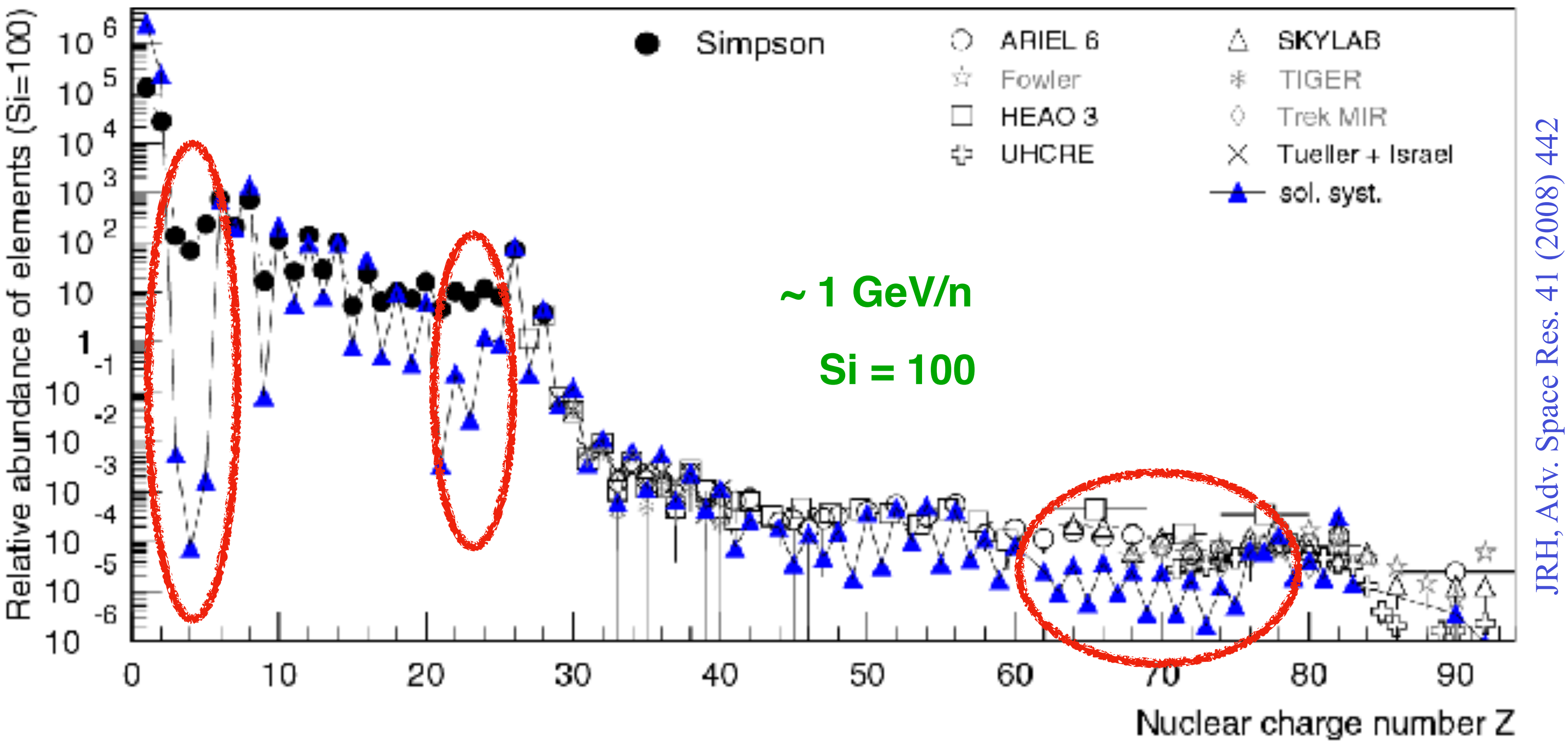

abundance of elements in CRs and solar system mostly similar

but few differences, e.g. Li, Be, B —> important to understand propagation of cosmic rays in Galaxy —> column density of traversed matter

primary cosmic rays generated at source e.g. p, He, Fe
spallation products —> secondary cosmic rays, e.g. Li, Be, B

THE ASTROPHYSICAL JOURNAL, 217:859–877, 1977 November 1

Age of cosmic rays

THE AGE OF THE GALACTIC COSMIC RAYS DERIVED FROM THE ABUNDANCE OF ^{10}Be*

M. GARCIA-MUNOZ, G. M. MASON, AND J. A. SIMPSON†
Enrico Fermi Institute, University of Chicago
Received 1977 March 14; accepted 1977 April 21

$\tau = 17 \cdot 10^6$ a

$^{10}Be \rightarrow {}^{10}B + e^-$ (τ=2.4 10^6 a)

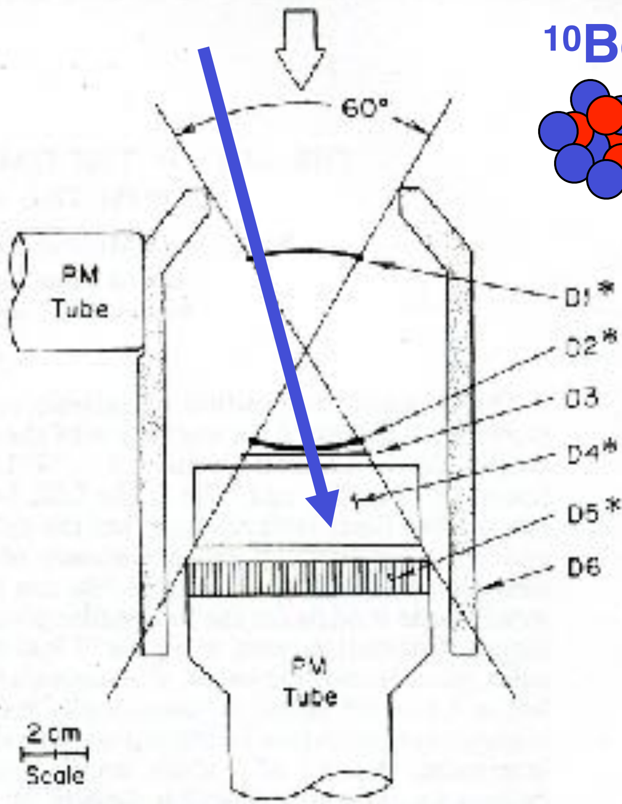

FIG. 1.—Cross section of the IMP-7 and IMP-8 telescopes. D1, D2, and D3 are lithium-drifted silicon detectors of thickness 750, 1450, and 800 μm, respectively. D4 is an 11.5 g cm^{-2} thick CsI (Tl) scintillator viewed by four photodiodes. D5 is a sapphire scintillator/Cerenkov radiator of thickness 3.98 g cm^{-2}, and D6 is a plastic scintillation guard counter viewed by a photomultiplier tube. Asterisks denote detectors whose output is pulse-height analyzed.

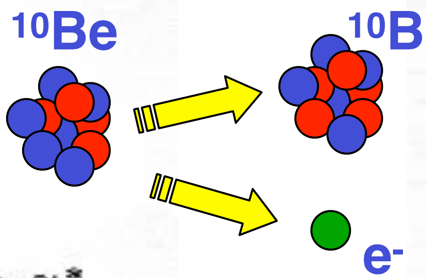

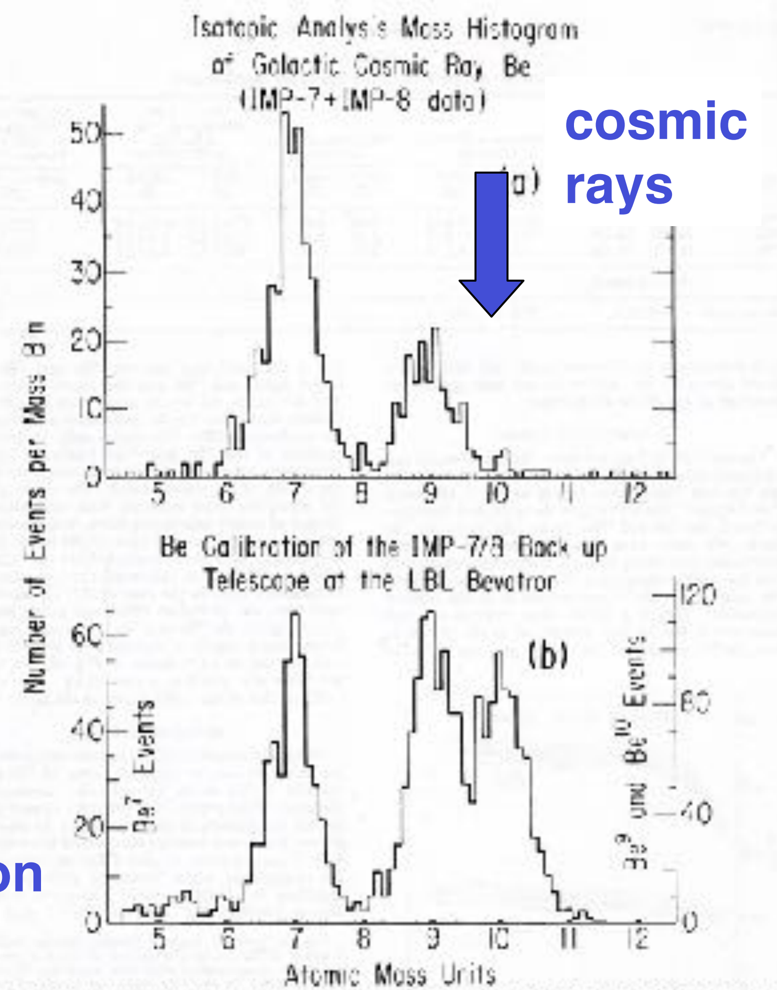

Path length of cosmic rays

VOLUME 29, NUMBER 7 PHYSICAL REVIEW LETTERS 14 AUGUST 1972

Composition of Cosmic-Ray Nuclei at High Energies*

Einar Juliusson, Peter Meyer, and Dietrich Müller
Enrico Fermi Institute and Department of Physics, University of Chicago, Chicago, Illinois 60637
(Received 26 May 1972)

We have measured the charge composition of cosmic-ray nuclei from Li to Fe with energies up to about 100 GeV/nucleon. A balloon-borne counter telescope with gas Cherenkov counters for energy determination was used for this experiment. Our first results show that, in contrast to low-energy observations, the relative abundances change as a function of energy. We find that the ratio of the galactic secondary nuclei to primary-source nuclei decreases at energies above about 30 GeV/nucleon.

g/cm²

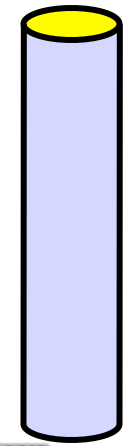

spallation

C → B + n + p

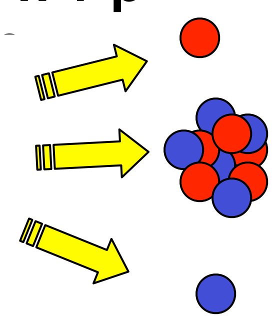

B/C-ratio

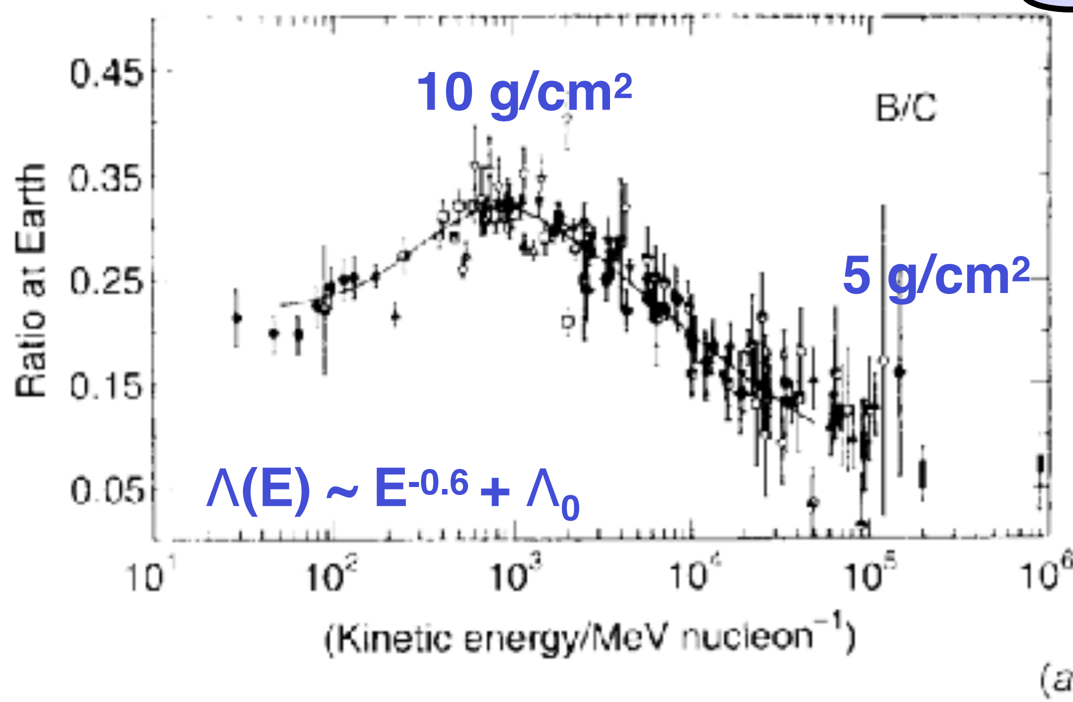

Origin of Cosmic Rays?

1927 R.A. Millikan: „death cries of atoms“

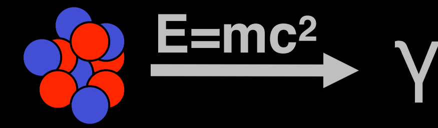

1933 Regener: E density in CRs ~ E density of B field in Galaxy

1934 Supernovae

Walter Baade Fritz Zwicky

1949 E. Fermi: acceleration at magnetic clouds

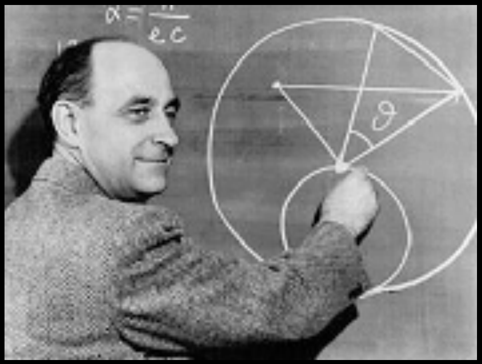

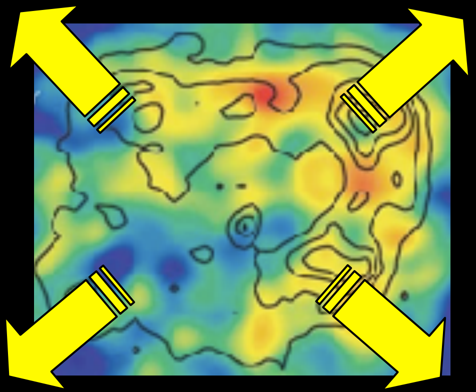

1978 R.D. Blanford, J.P. Ostriker: acceleration at strong shock front (1st order Fermi acceleration)

Beyond the boundaries of our Solar System

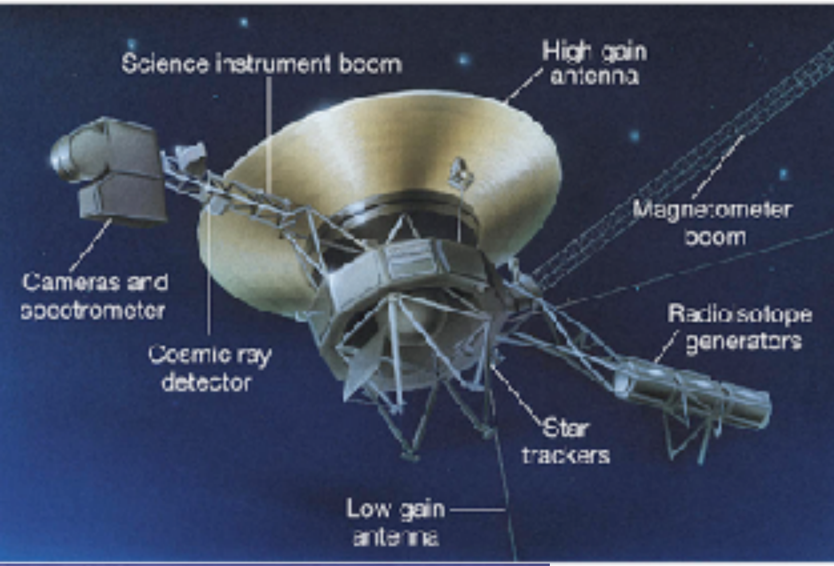

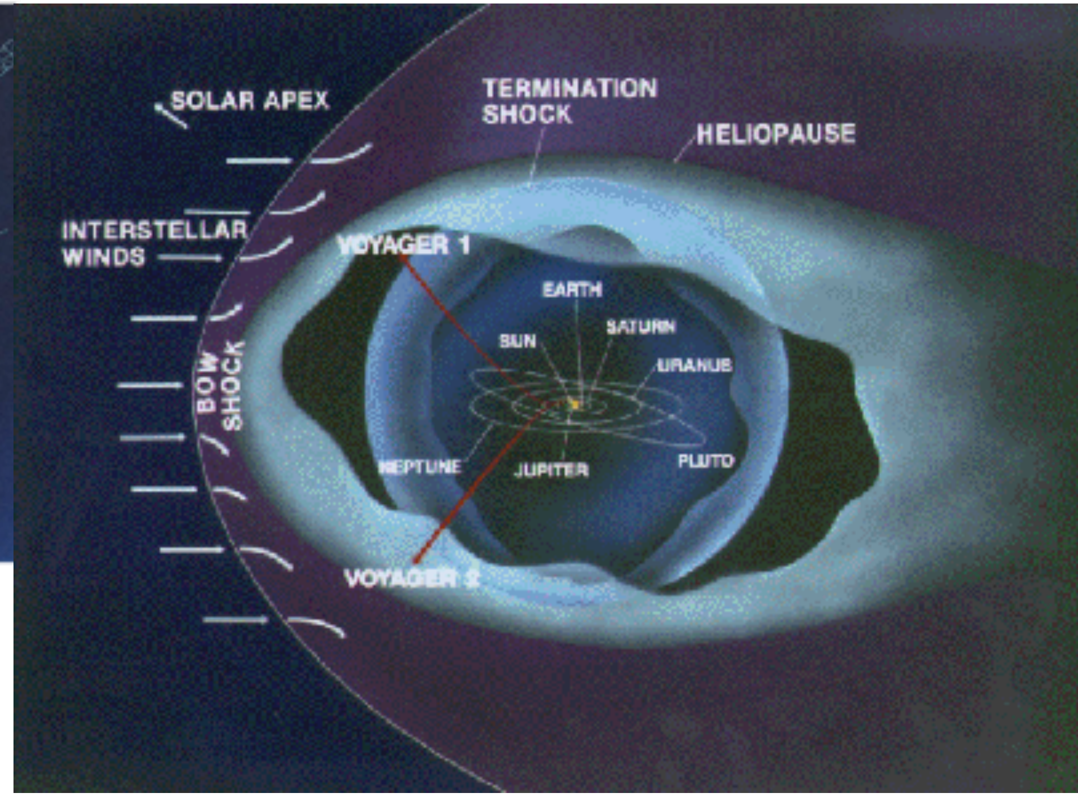

passage through termination shock ended
Voyager 1: 94 AU, December 2004
Voyager 2: 84 AU, August 2007

February 2024: Voyager 1: 162 AU from Sun
Voyager 2: 136 AU from Sun

$$\Delta T = cd \approx 22 \text{ h}$$

Voyager 2: 20 August 1977
Voyager 1: 5 September 1977
Kenedy Space Center

Galactic Cosmic Rays and the Heliosphere

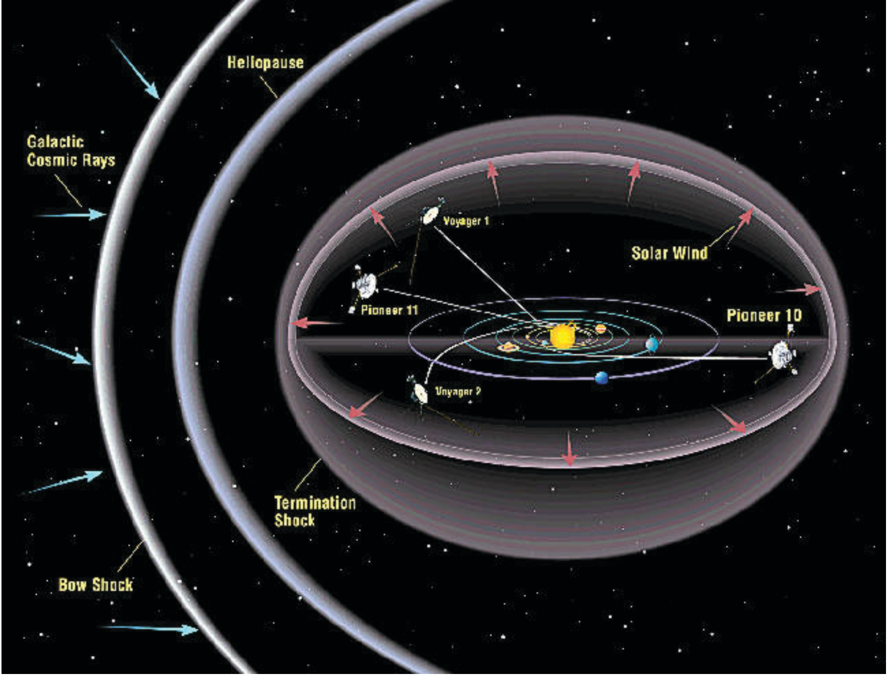

August 25th, 2012
Interstellar Space